Design and Performance analysis of Novel Decoding Techniques for Non-Orthogonal Multiple Access for 5G and Beyond-5G Wireless Networks

by

Elie Sfeir

MANUSCRIPT-BASED THESIS PRESENTED TO ÉCOLE DE TECHNOLOGIE SUPÉRIEURE IN PARTIAL FULFILLMENT FOR THE DEGREE OF DOCTOR OF PHILOSOPHY
Ph.D.

MONTREAL, MARCH 6, 2023

ÉCOLE DE TECHNOLOGIE SUPÉRIEURE
UNIVERSITÉ DU QUÉBEC

BOARD OF EXAMINERS

THIS THESIS HAS BEEN EVALUATED

BY THE FOLLOWING BOARD OF EXAMINERS

M. Georges Kaddoum, Thesis supervisor
Department of Electrical Engineering, École de Technologie Supérieure

M. Kaiwen Zhang, President of the board of examiners
Département de génie logiciel et des TI, École de Technologie Supérieure

M. Frédéric Nabki, Member of the jury
Département de génie électrique, École de Technologie Supérieure

M. Jean-Francois Bousquet , External examiner
Département de Génie Électrique et Informatique, Université Dalhousie

THIS THESIS WAS PRESENTED AND DEFENDED

IN THE PRESENCE OF A BOARD OF EXAMINERS AND THE PUBLIC

ON JANUARY 25, 2023

AT ÉCOLE DE TECHNOLOGIE SUPÉRIEURE

FOREWORD

This dissertation comes as the result of the author's Ph.D. under the supervision of Professor Georges Kaddoum from September 2018 to December 2022. It is a manuscript-based thesis based on four published journals. This work focuses on non-orthogonal multiple access (NOMA), which enables massive connectivity and improved spectral efficiency which are essential for upcoming generations of wireless communications. This work studies the effect of impairments on the viability of NOMA within different challenging scenarios, which include several defects such as AM/PM nonlinearities and impulsive noise. We showed the effect of the studied imperfections and proposed suitable techniques for mitigating their deleterious effects. This led to improving the implementations of NOMA within different conditions of the network, thus enabling better BER performance, spectral efficiency, and sum rates. This work can also be extended for practical implementation in the fifth (5G) and sixth (6G) upcoming generations.

In this dissertation, the first chapter presents an overview of machine learning and information theory tools that we utilized. The second chapter presents an extensive literature review on NOMA, depicting its different categories, system models, and newly evolved applications. Then, the following four chapters are written based on the author's journal papers. Last but not least, the conclusion and recommendations for future work are given in the last chapter.

ACKNOWLEDGEMENTS

Firstly, I would like to express my sincere gratitude and thankfulness to my advisor, Professor Georges Kaddoum, for his immense knowledge, unparalleled support, patience, motivation, and encouragement throughout this process. This work would not have been possible without his perspicacity, guidance, and professional comments.

I would like to thank also Dr. Rangeet Mitra for his time, insights and professional comments.

I would also like to truly thank my labmates in LACIME for the stimulating discussions and the good moments we did have together, including Dr. Ali, Ibrahim, Dr. Bassant, Dr. Victor, Dr. Michael, Dr. Zeeshan, Dr. Dat, Dr. Jung, Christian, Dr. Khaled, Dr. Sahabul. I would also like to thank my ETS friends for their support including Dr. Claude and Dr. Georges.

I thank my siblings and friends who were always beside me, motivating me and fuelling my energy throughout this journey.

Last but not least, I would like to thank my beautiful parents, Denise & Jean, who sacrificed a lot for me, supported me, and vigorously pushed me to achieve more. I will be indebted to them forever.

Conception et analyse des performances de nouvelles techniques de décodage pour l'accès multiple non orthogonal des réseaux sans fil de la 5G et d'au-delà

Elie Sfeir

RÉSUMÉ

Le domaine des communications sans fil a connu plusieurs évolutions qui ont considérablement changé notre mode de vie. Ces évolutions ont été motivées non seulement par le besoin de plus larges débits de données, mais également par les exigences de performance toujours plus strictes d'une pléthore de nouvelles applications technologiques. La croissance explosive continue du nombre d'appareils connectés combinée à l'émergence de plusieurs nouvelles applications telles que l'internet des objets (IdO), la télémédecine, la technologie des véhicules, les maisons et appareils intelligents, poussent les ingénieurs et les chercheurs à innover et à concevoir de nouvelles technologies d'accès multiple viables, capables de couvrir les demandes croissantes de connectivité et de débits de données plus élevés.

L'accès multiple non orthogonal (NOMA), par opposition aux techniques traditionnelles d'accès multiple orthogonal (OMA), permet à plusieurs utilisateurs de partager le même élément de ressource orthogonal. Ainsi, NOMA est une technologie prometteuse et un excellent candidat pour satisfaire la plupart des besoins des réseaux de cinquième génération (5G), notamment une connectivité massive, une efficacité spectrale plus élevée et des débits d'utilisation plus élevés. Les recherches en NOMA ont conduit à la mise au point de plusieurs architectures divisées en deux catégories principales distinguées par la nature du multiplexage des utilisateurs, qui est soit dans le domaine de puissance (PD-NOMA), soit dans le domaine de code (CD-NOMA).

Parmi les architectures multiples de CD-NOMA, l'accès multiple par code clairsemé (SCMA), qui consiste en un mappage d'un ensemble de code pour chacun des utilisateurs du réseau, a attiré une attention considérable pour satisfaire les besoins des prochaines générations, couvrant spécifiquement une connectivité massive et une efficacité spectrale supérieure. Cependant, comme toute autre nouvelle technologie, diverses dégradations de la transmission peuvent compromettre les performances. Cette thèse met en lumière la technologie SCMA et étudie son application dans plusieurs scénarios. Nous analysons les performances de SCMA en présence de plusieurs dégradations qui pourraient gravement détériorer la performance du système de communication et présentons des solutions pour atténuer les dégradations de performance. Aussi, nous étudions PD-NOMA dans des scénarios impliquant des dégradations et proposons des solutions pour atténuer la détérioration des performances.

Dans ce contexte, le troisième chapitre présente le modèle de simulation pour SCMA avec une analyse détaillée sur le taux d'erreurs binaire (BER), en présence des non-linéarités de l'amplicateur de puissance (PA). Les effets néfastes des non-linéarités sont montrés. Les techniques de traitement du signal se sont avérées être des solutions convaincantes pour atténuer la non-linéarité en général, en particulier les techniques basées sur les espaces de Hilbert à noyau reproduisant (RKHS) qui jouissent d'une légère complexité et guarantissent la représentation exacte de la fonction non linéaire. Ainsi, nous proposons une solution utilisant les caractéristiques

de Fourier aléatoires (RFF) pour atténuer les effets de la non-linéarité, ce qui permet d'améliorer le BER par rapport à l'algorithme de passage de message classique (MPA) fonctionnant dans des conditions linéaires.

Dans le quatrième chapitre, nous abordons le défi de mitigation du bruit impulsif qui sera commun dans les écosystèmes du 5G, en particulier l'IdO. La présence d'interférence électromagnétique, désignée par le bruit impulsif, dégrade les performances des applications IdO. De plus, étant donné la superposition de mots de code dans SCMA, l'effet serait plus prononcé. Par conséquent, nous étudions l'implémentation de la SCMA en présence de bruit impulsif. Nous étudions l'impact du bruit impulsif sur le BER et proposons une solution basée sur la correntropie maximale. Notre modèle transfère des gradients de potentiel d'information (IP) au lieu du logarithme du rapport de vraisemblance (LLR) normalement utilisé dans le MPA conventionnel. Les gains de performance obtenus montrent la viabilité de la solution même dans des scénarios très impulsifs.

Dans le cinquième chapitre, nous proposons une autre méthode pour atténuer l'effet de non-linéarité. Notre nouvelle méthode est basée sur la décomposition de Bussgang et présente une complexité moindre, ce qui la rend intéressante pour une implémentation dans les réseaux internet des objets industriels (IIoT). Nous calculons le coefficient de Bussgang et mettons à jour les nouveaux gains de canal avec le coefficient obtenu. De plus, une analyse montrant la convergence de la méthode proposée avec une comparaison avec la solution basée sur les RFF est fournie. Les résultats obtenus confirment que la technique d'accès multiple SCMA est une solution viable pour divers scénarios, même en présence de conditions non idéales.

Dans le sixième chapitre, nous considérons le PD-NOMA en présence des non-linéairités du PA. Nous montrons l'effet néfaste des non-linéarités des PA sur le BER des utilisateurs superposés dans PD-NOMA, en particulier pour l'utilisateur qui effectue l'annulation successive d'interférence (SIC). En utilisant le RKHS, nous proposons un algorithme de décodage basé sur les RFF pour atténuer ces imperfections matérielles et atteindre un BER qui se rapproche de celui du scénario linéaire.

Mots-clés: NOMA, SCMA, non-linéarité, bruit impulsif

Design and Performance analysis of Novel Decoding Techniques for Non-Orthogonal Multiple Access for 5G and Beyond-5G Wireless Networks

Elie Sfeir

ABSTRACT

The field of wireless communications has witnessed several evolutions which have significantly changed our lifestyle. These evolutions were driven by not only the need of increase in data rates, but also the ever-increasing stringent performance requirements of a plethora of novel technological applications. The continuous explosive growth in the number of connected devices combined with the emergence of several new applications such as Internet of Things (IoT), telemedicine, vehicular technology, smart homes, and appliances is pushing engineers and researchers, to innovate and conceive new viable multiple access technologies capable of covering the increasing demands for higher connectivity and data rates.

Non-orthogonal multiple access (NOMA), as opposed to the traditional orthogonal multiple access (OMA) techniques, allows multiple users to share the same orthogonal resource element. Thus, NOMA is a promising technology and an excellent candidate to satisfy fifth generation (5G) network needs, i.e., massive connectivity, higher spectral efficiency, and higher user rate. Research in NOMA has led to the inception of several architectures for NOMA often categorized based on the users' multiplexing, which is either in the power domain (PD-NOMA) or the code domain (CD-NOMA).

Among CD-NOMA architectures, sparse code multiple access (SCMA), which is based on codebook mapping for network users, has attracted significant attention given its ability to satisfy the massive connectivity and higher spectral efficiency requirements of next generation networks. Like every new wireless communication technology, the implementation within practical networks presents multiple inevitable teething challenges and impediments. This thesis sheds light on SCMA technology and investigates its application within various scenarios. We analyze SCMA's performance in the presence of several impairments that could severely deteriorate the communication performance and present solutions for mitigating the induced performance degradation. Also, we study PD-NOMA within scenarios involving impairments and propose solutions for mitigating performance degradation.

In this context, the third chapter presents the simulation model along with a detailed analysis of the bit error rate (BER) performance for SCMA in the presence of power-amplifier (PA) nonlinearities. The detrimental effects of PA nonlinearities are shown. Signal processing techniques have been found to be compelling solutions for mitigating device nonlinearities, especially reproducing kernel Hilbert Spaces (RKHS) based techniques that enjoy slight complexity combined with their ability to exactly represent a nonlinear function. Thereby, we propose a Random Fourier Features (RFF) based solution to mitigate nonlinearity hurdles, which achieves improved BER performance compared to the classical message passing algorithm (MPA) operating in linear conditions.

In the fourth chapter, we tackle the challenge of mitigating impulsive noise, which will be common within the 5G ecosystems, specifically for IoT applications. The presence of electromagnetic interference, known as impulsive noise, degrades the performance of IoT applications. Additionally, given the superposition of codewords in SCMA, the performance degradation is more pronounced. Therefore, we study the implementation of SCMA in the presence of impulsive noise. We study the impact of impulsive noise on the BER performance. To mitigate the induced performance degradation, we propose a Maximum-Correntropy-based solution. Our proposed model transfers information potential (IP) gradients instead of the log-likelihood ratio (LLR) used in the conventional MPA. The achieved performance gains show the viability of the solution, even within highly impulsive scenarios.

In the fifth chapter, we propose another method for alleviating the effect of nonlinearities. Our new approach is based on the Bussgang decomposition and requires a relative low complexity, making it attractive for implementation within industrial internet of things (IIoT) networks. We compute the Bussgang coefficient and update the new channel gains with the obtained coefficient. Additionally, an analysis is provided that shows the convergence of the proposed method along with a comparison with the RFF based solution. The obtained results ascertained that SCMA is a viable solution for implementation within various challenging conditions and environments.

In the sixth chapter, we consider PD-NOMA in the presence of PA nonlinearities. We show the harmful effect of PA nonlinearities on the BER performance of superposed users in PD-NOMA, especially for the users performing the successive interference cancellation (SIC). Using RKHS, we propose an RFF based decoding algorithm to mitigate these hardware imperfections and achieve a BER performance that approaches the linear scenario.

Keywords: NOMA, SCMA, nonlinearity, impulsive Noise

TABLE OF CONTENTS

Page

LIST OF TABLES

Page

LIST OF FIGURES

Page

LIST OF ALGORITHMS

Page

LIST OF ABBREVIATIONS

1G	First Generation
2G	Second Generation
3G	Third Generation
4G	Fourth Generation
5G	Fifth Generation
6G	Sixth Generation
AM-AM	Amplitude Modulation–Amplitude Modulation
AM-PM	Amplitude Modulation–Phase Modulation
AR	Augmented Reality
AWGN	Additive white Gaussian noise
B5G	Beyond Fifth Generation
BER	Bit Error Rate
BLER	Block Error Rate
BP	Belief Propagation
BPSK	Binary PSK
C-NOMA	Cooperative NOMA
CB	Codebook
CD-NOMA	Code Domain NOMA
CDM	Code Domain Multiplexing

CDMA	Code Division Multiple Access
CNN	Convolutional Neural Network
CSI	Channel State Information
CTU	Contention Transmission Unit
DNN	Deep Neural Network
DoF	Degree of Freedom
E2E	End-to-End
ECC	Error Correntropy Criterion
EEC	Error Entropy Criterion
EH	Energy Harvesting
eMBB	Enhanced Mobile Broadband
EP	Expectation Propagation
FBMC	Filter Bank-Based Multicarrier
FDMA	Frequency Division Multiple Access
FN	Function Nodes
GAN	Generative Adversial Network
GSNR	Generalized signal-to-noise ratio
HetNets	Heterogeneous Networks
HPA	High-Power Amplifiers
ICI	Inter Carrier Interference

ICSI	Imperfect Channel State Information
i.i.d.	Independent and Identically Distributed
IIoT	Industrial Internet Of Things
IM	Index Modulation
IMT	International Mobile Telecommunications
IN	Impulsive noise
IoT	Internet of Things
IP	Information Potential
IQI	In-Phase/Quadrature-Phase Imbalance
ISI	Inter Symbol Interference
ITL	Information-Theoretic Learning
JMPA	Joint Message Passing Algorithm
KKT	Karush-Kuhn-Tucker
LDS	Low-Density Spreading
LLR	Log-Likelihood Ratio
LMS	Least Mean Square
LSTM	Long Short-Term Memory
LTE	Long-Term Evolution
MAI	Multiple Access Interference
MAP	Maximum a Posteriori

MCC	Maximum Correntropy Criterion
MEE	Minimum Error Entropy
MIMO	Multiple-Input Multiple-Output
MIP	Mutual Incoherence Property
mmWave	Millimetre Wave
mMTC	massive Machine-Type Communications
MPA	Message Passing Algorithm
MSE	Mean Squared Error
MU-m-MIMO	multi user massive multiple input multiple output
MUD	Multi User Detection
NOMA	Non-Orthogonal Multiple Access
OFDM	Orthogonal Frequency Division Multiplexing
OFDMA	Orthogonal Frequency Division Multiple Access
OMA	Orthogonal Multiple Access
OMP	Orthogonal Matching Pursuit
PA	Power amplifier
PDF	Probability density function
PDM	Power Domain Multiplexing
PDMA	Pattern Division Multiple Access
PD-NOMA	Power Domain NOMA

PER	Packet Error Rate
PN	Pseudo-random Noise
QAM	Quadrature Amplitude Modulation
QIP	Quadratic Information Potential
QoS	Quality of Service
QPSK	Quadrature PSK
RB	Resource Block
RD	Random Direction
RE	Resource Element
RIS	Reconfigurable Intelligent Surface
RFF	Random Fourier Features
RFO	Residual Frequency Offset
RL	Reinforcement Learning
RKHS	Reproducing Kernel Hilbert space
RSMA	rate splitting multiple access
RWMM	Random Waypoint Mobility Model
RWP	Random Waypoint
SCMA	Sparse Code Multiple Access
SDMA	Space-Division Multiple Access
SIC	Successive Interference Cancellation

SNR	Signal-to-Noise-Ratio
TDMA	Time Division Multiple Access
UAV	Unmanned Aerial Vehicle
UDN	Ultra-Dense Network
UE	User Equipment
URLLC	Ultra-Reliable Low Latency Communication
UVLC	Underwater Visible Light Communication
VLC	Visible Light Communication
VN	Variable Nodes
VR	Virtual Reality

LIST OF SYMBOLS AND UNITS OF MEASUREMENTS

x	Scalar
$\|x\|$	Absolute value
$\mathbf{x}$	Vector
$\mathbf{x}^T$	Transpose
$\mathbf{X}$	Matrix
$\mathbf{X}^\dagger$	Pseudo-inverse
$\mathcal{S}$	Set
$\|\mathcal{X}\|$	Cardinality of a set
$\mathbb{R}$	Set of real numbers
$\mathbb{C}$	Set of complex numbers
$\mathcal{N}(\cdot,\cdot)$	Normal distribution
$U(\cdot,\cdot)$	Uniform distribution
$\mathbb{E}(\cdot)$	Expectation operator
$\mathbb{P}(\cdot)$	Probability function
$\exp(\cdot)$	Exponential function
$\log_2(\cdot)$	Base-2 logarithm
$\angle(\cdot)$	Angle
$< \cdot, \cdot >$	Inner product
$\mathcal{H}$	Hilbert Space

real (·)	Real part of a complex number
imag (·)	Imaginary part of a complex number
diag(·)	Diagonal matrix
$\mathbf{y}_{tr}$	the received signal during the training phase

INTRODUCTION

0.1 Motivation

The recent advancements in telecommunications have shaped our lives and impacted our generations. This would not have been achieved without the tremendous and continuous improvement in the wireless network technologies over the course of the different generations of wireless communication systems. Wireless communication systems have witnessed several evolutions where each generation, characterized by its distinct architecture, was conceived to satisfy the demands for increased data rates, faster and more reliable communication. The first generation systems (1G) of wireless networks was analog and based on frequency division multiple access (FDMA), where the bandwidth is divided into channels, and each channel can be assigned to only one user at a time. In the second generation (2G), instead of dividing the frequency, a division over time was proposed, namely, time division multiple access (TDMA). In this context, the different users are allocated different time slots for transmitting information on the same frequency. Thus, the users transmit, one after the other, each during their assigned time slot. The third generation (3G) was based on code division multiple access (CDMA). CDMA is a wideband communication technology that does not use time or frequency as a resource but codes instead. Here, each user is assigned a specific spreading code used to multiply his information sequence. Precisely, the low bandwidth data message (voice or data) is multiplied by a large pseudo-random noise (PN) sequence. Thus, users in CDMA can use the same frequency simultaneously but with different codes. Besides, the information sequence can be retrieved at the receiver by multiplying the received message by the same code used at the transmitter. Moreover, the fourth generation (4G) of wireless communications, also known as long-term evolution (LTE), was based on orthogonal frequency division multiplexing (OFDM). OFDM is another wideband communication technology which, unlike CDMA, consists of a multi-carrier modulation technique. The bandwidth B, instead of having one single carrier, is

divided into N subcarriers that are separated by B/N. On each of these subcarriers, a different stream of data is sent. As a result, the N subcarriers carry N streams; thus, higher data rates can be achieved. Moreover, the orthogonality reduces the intercarrier interference (ICI), while a cyclic prefix is added to mitigate intersymbol interference (ISI). Finally, with the emergence and vivid tremendous expansion of new applications, such as the Internet of Things (IoT), vehicular technologies, eHealth applications, augmented reality (AR), virtual reality (VR), and the ever-increasing number of requested connections, the fifth generation (5G) is satisfying higher data rates, massive connectivity, higher spectral efficiency, lower latency, and higher reliability Dangi, Lalwani, Choudhary, You & Pau (2021).

The stringent requirements of 5G specifications are diverse. They cover several aspects of wireless communications, including a peak data rate of 20 Gbit/s, connection density of one million devices per square kilometer, and spectrum efficiency of three times the one of international mobile telecommunications-Advanced (IMT-advanced). The complete diagram of 5G planned services is shown in Fig. 0.1.

Therefore these requirements lead us to define 5G use cases tailored for specific applications. These use cases are shown in Fig. 0.2 and summarized as follows:

- Enhanced mobile broadband (eMBB), which encompasses the applications needing higher throughput and spectral efficiency, such as 3D videos and video calling applications.
- Massive machine-type communications (mMTC), which supports an extremely high connection density of low consumption devices, such as smart metering, sensors, and IoT devices.
- Ultra-reliable low latency communication (URLLC), which covers mission-critical applications where errors or delays are not tolerated, such as telemedicine surgery, autonomous cars, and industrial automation.

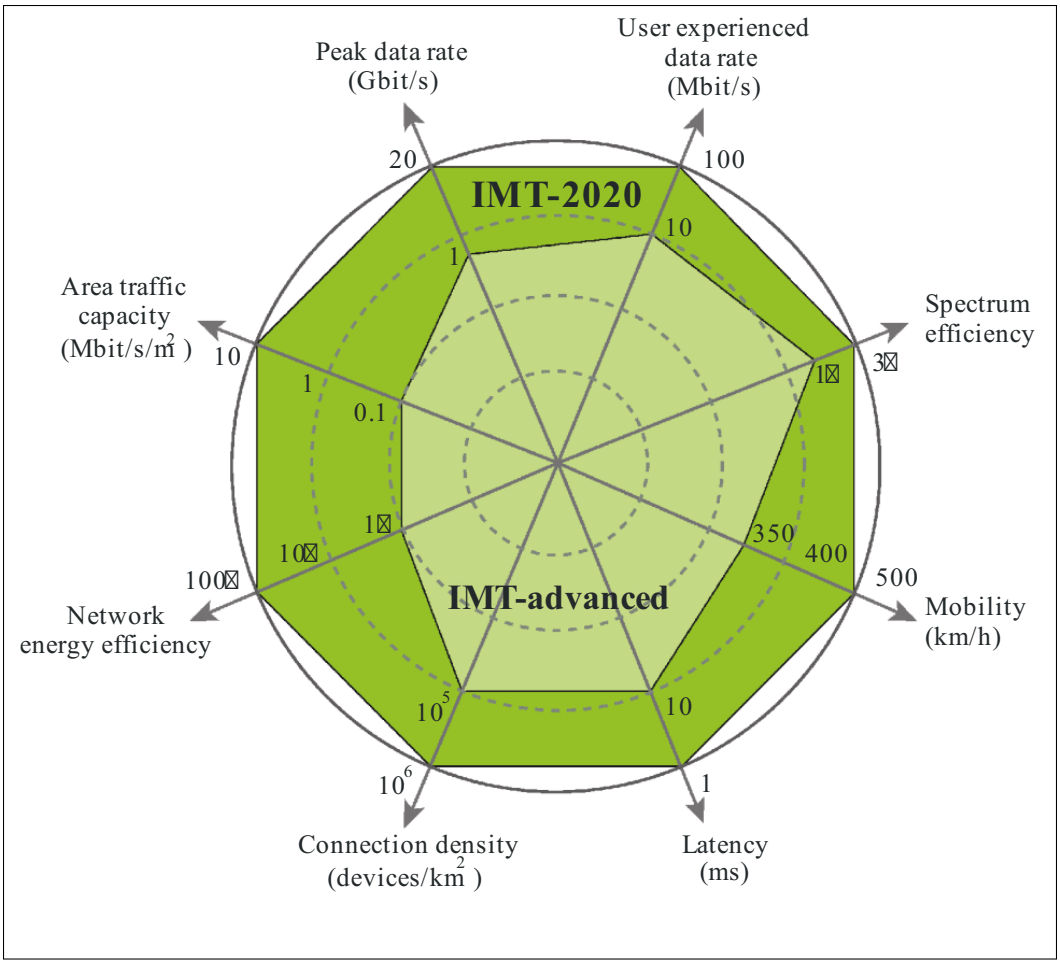

Figure 0.1 5G envisioned services specifications Series (2015)

That being said, much effort in research and industry all over the world is being put into introducing new ideas, conceiving new architectures, and establishing new technologies that will make these aspirations a reality by giving birth to a new evolved wireless mobile generation. In this vein, many technologies have been proposed as strong candidates for the 5G standard, including

- Massive multiple-input multiple-output systems (MIMO).
- Millimeter-wave (mmWave) communications.
- Heterogeneous networks (HetNets).
- Ultra-dense networks (UDNs).

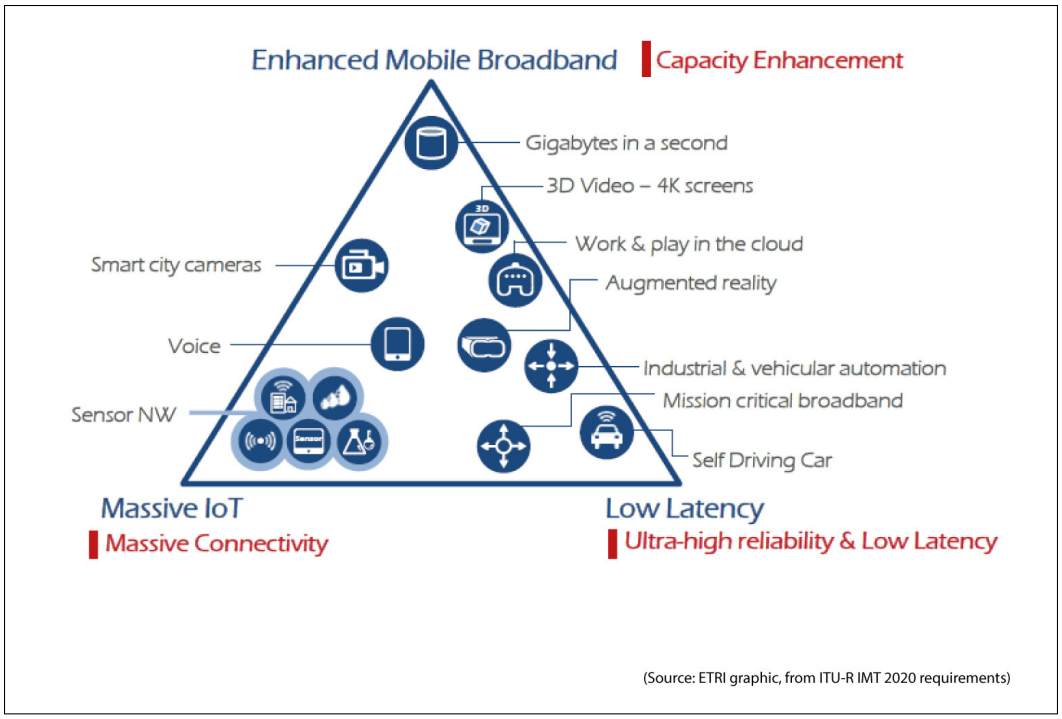

Figure 0.2 5G use cases Mallinson (2016)

- Non-orthogonal multiple access (NOMA).

Implementing these new technologies necessitates the development of new mathematical models to represent the system model and study its performance. On the other hand, the QoS requirements are no longer limited to satisfying a specific support level of data rates but to other more complex needs, such as service coverage over high mobility scenarios, high reliability, and massive connectivity.

0.2 Problem Statement

As the world's population is rapidly growing and becoming increasingly urbanized, improving our cities through enabling connectivity and automation of the different resources and operations is a critical global necessity. In this context, massive machine-type communication is defined as an enabler for wireless connectivity for a large number of low-complexity, low-power machine-type

devices Bockelmann, Pratas, Nikopour, Au, Svensson, Stefanovic, Popovski & Dekorsy (2016). Specifically, mMTC includes a wide range of nonconventional UEs, such as smart devices, IoT devices, energy meters, sensors for air and water quality monitoring, electronic billboards, charging stations for electric vehicles, as shown in Figure 0.3. Consequently, 5G is expected to provide a high connection density of about one million devices per square kilometer, which is ten times the current LTE connection density, which is about a hundred thousand devices per square kilometer. These devices will sporadically send and receive short packets of data. This high activity will increase the demands for more stringent requirements, including more bandwidth, higher data rates, and more connections. Revisiting the previous generations, they have all been based on orthogonal multiple access (OMA) techniques, where users are allocated orthogonal resources in time, frequency, or code to avoid multiple access interference (MAI) as much as possible. However, in OMA models, we are always bounded by the number of resources due to the orthogonality constraint, which limits their scalability and ability to satisfy the above-mentioned requirements. Therefore new convenient architectures tailored to fulfill the afore-mentioned requirements are sought. In this context, NOMA was introduced as a compelling architecture for enabling massive connectivity, higher spectral efficiency, higher cell-edge throughput, and data rates. Meanwhile, NOMA architectures are divided into two main categories: power domain NOMA (PD-NOMA) and code domain NOMA (CD-NOMA). The basic idea behind NOMA is to allow more than one user to send data on the same orthogonal resource, leading to a higher connection density and spectral efficiency, making it a potential candidate for 5G Dai *et al.* (2015). However, several performance degradations are expected to arise when it comes to realistic implementations. Therefore it is essential to study the impact of these impairments and propose suitable mitigation techniques. Particularly the growing density of connected devices combined with the sporadic nature of their activity give rise to electromagnetic interference, commonly known as impulsive noise that could jeopardize the performance of communication devices. Additionally, imperfections in hardware, such as

nonlinear hardware, are very likely, which could also threaten the system's performance if not mitigated. Meanwhile, as previously stated, most newly connected devices are nonconventional and of low complexity and hence might not be able to handle complex algorithms; therefore, seeking low complexity mitigation algorithms is crucial.

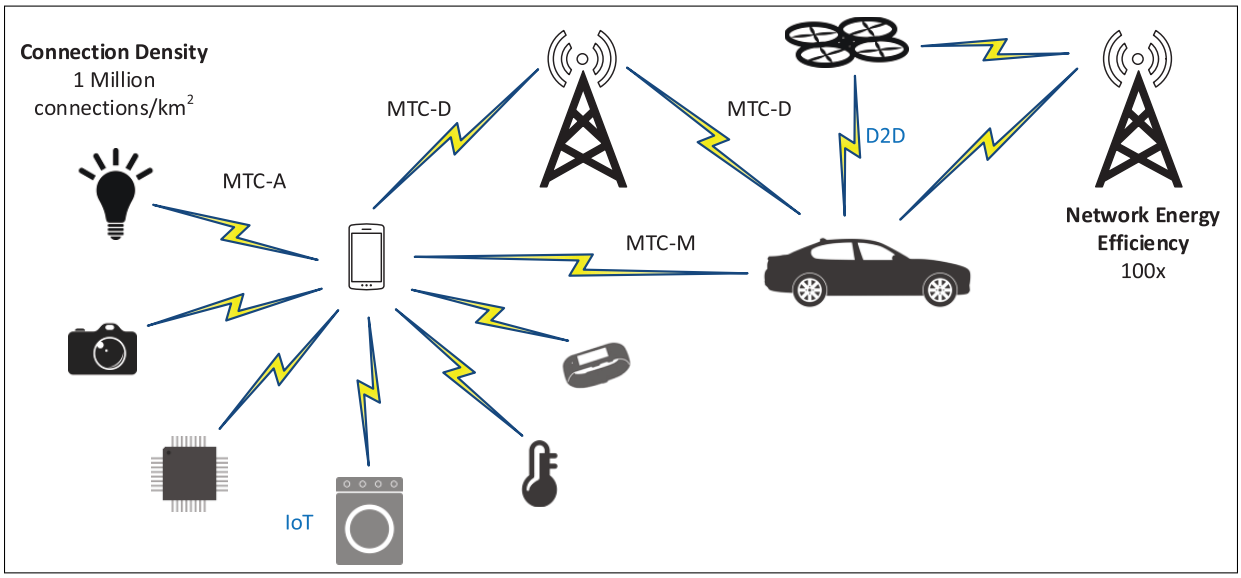

Figure 0.3 Various mMTC devices Morocho-Cayamcela *et al.* (2019)

0.3 Research Objectives

In this thesis, we focus on the mMTC use case, particularly achieving massive connectivity, by considering NOMA. In this regards, the practical implementation of NOMA presents multiple challenges, such as power amplifier (PA) nonlinearities, impulsive noise, and some devices' limited computational complexity. That being said, our research objectives are as follows:

- Non-ideal hardware, specifically PA nonlinearity, is a frequent defect in electronics; consequently, we will study the impact of PA nonlinearities on a CD-NOMA technique, sparse code multiple access (SCMA). We aim to propose a suitable mitigation technique for PA nonlinearities using the theory of reproducing kernel Hilbert space (RKHS), which proved to enable immune solutions to such flaws in various applications, such as ultraviolet communica-

tions Bhatia, Jain, Garg & Mitra (2021), visible light communications Mitra, Miramirkhani, Bhatia & Uysal (2018), Jain (2022), Miramirkhani, Karbalayghareh, Zeydan & Mitra (2022), Mitra, Miramirkhani, Bhatia & Uysal (2020b), fiber communication systems Jain, Agrawal, Bhatia & Prakash (2019a). This approach will be considered for both SCMA and PD-NOMA.

- Many of the new proposed technologies for mMTC, such as the industrial internet of things (IIoT), give rise to electromagnetic interference, commonly known as impulsive noise. Hence we aim to study the impact of impulsive noise on the bit error rate (BER) performance of SCMA and propose a suitable mitigation technique.
- Among the newly deployed devices are low-power devices with limited computational capability, where algorithms with little complexity are requested. Hence we seek to explore less complex algorithms for message decoding at the receiver and utilize our previously developed algorithms to benchmark their BER performance.

0.4 Contributions and Outline

NOMA is a potential candidate for enabling mMTC. NOMA architectures are divided into two main categories: PD-NOMA and CD-NOMA. SCMA, a CD-NOMA technique for achieving higher connection densities, higher cell-edge throughput, and spectral efficiency, is a potential candidate for next generation wireless communications. On the other hand, PD-NOMA is particularly appealing as it improves user fairness while enhancing spectral efficiency and benefits from a simplistic successive interference cancellation (SIC) decoding at the receiver. Hence, throughout our research, we envision implementing NOMA, precisely SCMA and PD-NOMA, within multiple challenging scenarios and show the viability of our proposed algorithms.

In the first chapter, we present machine learning and information theory tools that were utilized for developing our algorithms. We present the corresponding theoretical proofs and theorems along with the motivation.

In the second chapter, we undertake a comprehensive literature review on NOMA, where we expose its different categories and depict the corresponding system models. We also consider some exciting applications from the literature highlighting the potential of NOMA and its new system developments.

Chapter 3 presents the first article where we study a frequent impairment in hardware, which is PA nonlinearity, and investigate its impact on the performance of SCMA. We show its deleterious effect and propose a RFF-based solution to mitigate it. We simulate the BER of our proposed method with respect to SNR, under different types and orders of severity of PA nonlinear models as well as for several SCMA codebooks. Our simulation results show a notable improvement in the BER performance with the proposed approach, almost reaching the ideal linear scenario. Additionally, we prove the optimality of our results using functional analysis and RKHS theorems and show that RFF improves the convergence of the MPA in the presence of nonlinearities.

Chapter 4 presents the second journal where we study another frequent impairment in wireless communications that impedes ideal wireless systems' performance, which is impulsive noise. We consider Gaussian-mixture based impulsive noise in downlink SCMA systems. We simulate the BER performance for different scenarios of impulsive noise severity and show the deleterious effect caused by impulsive noise. To mitigate this problem, we use information theoretic learning and propose a maximum-correntropy based receiver. Our novel proposed receiver consists in propagating information potential gradients instead of log-likelihood probabilities due to its particular immunity to impulsive noise. We simulate the proposed receiver under different impulsive noise scenarios. Our results show improved BER performance and are backed by analytical proofs using theorems from information theoretic learning.

Chapter 5 presents our third work, where we propose a nonlinearity mitigation technique for computationally lightweight devices. We use Bussgang's decomposition to propose a low-complexity detector, which is suitable for hardware-limited IIoT devices, where satisfying a low

computational cost outweighs the importance of a maximum BER performance. We simulate our new proposed Bussgang-based MPA detector in different channel conditions and benchmark its BER performance with our RFF-based receiver. We also provide analytical proofs for the error floor and the error complexity. The assessment of computational complexity and error floor validates the importance of switching between the different methods for hardware-limited IIoT systems, where reaching a particular degree of QoS at minimal computational cost is more important than obtaining a globally ideal BER performance.

Chapter 6 presents our fourth and last work, where we consider PD-NOMA in the presence of PA nonlinearities. We show the damage caused by the PA nonlinearities on the BER performance of the superposed users, especially for the SIC user who has to decode the other user's information before his own. We propose an RFF-based decoding algorithm for mitigating this impairment. We simulate our proposed algorithm under different PA nonlinearities, such as AM-AM and AM-PM, and under different severity levels. Our proposed algorithm shows notable improvement in the BER performance of the users, especially for the SIC user whose performance approaches that of the ideal linear scenario. Additionally, we present an analytical validation for the obtained simulation results using the theorems of functional analysis.

Author's Publications

The author's Ph.D. resulted in research articles, which are listed below. The journal publications are denoted by "J".

- J1: **E. Sfeir**, R. Mitra, G. Kaddoum, and V. Bhatia, "RFF Based Detection for SCMA in Presence of PA Nonlinearity", in IEEE Communication Letters, July 2020. DOI: https://doi.org/10.1109/LCOMM.2020.3010698

- J2: **E. Sfeir**, R. Mitra, G. Kaddoum, and V. Bhatia, "Performance Analysis of Maximum-Correntropy based detection for SCMA", in IEEE Communication Letters, December 2020. DOI: https://doi.org/10.1109/LCOMM.2020.3010698

- J3: **E. Sfeir**, R. Mitra, G. Kaddoum, and V. Bhatia, "Comparative Analytical Study of SCMA Detection Methods for PA Nonlinearity Mitigation", in MDPI Sensors, December 2021. DOI: https://doi.org/10.3390/s21248408

- J4: **E. Sfeir**, R. Mitra, and G. Kaddoum, "A Random Fourier Feature Based Receiver Detection for Enhanced BER Performance in Nonlinear PD-NOMA", in IEEE Transactions on Vehicular Technology, October 2022, doi: 10.1109/TVT.2022.3213811.

CHAPTER 1

OVERVIEW OF MACHINE LEARNING AND INFORMATION THEORY TOOLS UTILIZED IN WIRELESS COMMUNICATIONS

Wireless communication systems are continuously evolving into more heterogeneous and complex networks with increasingly tight conditions and challenging operating environments. Thanks to advances in computer hardware and the availability of an enormous amount of data, machine learning solutions for various applications in wireless systems have gained increasing traction. On the other hand, since its inception, information theory has been a powerful tool for studying the performance limits of wireless systems and for adaptive filtering scenarios. Hence, in our work, we envision utilizing tools from machine learning and information theory to build our algorithms. That being said, we will, in the coming sections, depict more details on the characteristics of these tools, which will be used later in our work.

1.1 Machine Learning in Wireless Communication

Future communications are envisioned to embrace a more dense and highly diversified network, leading to increased interference and more frequent impairments caused by nonlinear hardware. On the other hand, in order to meet the challenge of achieving massive connectivity and 10-100 times higher data rates compared to present generation rates, new tools are emerging. Machine learning and deep learning tools have been actively exploited in wireless communication problems due to their ability to address the arising challenges of enabling higher rates and massive connectivity within the different scenarios of the evolving wireless domain. In this context, we will present, in what follows, some of the interesting recent machine learning tools utilized in wireless communications, while focusing more on the tools we envision utilizing within our research work.

1.1.1 Neural networks and Deep Learning

Neural networks have been employed in several works. A deep neural network decoding based approach was proposed for SCMA by Lin, Feng, Zhang, Yang & Zhang (2020) to achieve better BER performance than the conventional decoder. Another approach for blind decoding in SCMA used convolutional neural networks (CNN) to reduce the computational complexity while achieving better BER performance than the conventional decoder Abidi, Hizem, Ahriz, Cherif & Bouallegue (2019). In Gui, Huang, Song & Sari (2018), a long short-term memory (LSTM)-aided NOMA system is proposed to learn the environment and estimate channel states.

1.1.2 Reproducing Kernel Hilbert Spaces

The theory of reproducing kernel Hilbert space (RKHS) dates back to the 1950's paper Aronszajn (1950). RKHS is defined as a complete inner product space. In Fig. 1.1, we show its algebraic structure diagram. Moreover, RKHS based solutions were shown to be exceptionally powerful and have received increasing attention in various applications, such as ultraviolet communications Bhatia *et al.* (2021), visible light communications Mitra *et al.* (2018), Jain (2022), Miramirkhani *et al.* (2022), Mitra *et al.* (2020b), and fiber communication systems Jain *et al.* (2019a). The motivation behind the use of RKHS is the result of the Riesz Representer's theorem that guarantees the existence of a unique representation in RKHS for a large category of nonlinear functions Schölkopf, Herbrich & Smola (2001), Príncipe, Liu & Haykin (2011), Theodoridis (2015). Consequently, any nonlinear function has a representation as follows

$$f(\cdot) = \sum_{\forall j} \beta_j \kappa(\mathbf{x}_j, \cdot), \tag{1.1}$$

where $\beta_j \in \mathcal{R}$. The use of RKHS is additionally motivated by the "kernel trick" through which the kernel applied to the vectors in the original low-dimensional space returns the dot product of the mapped vectors in the high-dimensional feature space. More formally, considering two

vectors $\mathbf{x}, \mathbf{z} \in X$ and a map ϕ from the original input space X to the RKHS $\mathcal{H}$, defined as

$$\phi : X \rightarrow \mathcal{H} \tag{1.2}$$

then the function obtained by computing the inner product of the obtained points in the RKHS,

$$k(\mathbf{x}, \mathbf{z}) = \langle \phi(\mathbf{x}), \phi(\mathbf{z}) \rangle, \tag{1.3}$$

is a kernel function Daumé III (2004). Hence no need for the explicit mapping to an RKHS space since the kernel is ensuring the implicit map. Here we would like to note that the kernel can be expressed in matrix form whose entries are obtained from the available data samples $\mathbf{x_1}, \mathbf{x_2}, \ldots, \mathbf{x_n}$, expressed as

$$K_{ij} = \langle \phi(\mathbf{x}_i), \phi(\mathbf{x}_j) \rangle. \tag{1.4}$$

This matrix is known as the Gram Matrix. RKHS based methods have various benefits discussed in Bhatia *et al.* (2021), including finding globally optimal solutions. In figure 1.2, we represent an original input space X and $\mathcal{H}$, the corresponding RKHS space, which is obtained by applying the mapping function ϕ on the original space.

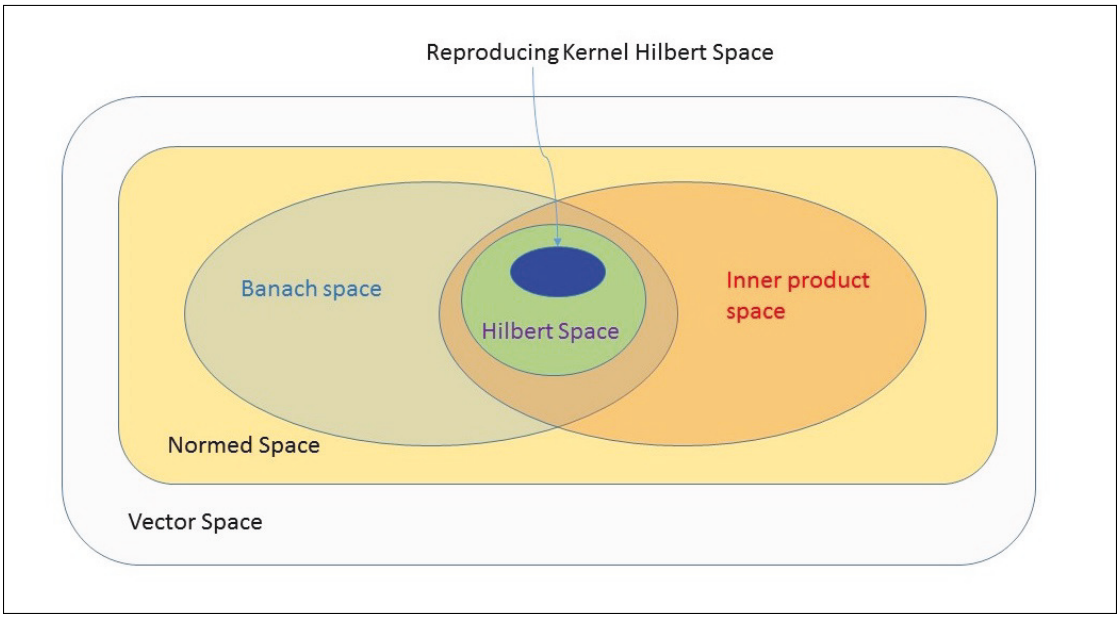

Figure 1.1 RKHS algebraic structure diagram

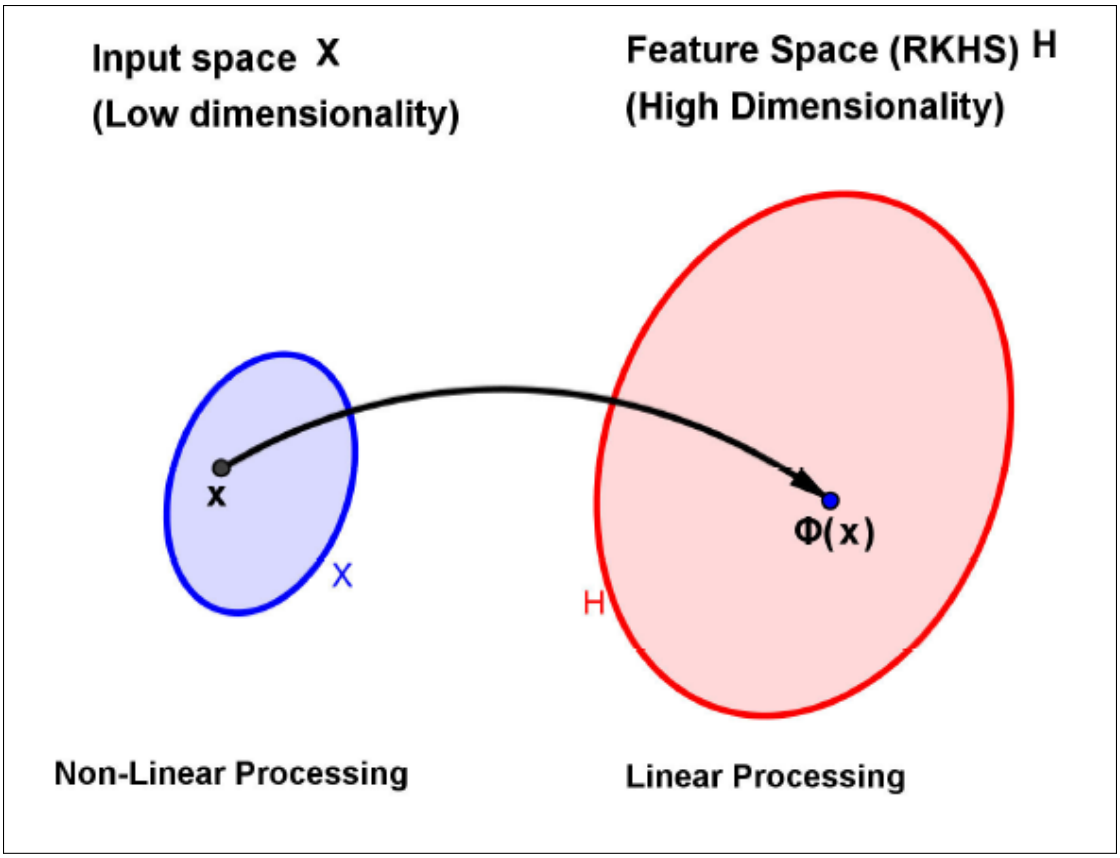

Figure 1.2 Mapping from input space X to feature space $\mathcal{H}$
Slavakis *et al.* (2014)

However, for large datasets, mapping to a higher dimensional space, leads to complex computations, causing slowness in the processing. In this context, another better alternative, which was presented in Rahimi, Recht et al. (2007), consists into explicitly mapping to a randomized low-dimensional feature space instead of maping to a higher dimensional space. RFFs allow us to do this by enabling explicit mapping to the feature space, which is the desired RKHS space.

RFF have been used in several applications, such as VLC Mitra, Bhatia, Jain & Choi (2021), Jain, Mitra & Bhatia (2021), Mitra, Jain & Bhatia (2020a), and massive MIMO Anand, Jain, Mitra & Bhatia (2021), Chhangani, Mitra & Bhatia (2020).

The randomized feature mapping function, the basis for an RFF, is defined as Anand *et al.* (2021), Bouboulis, Pougkakiotis & Theodoridis (2016), Mitra *et al.* (2020a)

$$\Psi : \mathbb{R}^d \rightarrow \mathbb{R}^D, \tag{1.5}$$

where $D < d$. The expanded expression of Ψ is formulated as

$$\Psi(\boldsymbol{\gamma}) = \sqrt{\frac{2}{D}} \begin{bmatrix} \cos\left(\boldsymbol{\omega}_1^T \boldsymbol{\gamma} + \eta_1\right) \\ \cos\left(\boldsymbol{\omega}_2^T \boldsymbol{\gamma} + \eta_2\right) \\ \vdots \\ \cos\left(\boldsymbol{\omega}_D^T \boldsymbol{\gamma} + \eta_D\right) \end{bmatrix}, \tag{1.6}$$

where each $\{\boldsymbol{\omega}_i\}_{i=1}^D$ is generated from the Gaussian filter kernel Fourier transform, expressed as Anand *et al.* (2021), Bouboulis *et al.* (2016)

$$K_{\mathbf{G}}(\omega) = \left(\frac{\sigma}{2\pi}\right)^D e^{(-0.5\sigma^2\|\omega\|^2)}, \tag{1.7}$$

which is equivalent to the normal distribution $\mathcal{N}\left(\mathbf{0}_D, \frac{1}{\sigma^2}\mathbf{I}_D\right)$, with $\mathbf{I}_D$, σ, and D representing the identity matrix of dimension D, the kernel-width hyperparameter, and the number of RFFs, respectively. Moreover, $(\cdot)^T$ denotes the transpose operator, each $\{\eta_i\}_{i=1}^D$ is drawn from a uniform distribution on the interval $[0, 2\pi]$ Bouboulis *et al.* (2016), Anand *et al.* (2021), and $\boldsymbol{\gamma} \in \mathbb{C}$ represents an independent random variable.

We would also like to note that another related technique is kernel density estimation, which is a non-parametric tool that estimates the function through data points. However, it suffers from being prohibitively expensive because the number of computations increases with the number of data points.

Using the kernel density estimation (KDE), expressed in (6.24), each evaluation point requires $O(N * d)$ kernel evaluations and $O(N * d)$ multiplications and additions Raykar, Duraiswami & Zhao (2010b).

$$f(\mathbf{x}) = \frac{1}{nh} \sum_{i=1}^{N} K\left(\frac{\mathbf{x} - \mathbf{x_i}}{h}\right) \tag{1.8}$$

Additionally, we would like to note that the RFF requires deriving the hyperplane $\mathbf{W}$ before mapping the original space to the new RKHS space of dimension D. Thus, the complexity is limited to $O(D + d)$ for each evaluation point Rahimi *et al.* (2007). This shows the decrease in computational complexity when using RFF instead of the generic kernel density estimation.

1.1.3 Reinforcement learning

Reinforcement learning (RL) uses experience to update the policies of an agent, i.e., it learns by trial and error. Reinforcement learning has been applied in many sequential decision making tasks, such as robotics and natural language processing, where the agents need to optimize their actions based on feedback from sensors or other external sources. The recent success of reinforcement learning in many sequential decision making tasks has led to its application in wireless communication as in Chen, González, Wang & Chen (2021).

1.2 Information theoretic learning

In adaptive filtering theory and applications, choosing the appropriate cost function (typically a statistical measure of the error signals) is of great importance for the successful learning of the weight parameters of the adaptive learning system, as shown in Fig. 1.3. The most common cost function is the mean squared error (MSE) due to its appealing properties including convexity and mathematical tractability Sayed (2011), Haykin (2008). This criterion is utilized in the least mean square (LMS) optimization algorithm, which showed robust results in scenarios where signals are Gaussian distributed. However, in non-Gaussian scenarios, criteria that consider higher order statistics are required. In this context, the information theoretic learning (ITL) framework, which is based on information theoretic quantities, like entropy and mutual information, is particularly attractive in the context of adaptive filtering in scenarios involving signal outliers or non-Gaussian noise. In Fig. 1.4, we show the relation between the basic

information theoretical descriptors: joint information, marginal entropy, conditional entropy, and mutual information. ITL, through its performance metrics, enables extracting more information than the second order statistics based methods, from the same available data. The main goal is to use descriptors from information theory as non-parametric cost functions when designing adaptive systems in supervised or unsupervised learning modes. More generally, the aim is to consider scalar descriptors of the probability density function (PDF), like entropy, for learning and parameters' adaptation.

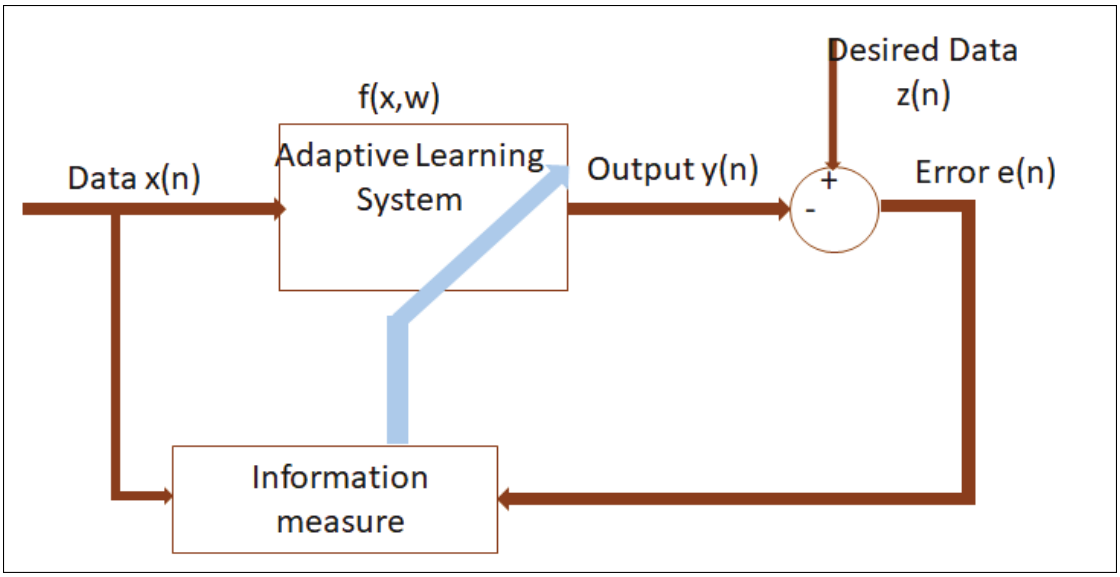

Figure 1.3 Adaptive learning scheme

1.2.1 Descriptors of information theory

As previously mentioned, ITL tools, in contrast to second order statistics based descriptors, do not restrain to the central moments of the data, such as mean and covariance. Indeed, ITL based descriptors, are based on the PDF of the random variable, which is known, to contain the data's whole statistical structure information. That being said, ITL based descriptors, enable extracting more information than second order statistics descriptors.

ITL descriptors are based on the α-norm with $\alpha = 2$, which is called the information potential (IP) Principe (2010), given as

$$E_X[p(x)] = \int p(x)p(x)dx, \tag{1.9}$$

which is also referred to as quadratic information potential (QIP) in Chen, Zhu, Hu & Principe (2013). This IP can also be viewed as the argument of the logarithm of the Renyi's entropy, where Renyi's entropy is expressed as

$$H_\alpha(X) = \frac{1}{1-\alpha} \log \int p^\alpha(x)dx. \tag{1.10}$$

For $\alpha = 2$, the logarithm can be dropped because it is a monotonic function, and the optimal parameters would not be affected. Hence, we obtain the expression of the IP given in (1.9).

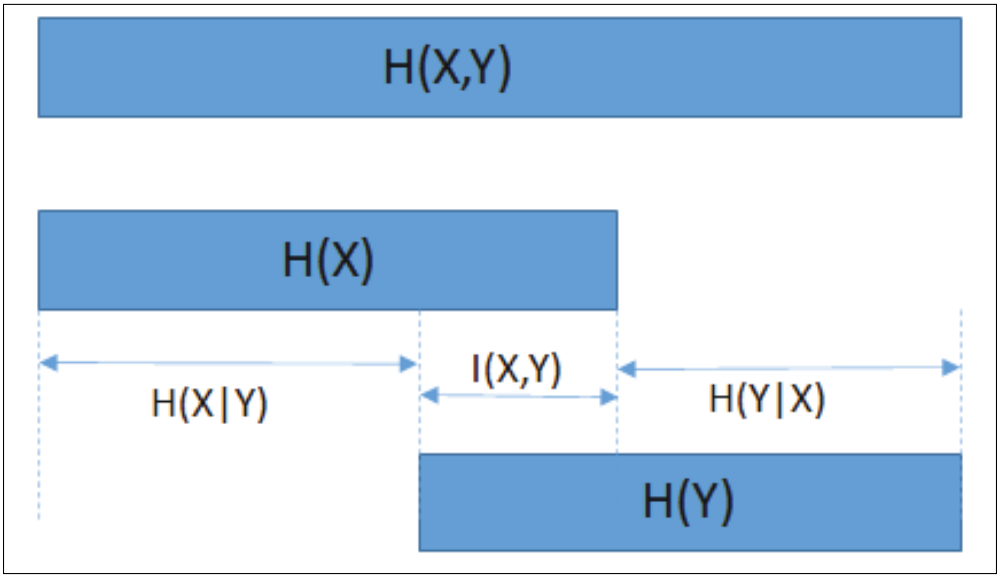

Figure 1.4 The relationship between joint information, marginal entropy, conditional entropy, and mutual information

1.2.2 Error entropy criterion and minimum error entropy

LMS is a gradient-descent algorithm with the MSE as the cost function. Here we will substitute the MSE with an information theoretical criterion that is error entropy. Since MSE considers only the second-order moment of the error distribution, which is optimal just in the case of Gaussian distributed errors, it makes sense to utilize alternative cost functions for adaptive filtering in the case of non-Gaussian error distributions. Error entropy criterion (EEC) is an information theoretical criterion. As its name indicates, the EEC is obtained by computing the entropy of the error e. The error entropy criterion gives rise to the minimum error entropy (MEE) algorithm, which learns to reduce the error signal's uncertainty as much as possible. Hence, we calculate the entropy of the error and minimize it with respect to the free parameters as follows

$$\min_{w} H[e] \quad s.t. e = z - f(x, w) \quad \& \quad E[e] = 0 \tag{1.11}$$

Renyi's entropy being defined as

$$H_2(e) = -\log V(e) \tag{1.12}$$

and the information potential (IP) as

$$V(e) = E[p(e)] \tag{1.13}$$

Hence minimizing the error entropy $H_2(e)$ is identical to maximizing the information potential $V(e)$. Thus the optimal results of error entropy minimization can be found by studying the information potential

$$\frac{\partial H_2(e)}{\partial \mathbf{w}} \rightarrow \frac{\partial V(e)}{\partial \mathbf{w}} = 0. \tag{1.14}$$

1.2.3 Kullback–Leibler divergence and mutual information

In this section, we shed light on another information theoretical criterion that could be utilized as a cost function for adaptive filtering, which is divergence. The divergence between two PDFs is defined as the dissimilarity between these two distributions and is expressed as

$$D_{KL}\left(p \parallel q\right) = \sum_{x} p\left(x\right) \log \frac{p(x)}{q(x)} = E_p \left[\log \frac{p\left(X\right)}{q(X)}\right]. \tag{1.15}$$

The mutual information can be seen as a particular case of the divergence, where $p(x)$ is substituted by $p(x, y)$, and $q(x)$ is replaced by the product of the marginal distributions, $p(x) * q(y)$. Hence the mutual information is expressed as

$$I(X, Y) = D_{KL}\left(p\left(X, Y\right) || p(X)q(Y)\right) \tag{1.16}$$

1.2.4 Correntropy

Among the different performance metrics of ITL, cross-entropy or simply correntropy is closely related to Renyi's quadratic entropy Chen *et al.* (2013) and is defined as a measure of similarity between two random variables induced by a kernel measure Liu, Pokharel & Principe (2006), Panda & Nanda (2021). Hence its mathematical expression is given as

$$v(X, Y) = E[< \Phi(X), \Phi(Y) >] = E[k_\sigma(X - Y)] = \int \int k_\sigma(x - y) p_{X,Y}\left(x, y\right) dxdy, \tag{1.17}$$

where Φ represents the nonlinear transformation to the feature space generated by the kernel mapping and k_σ is the Gaussian kernel of bandwidth σ that is obtained by using silverman's rule. From (1.17), we see that for $k_\sigma(x - y) = xy$, we have the exact expression of the correlation between two random variables. Hence, the correntropy can be seen as a generalization of the correlation concept. Since, in practical scenarios, the PDF is not available, we use the finite

number of available samples $\{(x_i, y_i)\}_{i=1}^{N}$ to estimate the correntropy, formulated as

$$\widehat{v}(\mathrm{X}, \mathrm{Y}) = \frac{1}{N}\sum_{i=1}^{N} k_\sigma(x_i - y_i) = \frac{1}{N}\sum_{i=1}^{N} k_\sigma(e_i) \tag{1.18}$$

The properties of the correntropy were highlighted in Liu, Pokharel & Principe (2007), where the positivity of the correntropy and the fact that it reaches its peak only if $X = Y$ are important to note. Moreover, the correntropy considers all the even moments of the error random variable $E = X - Y$. The motivation behind using correntropy lies in the fact that it is simpler to derive than the EEC Principe (2010).

1.2.5 Maximum correntropy criterion

Using the error correntropy criterion (ECC) cost function yields the maximum correntropy criterion (MCC) algorithm, which maximizes the correntropy, i.e., $\max_{\theta} \widehat{v}(E)$, where E is the random variable accounting for the difference between the two random variables X and Y, i.e., $E = X - Y$, θ is the MCC's hyperparameter, and $\hat{v}$ is the estimated correntropy. The PDF of the error E is expressed as

$$\hat{p}_E(e) = \frac{1}{N}\sum_{i=1}^{N} G_\sigma(e - e_i), \tag{1.19}$$

where G_σ is the Parzen window function and N is the number of used sample points. For $e = 0$, comparing with Eq. (1.18), we get

$$\hat{v}(E) = \hat{v}(X, Y) = \hat{p}_E(0) \tag{1.20}$$

Hence, according to Eq. (1.20), maximizing the correntropy, which is the aim of MCC, leads to maximizing the error's PDF at zero, which is increasing the similarity between the random variables by reducing the difference's error.

Due to the aforementioned characteristics, the MCC algorithm has shown robustness in several

non-Gaussian noise scenarios Principe (2010), Liu *et al.* (2007). Additionally, the correntropy-induced loss (C-loss) has drawn attention and utility in fighting non-Gaussian noise defects Chen & Wang (2018). Several correntropy based methods were derived, such as kernel maximum correntropy (KMC) Zhao, Chen & Principe (2011), correntropy kernel learning (CKL) Liu & Chen (2013), and the kernel recursive maximum correntropy (KRMC) Wu, Shi, Zhang, Ma, Chen & Senior Member (2015b).

1.3 Conclusion

We presented in this chapter an overview of several tools from machine learning and information theory, and showed some of their applications in the wireless communications. We will utilize some of these tools in the algorithms we develop in order to fulfill our objectives. We focus on RKHS from machine learning for linearization in scenarios involving hardware nonlinearities and we will utilize correntropy from information theory for impulsive noise mitigation.

CHAPTER 2

LITERATURE REVIEW

In this chapter, we undertake a comprehensive literature review on non-orthogonal multiple access (NOMA), including both power-domain NOMA (PD-NOMA) and code-domain NOMA (CD-NOMA). We show its practical implementation within the existing literature. This chapter is organized as follows: Section 2.1 defines NOMA and unveils its novelty and the motivation behind using it. Section 2.2 depicts the architecture and presents NOMA's main categories, mainly PD-NOMA and CD-NOMA, and highlights their characteristics and differences. Later, in section 2.3, we provide a deeper study on a CD-NOMA technique, sparse code multiple access (SCMA), where we depict its architecture, recent applications, and advantages. We would like to note that in some of the literature, NOMA and PD-NOMA were used interchangeably to indicate PD-NOMA. However, in our work, NOMA refers to the original non-orthogonal multiple access concept definition, which encompasses the power-domain NOMA denoted by PD-NOMA and the code-domain expressed by CD-NOMA.

2.1 What is NOMA?

Wireless communications have drastically evolved and shaped our lifestyle through the last decades. The first generation was based on analog time division multiple access (TDMA) and enabled the first wireless communication in the 80s. The second generation was the enabler for data communication based on frequency division multiple access (FDMA), where the division was done in frequency. For the 3rd generation, based on code division multiple access (CDMA), the utilization of code division enabled higher data rates, enabling data transfer over mobiles and mobile phone applications. The 4th generation, which was based on OFDM to mitigate intersymbol interference (ISI), enabled video streaming and video-based applications. However, all of the previous technologies were based on OMA, where due to the orthogonality constraint, we are always bounded by the number of resources, which limits our goals. Hence, new multiple access techniques are required in order to cope with the increasing demands for connectivity

and fulfill the new requested needs for data rates. NOMA, in simple terms, enables overloading subcarriers with multiple users, thus enabling higher spectral efficiency and high data rates. In the coming sections, we go over a detailed study of the different NOMA categories, their system model, and some of their advanced applications.

2.2 NOMA architectures

This section will go through the available NOMA techniques and expose the different architectures in the literature, their characteristics and associated advantages/disadvantages before delving into a special category of that family, which is SCMA. In contrast to OMA, NOMA technologies share the resources (either time, frequency or code) between many users. Depending on the resource being shared, NOMA techniques can be divided into two main categories: PD-NOMA and CD-NOMA Dai *et al.* (2015). We will expose each of these categories in the coming section.

2.2.1 PD-NOMA

PD-NOMA exploits the power domain to serve multiple users in the same degree of freedom (DoF). Every user is allocated a number of subcarriers, which can be shared with other users. Hence, if we consider the downlink with J users sharing the same subcarriers with their channel gains ordered such that: $|h_1|^2 \geq |h_2|^2 \geq \cdots \geq \left|h_j\right|^2$. In the downlink scenario, the signal received by user j is given by:

$$y_j = h_j \sum_{i=1}^{J} \sqrt{\beta_i P} s_i + n_j \tag{2.1}$$

where h_j is the channel gain between user j and the transmitter, β_i is the amount of power allocated to user i, P is the total amount of power, and n_j is the receiver noise at user j. In this context, the selection of the users sharing a resource should be made wisely in order to have the lower possible level of interference between users. At the receiver each user's information is recovered by successive interference cancellation (SIC) Hojeij, Farah, Nour & Douillard (2015), Farah, Sfeir, Nour & Douillard (2017). SIC consists of decoding the strongest signal while considering the weakest signal as noise. Once the strongest signal is decoded, it is subtracted

from the total signal and the difference is decoded to recover the weakest signal. In Hojeij *et al.* (2015), the authors propose a NOMA resource allocation algorithm, which covers user pairing, power distribution between allocated subbands, and the power division between paired users. In Figure 2.1, we graphically show the difference between OMA and NOMA models where blocks of different colors refer to different users.

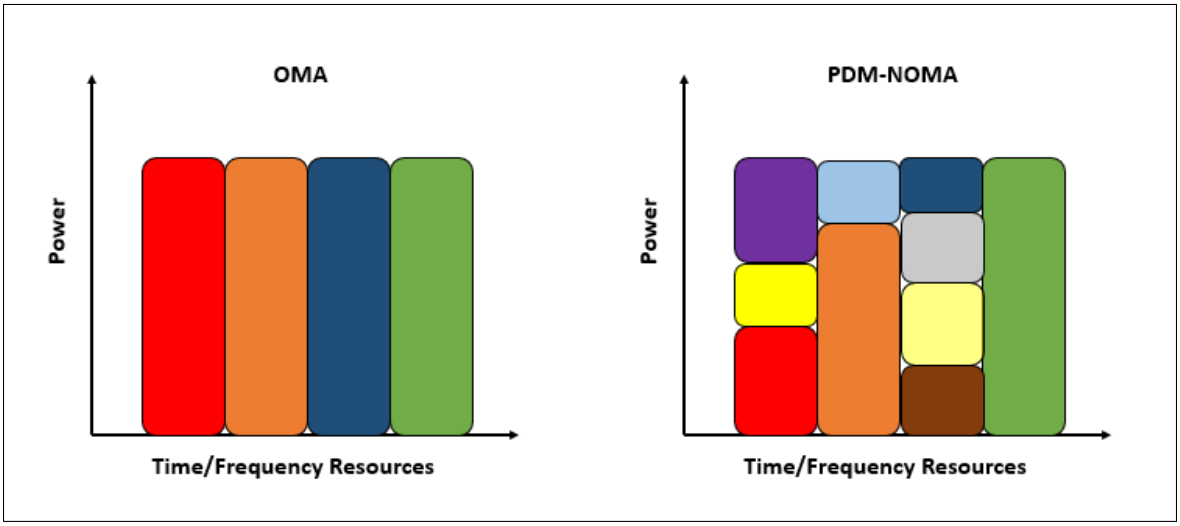

Figure 2.1 Resource allocation in OMA versus PDM-NOMA

2.2.2 CD-NOMA

In CD-NOMA each user is assigned a code to be used on his subcarriers. CD-NOMA techniques include low-density spreading (LDS) Hoshyar, Wathan & Tafazolli (2008) Razavi, Mohammed, Imran, Hoshyar & Chen (2012), SCMA Nikopour & Baligh (2013), and pattern division multiple access (PDMA) Dai, Chen, Sun, Kang, Wang, Shen & Xu (2014). The basic idea behind these techniques is to introduce redundancy by code spreading to facilitate the separation of the users at the receiver. At the receiver, multi-user detection (MUD) is performed in order to recover each user's signal. Usually, MUD is performed using the message passing algorithm (MPA), which is based on the maximum a posteriori probabilities (MAP). MPA is seen as a trade-off algorithm between high performance and low complexity and takes benefit from the sparseness

of the network. If an extremely low bit error rate is required, the exhaustive search algorithm, which is of exponential order and hence of high complexity, can be used.

LDS, one of the CD-NOMA schemes, is like CDMA where we have a different spreading code for each user, and the used codes (spreading codes) are sparse (they have many zeros). The sparsity will allow to have less interfering users on some chips and reduce decoding complexity by enabling the use of the MPA decoder of lower complexity than the exhaustive search.
PDMA, another CD-NOMA scheme, consists in the joint design of the transmitter and the receiver, and in following a code pattern offering a different order of transmission diversity to reduce the error propagation of the SIC. Sparsity in PDMA is useful when applying belief propagation algorithms Chen, Ren, Gao, Kang, Sun & Niu (2016).
SCMA is based on LDS-CDMA which consists of using LDS codes in CDMA Dai *et al.* (2015). Thus the interference between users is reduced and overloading is allowed due to the sparsity. The difference between LDS and SCMA is that codebooks in SCMA are built based on multidimensional constellation designs. There is a constellation for each user, and its size is equal to the number of possible signals for each user. There is no longer a single modulation block and a single spreader but these two blocks are combined in one single block, which is the SCMA encoder, shown in Figure 2.2. The constellation design is an optimization problem aiming to achieve the best distance properties between the different constellations which is necessary for the reduction of the bit error rate (BER) Taherzadeh, Nikopour, Bayesteh & Baligh (2014).
Moreover, the MPA algorithm, which can be used given the sparsity property of the codes, renders the decoding at the receiver easier than using MAP, which should be used if there is no sparsity.

Thus, SCMA implementation consists of 3 steps:

- Codebook design and mapping
- Multiple access design
- Decoding at the receiver

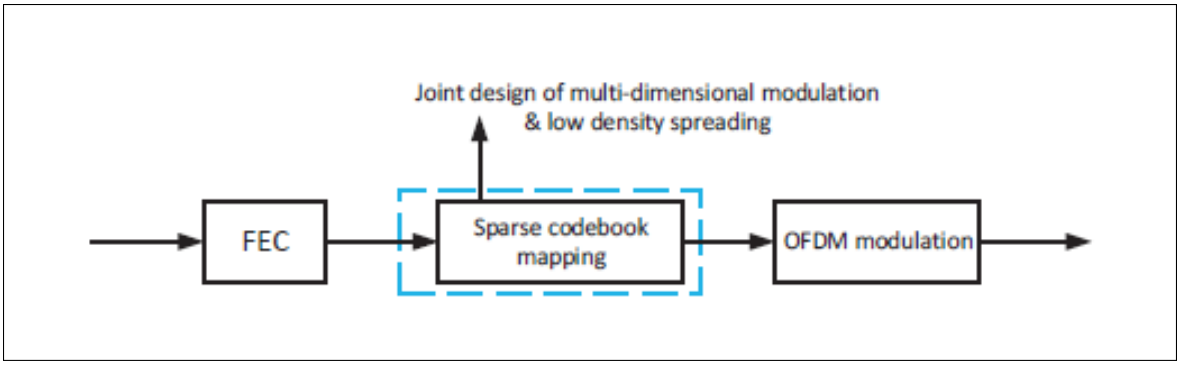

Figure 2.2 SCMA System Model
Taken from Wu *et al.* (2017)

In the following section, we go more in depth in the different parts of the SCMA scheme, which is employed in our research work.

2.3 SCMA Design and Overview

2.3.1 SCMA codebook design

In contrast to LTE systems where the modulation and the spreading are performed in two separate blocks, in SCMA, the modulator and spreader are merged into one block, which is a joint multi-dimensional modulation & low-density spreading. The coded bits of an information stream are directly mapped (i.e., without modulation) to a codeword from a codebook designed on a multi-dimensional constellation. Figure 2.3 shows the difference between SCMA and LDS/SCMA architectures from the transmitter side. It is noted here that at the receiver side, the despreader and demodulator are also substituted by a single block, namely the SCMA decoder.

On the other hand, the multidimensional characteristic of SCMA codewords achieves a system capacity benefit. In fact, in CDMA, the codebook is linear whereas in SCMA, the codebook is multidimensional. The major difference between LDS-CDMA and SCMA lies in the multidimensional constellation, which brings the shaping gain. This multidimensional constellation implies also an increase in the system capacity, and hence allows higher throughputs while sparseness enables massive connections Wu *et al.* (2017), Liu, Wang, Bao & Liu (2018).

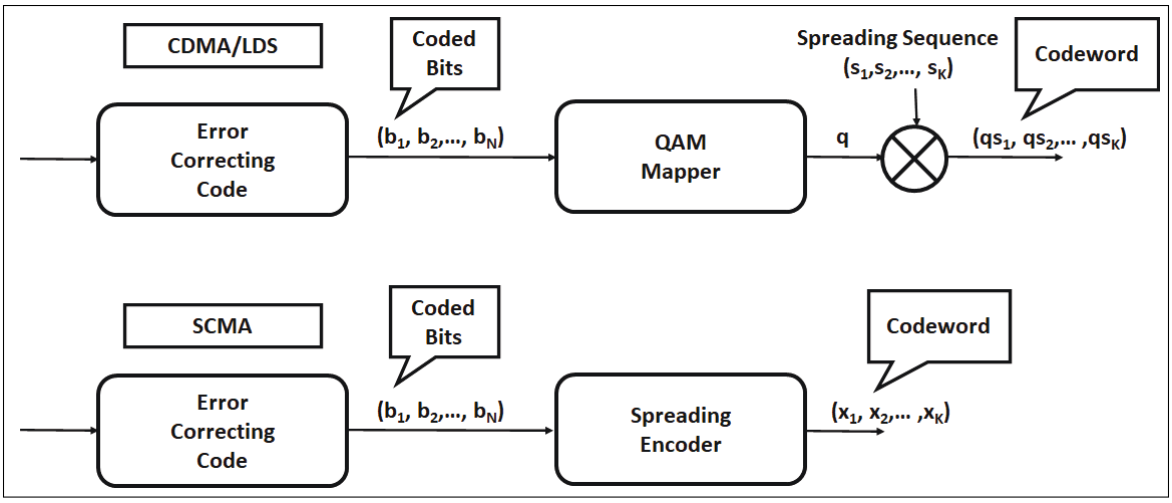

Figure 2.3 Comparison between SCMA and LDS/CDMA,
taken from Nikopour & Baligh (2013)

For example, in Figure 2.4 Wu *et al.* (2017), a 4-D real constellation is used instead of 2-D

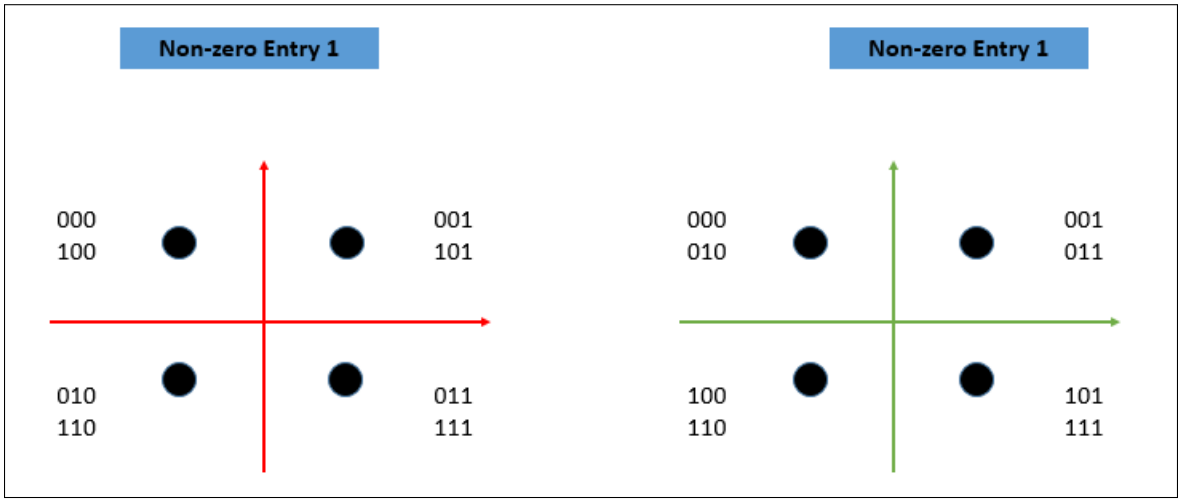

Figure 2.4 Example of SCMA 8-point codebook
Taken from Wu *et al.* (2017)

quadrature amplitude modulation (QAM). We consider 2 entries (active subcarriers) for each user, which lead to a 4-D real constellation. In the 4-D real constellation (or 2-D complex constellation), we have a 2-D constellation, on each entry. It is clear from this figure that on each entry we have 4 projection points because, on each entry there is a superposition of 2

different points of the 4-D constellation. However, if we have a 2-D constellation with one entry, we would have obtained 8 projection points on the same entry for the 8-QAM. A general formula for SCMA constellation is that if we have d_v active subcarriers per user, then we have a $2 * d_v$-D real constellation or d_v-D complex constellation Vameghestahbanati, Marsland, Gohary & Yanikomeroglu (2019). In our previous example, we have $d_v = 2$, the size of the constellation M=8 (since it is 8-QAM), N=4 (the dimension is 4), the number of users that are using a subcarrier $d_f = 3$.

This feature of reducing the number of projection points has also an important effect on reducing the decoding complexity. Additionally, the multilayer combination through N-dimensional codes allows us to increase the capacity of the system by overloading, and leads to a more energy-efficient transmission with less complexity. It allows the superposition of many symbols from different users on each resource element (RE). Thus, it allows massive connections since the number of allowed users is no longer strictly limited to the number of available resources as it was in the case of OMA.

On the other hand, the sparse spreading characteristic of SCMA reduces symbol collisions. Furthermore, the multidimensional benefit can be expressed by two metrics: coding gain and shaping gain. For the coding gain, each increase of 0.4 dB leads to doubling the decoding complexity at the receiver side as the constellations becomes denser Forney & Wei (1989). Hence, we are more interested in increasing the shaping gain, despite being limited to 1.53 dB Forney & Wei (1989). The shaping gain is 0 for a cube region and is maximum for a sphere Forney & Wei (1989).

Equation (2.2) shows the most used codebook in the literature Sergienko & Klimentyev (2017). Another codebook conceived in the aim of maximizing the sum-rate, is shown in equation (2.3) Zhang, Xiao, Xiao, Chen, Xia, Chen & Ma (2016).

$$
\mathbf{CB}_1 = \begin{bmatrix} 0 & -0.1815 - 0.1318j & 0 & 0.7851 \\ 0 & -0.6351 - 0.4615j & 0 & -0.2243 \\ 0 & 0.6351 + 0.4615j & 0 & 0.2243 \\ 0 & 0.1815 + 0.1318j & 0 & -0.7851 \end{bmatrix}^{\mathrm{T}}
$$

$$
\mathbf{CB}_2 = \begin{bmatrix} 0.7851 & 0 & -0.1815 - 0.1318j & 0 \\ -0.2243 & 0 & -0.6351 - 0.4615j & 0 \\ 0.2243 & 0 & 0.6351 + 0.4615j & 0 \\ -0.7851 & 0 & 0.1815 + 0.1318j & 0 \end{bmatrix}^{\mathrm{T}}
$$

$$
\mathbf{CB}_3 = \begin{bmatrix} -0.6351 + 0.4615j & 0.1392 - 0.1759j & 0 & 0 \\ 0.1815 - 0.1318j & 0.4873 - 0.6156j & 0 & 0 \\ -0.1815 + 0.1318j & -0.4873 + 0.6156j & 0 & 0 \\ 0.6351 - 0.4615j & -0.1392 + 0.1759j & 0 & 0 \end{bmatrix}^{\mathrm{T}}
$$

$$
\mathbf{CB}_4 = \begin{bmatrix} 0 & 0 & 0.7851 & -0.0055 - 0.2242j \\ 0 & 0 & -0.2243 & -0.0193 - 0.7848j \\ 0 & 0 & 0.2243 & 0.0193 + 0.7848j \\ 0 & 0 & -0.7851 & 0.0055 + 0.2242j \end{bmatrix}^{\mathrm{T}}
$$

$$
\mathbf{CB}_5 = \begin{bmatrix} -0.0055 - 0.2242j & 0 & 0 & -0.6351 + 0.4615j \\ -0.0193 - 0.7848j & 0 & 0 & 0.1815 - 0.1318j \\ 0.0193 + 0.7848j & 0 & 0 & -0.1815 + 0.1318j \\ 0.0055 + 0.2242j & 0 & 0 & 0.6351 - 0.4615j \end{bmatrix}^{\mathrm{T}}
$$

$$
\mathbf{CB}_6 = \begin{bmatrix} 0 & 0.7851 & 0.1392 - 0.1759j & 0 \\ 0 & -0.2243 & 0.4873 - 0.6156j & 0 \\ 0 & 0.2243 & -0.4873 + 0.6156j & 0 \\ 0 & -0.7851 & -0.1392 + 0.1759j & 0 \end{bmatrix}^{\mathrm{T}}
$$

(2.2)

$$\boldsymbol{C}_1 = \begin{bmatrix} -1.3498 & -0.4218 & 0.4218 & 1.3498 \\ 0 & 0 & 0 & 0 \\ -0.1980 - 0.3724i & 0.6337 + 1.1918i & -0.6337 - 1.1918i & 0.1980 + 0.3724i \\ 0 & 0 & 0 & 0 \end{bmatrix},$$

$$\boldsymbol{C}_2 = \begin{bmatrix} 0 & 0 & 0 & 0 \\ -0.1980 - 0.3724i & 0.6337 + 1.1918i & -0.6337 - 1.1918i & 0.1980 + 0.3724i \\ 0 & 0 & 0 & 0 \\ -1.3498 & -0.4218 & 0.4218 & 1.3498 \end{bmatrix},$$

$$C_3 = \begin{bmatrix} -0.6337 - 1.1918i & -0.1980 - 0.3724i & 0.1980 + 0.3724i & 0.6337 + 1.1918i \\ 0.2109 - 0.3653i & -0.6749 + 1.1690i & 0.6749 - 1.1690i & -0.2109 + 0.3653i \\ 0 & 0 & 0 & 0 \\ 0 & 0 & 0 & 0 \end{bmatrix},$$

$$C_4 = \begin{bmatrix} 0 & 0 & 0 & 0 \\ 0 & 0 & 0 & 0 \\ -1.3498 & -0.4218 & 0.4218 & 1.3498 \\ 0.2109 - 0.3653\text{i} & -0.6749 + 1.1690\text{i} & 0.6749 - 1.1690\text{i} & -0.2109 + 0.3653\text{i} \end{bmatrix},$$

$$C_5 = \begin{bmatrix} 0.2109 - 0.3653i & -0.6749 + 1.1690i & 0.6749 - 1.1690i & -0.2109 + 0.3653i \\ 0 & 0 & 0 & 0 \\ 0 & 0 & 0 & 0 \\ -0.6337 - 1.1918\text{i} & -0.1980 - 0.3724\text{i} & 0.1980 + 0.3724\text{i} & 0.6337 + 1.1918\text{i} \end{bmatrix},$$

$$\boldsymbol{C}_6 = \begin{bmatrix} 0 & 0 & 0 & 0 \\ -1.3498 & -0.4218 & 0.4218 & 1.3498 \\ 0.2109 - 0.3653\text{i} & -0.6749 + 1.1690\text{i} & 0.6749 - 1.1690\text{i} & -0.2109 + 0.3653\text{i} \\ 0 & 0 & 0 & 0 \end{bmatrix}. \tag{2.3}$$

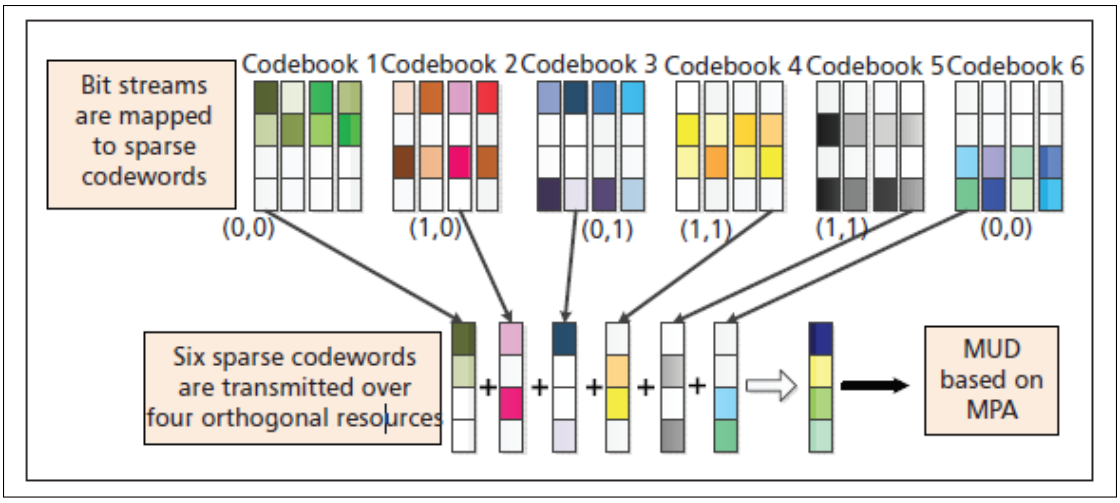

Figure 2.5 SCMA Encoding and Multiplexing, taken from Dai *et al.* (2015)

2.3.2 SCMA Encoding And Multiplexing

In Figure 2.5, we show a model for SCMA encoding and multiplexing where we have 6 codebooks, each corresponding to one user (total of 6 users). Each codebook consists of 4 codewords that correspond to the 4 possible data information of each user i.e. 00, 01, 10, 11. Each codeword consists of 4 bits, 2 sparse bits and 2 data bits. For Example, the first codebook of user 1 contains four codewords, namely 0000, 1000, 0100, 1100, which correspond to the data bits 00, 10, 01, 11, respectively. Note that within the same codebook, the position of the sparse bits is always the same and differs from a codebook to another (for codebook 1, the sparse bits are the last bits). Moreover, each bit is mapped to a subcarrier; therefore, since we have 4 bits, we need 4 subcarriers. Consequently, since the number of users is 6, the overloading is of 150%. Finally, since the sparse bits should differ from a codebook to another, we can get the limiting number of layers J in a SCMA block as $J = \binom{K}{N}$, where each user usually has one layer. Here, K is the number of subcarriers (4 in our case) and N denotes the number of data bits (2 in this case); therefore, the limit for J is $\binom{4}{2} = 6$.

The SCMA encoder is modelled by the following mapping function: $f : \mathbb{B}^{log_2(M)} \rightarrow \mathcal{X}$ where $\mathcal{X} \subset \mathbb{C}^K$ with cardinality $\mathcal{X} = M$, M being the modulation order. Then, $\mathbf{x} = f(\mathbf{b})$, where

$\mathbf{x}$ is a sparse vector with $N < K$ non-zero entries. This encoding function f can be considered as a composition of two functions where the first is a constellation mapping $g : \mathbb{B}^{log_2(M)} \rightarrow C$, $C \subset \mathbb{C}^K$ while the second function is a binary mapping $\mathbf{V} \in \mathbb{B}^{K*N}$. Thus, we have $f = \mathbf{V}g$ where $\mathbf{V}$ maps the N-dimensional codeword to a K-dimensional one. In order to satisfy the sparsity condition for $\mathbf{x}$, $\mathbf{V}$ must contain $K - N$ all-zero rows. The mapping matrix $\mathbf{V}$ can be constructed by taking the $N * N$ identity matrix $\mathbf{I}_N$ and adding $K - N$ columns of zeros to it.

A SCMA system is defined by a set of layers $\mathcal{S}([\mathbf{V}_j]_{j=1}^J, [g_j]_{j=1}^J, J, M, N, K)$. The received signal is given by

$$\begin{aligned} \mathbf{y} &= \sum_{j=1}^{J} \text{diag}(\mathbf{h}_j)\mathbf{x}_j + \mathbf{n} \\ &= \sum_{j=1}^{J} \text{diag}(\mathbf{h}_j)\mathbf{V}_j g_j(\mathbf{b}_j) + \mathbf{n}. \end{aligned} \tag{2.4}$$

Where $\mathbf{x}_j = (x_{1j}, ..., x_{kj})^T$ is the SCMA codeword of the j^{th} layer with size $K > N$, where $K - N$ are zeros, $\mathbf{h}_j = (h_{1j}, ..., h_{kj})^T$ is the channel vector of layer j, and $\mathbf{n} \sim \mathcal{CN}(0, N_0\mathbf{I})$ is the complex Gaussian noise.

The structure of SCMA is conveyed through a factor graph representation. Let $\mathbf{F} \in \mathbb{B}^{K*N}$ be the factor graph matrix, each element $[\mathbf{F}]_{kj}$ is set to 1 if there is transmission on resource k. $\mathbf{F}$ is obtained from $\{\mathbf{V}_j\}_{j=1}^J$ as $\mathbf{F} = (\mathbf{f}_1, ..., \mathbf{f}_J)$ where $\mathbf{f}_j = \text{diag}(\mathbf{V}_j {\mathbf{V}_j}^T)$. The number of layers for each user is given by the vector $\mathbf{d} = (d_1, ..., d_K)^T = \sum_{j=1}^{J} \mathbf{f}_j$.

In Yuan (2016), an SCMA model, where data streams are directly mapped to codewords is proposed as an enhanced version of LDS, illustrated in Figure 2.3. Each of the 6 users has his codebook and each codebook has its codewords that contain zeros in the same dimensions. The position of the zeros differs from a codebook to another to avoid collision and interference between different users. In Figure 2.5, each user has its two bits that are mapped to a complex codeword. Codewords for all users are then multiplexed over four OFDM subcarriers (orthogonal

subcarriers). The SCMA codebook design is a challenging problem since different layers are being multiplexed with different codebooks to achieve multiple access.

2.3.3 SCMA Receiver

For MUD, the MPA algorithm is used with relatively low complexity due to the sparsity property of SCMA. The MPA is optimal in terms of performance and complexity and is based on the MAP. One would use the exhaustive search over all possible combinations of codewords to recover each user data, which is of exponential complexity; however, with MPA, the complexity is reduced due to the sparseness.

In order to represent the evolution of the MPA, we use the factor graph which helps us represent the evolution of the messages through the different stages of MPA, Wu *et al.* (2017). In Figure 2.6 we see an example of a factor graph, which aims to provide an original graphical description of the factorization of a global function into a product of local functions. In the factor graph of Figure 2.6, the four squares are the function nodes which represent the set of subcarriers. The six circles that are connected to the squares, are the variable nodes which represent the layers, i.e. the set of users.

In Alizadeh, Bélanger, Savaria & Boyer (2016), the SCMA decoding algorithm was analyzed and 4 solutions were considered to optimize it from the perspective of latency and hardware resource utilization. The best solution was the one that minimizes the product of the decoding area by the time analysis. In Wei & Chen (2016), a decoding algorithm based on list sphere decoding is presented. It achieves the near maximum likelihood performance and reduces the complexity of the original MPA detection. The simulation results showed a good trade-off between the BER performance and computational complexity.

Using MPA instead of MAP reduces the complexity from the order of $O(M^J)$ to $O(M^{d_f})$, where J is the number of users and d_f the number of degrees of freedom which is the number of users connected to a single subcarrier.

The MPA consists of 3 steps:

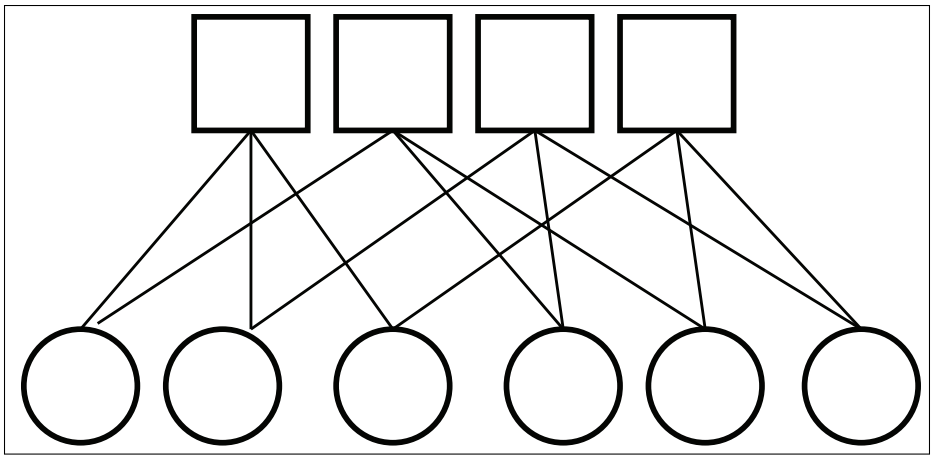

Figure 2.6 Factor graph schematic of an SCMA system with 6 layers, 4 users, 2 subcarriers and 3 degrees of freedom

- Initialization and computation of the initial conditional probabilities
- Iterative message transfer between the variables and the function nodes
- Calculation of the log-likelihood ratio (LLR) at the output

The network is usually initialized with equiprobable values for all codewords on each function node, where each layer is assumed to be assigned to a user k out of the total K users. Moreover, since each user has his codebook consisting of M codewords, each codeword has a probability of $1/M$ as shown in Figure 2.7. Hence, the first messages that have to be sent from the variable nodes to the corresponding connected function nodes. The messages, denoted by I, are transferred between the variable nodes, denoted by v_i, and the function node, denoted by f, as shown below.

$$I^{init}_{v_1 \to f}(m1) = I^{init}_{v_2 \to f}(m2) = I^{init}_{v_3 \to f}(m3) = \frac{1}{M} \tag{2.5}$$

The 2nd step of the MPA consists of two phases that are repeated iteratively until convergence or until we reach a certain number of predefined iterations.

The first phase consists of computing messages at the function nodes using equation (2.6) given the known or estimated channel $h_{n,k}$ and the possible transmitted codeword $C_{k,n}(m_k)$.

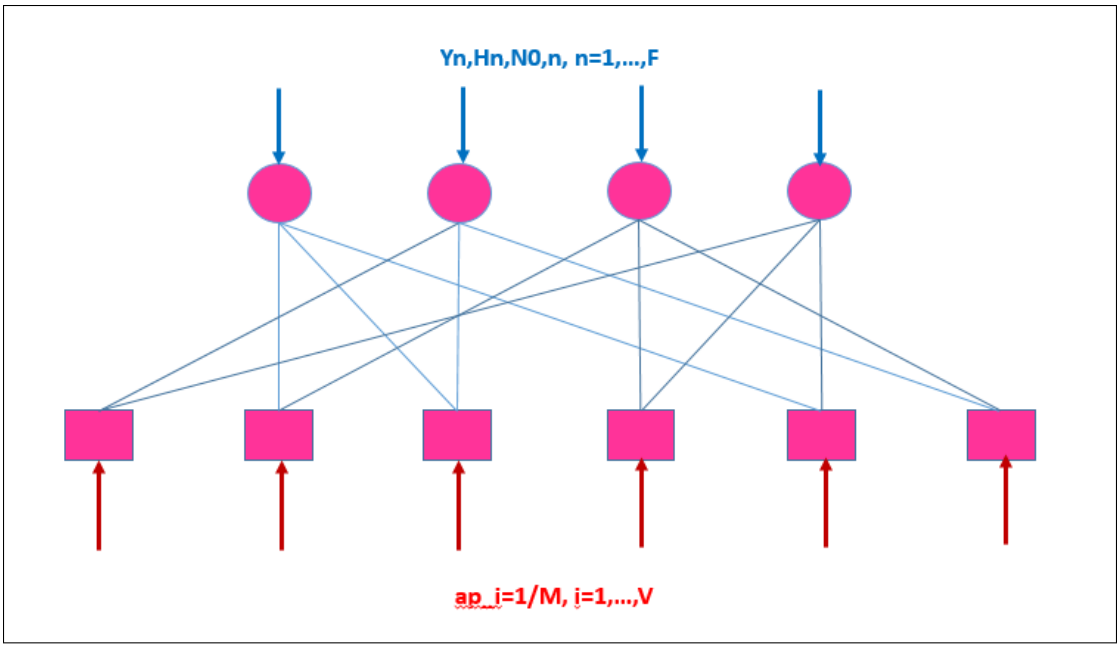

Figure 2.7 Message Passing Part 1

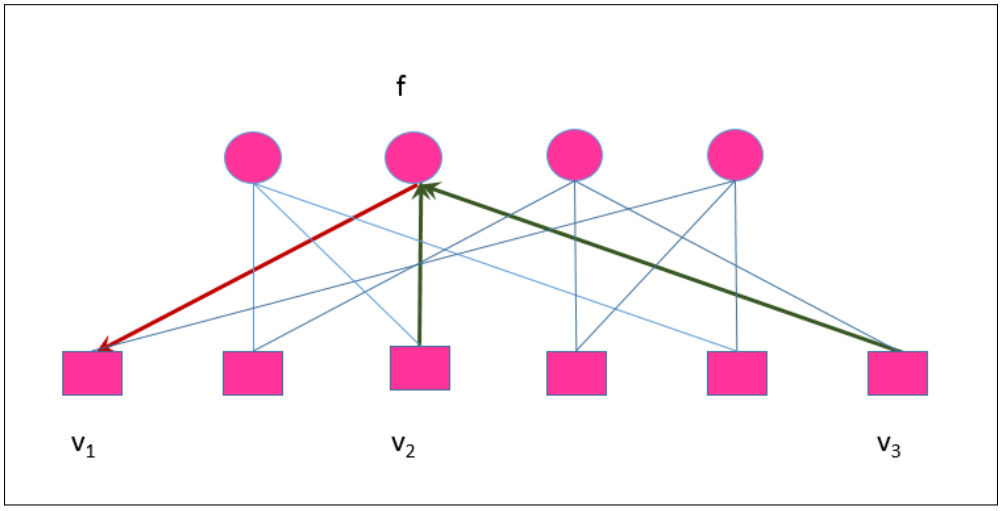

Figure 2.8 Message Passing Part 2-a

$$z_n\left(y_n, m_1, m_2, m_3, N_{0,n}, H_n\right) = \frac{-1}{N_{0,n}} \left\| y_n - \left(h_{n,1} C_{1,n}\left(m1\right) + h_{n,2} C_{2,n}\left(m_2\right)\right)\right\| \qquad (2.6)$$

$$\phi_n\left(y_n, m_1, m_2, m_3, N_{0,N}, H_n\right) = exp\left(z_n\left(y_n, m_1, m_2, m_3, N_{0,N}, H_n\right)\right) \tag{2.7}$$

The message passing takes place from all function nodes (that represent subcarriers) to their respective connected variable nodes (that represent layers, i.e. users) as shown in Figure 2.8. Meanwhile, the second phase consists of calculating the response messages at the variable nodes before passing them back to function nodes as shown in Figure 2.9.

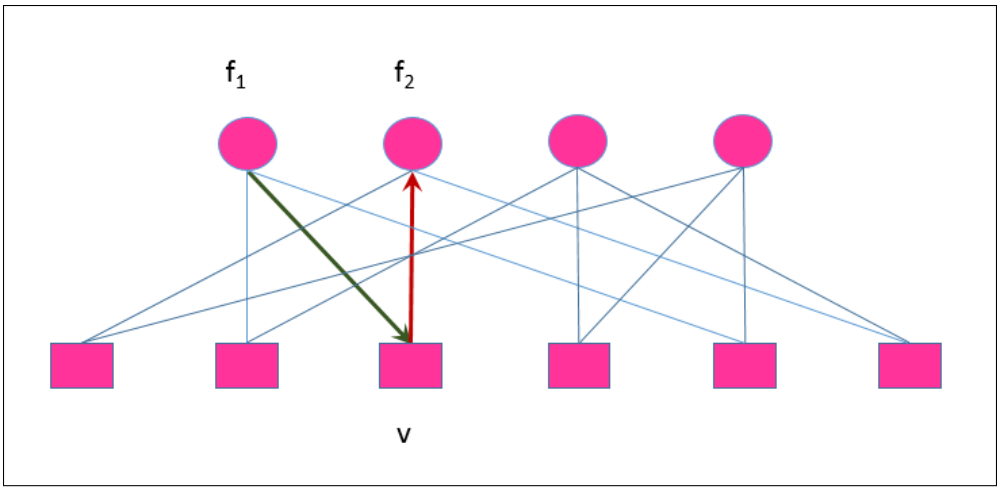

Figure 2.9 Message Passing Part 2-b

The beliefs at each variable node are computed as:

$$I_{f\to v_1}(m_1) = \sum_{m_2=1}^{M}\sum_{m_3=1}^{M} \phi_n\left(y_n, m_1, m_2, m_3, N_{0,N}, H_n\right) I^{init}_{v_2\to f}(m2)\, I^{init}_{v_3\to f}(m3) \;\; m_1 = 1, ..., M \tag{2.8}$$

$$I_{f\to v_2}(m_2) = \sum_{m_1=1}^{M}\sum_{m_3=1}^{M} \phi_n\left(y_n, m_1, m_2, m_3, N_{0,N}, H_n\right) I^{init}_{v_1\to f}(m1)\, I^{init}_{v_3\to f}(m3) \;\; m_2 = 1, ..., M \tag{2.9}$$

$$I_{f\to v_3}(m_3) = \sum_{m_1=1}^{M}\sum_{m_2=1}^{M} \phi_n\left(y_n, m_1, m_2, m_3, N_{0,N}, H_n\right) I^{init}_{v_1\to f}(m1)\, I^{init}_{v_2\to f}(m2) \;\; m_3 = 1, ..., M \tag{2.10}$$

After receiving messages from the function nodes, the variable nodes update their beliefs about each of the M codewords using:

$$I_{v\to f_1}(m) = normalize(ap_v(m)I_{f_2\to v}(m)), \quad m = 1, ..., M \tag{2.11}$$

$$I_{v\to f_2}(m) = normalize(ap_v(m)I_{f_1\to v}(m)), \quad m = 1, ..., M \tag{2.12}$$

When the number of fixed iterations is reached, we can compute the guess on each codeword at each variable node v using:

$$G_v(m) = ap_v(m)I_{f_1\to v}(m)I_{f_2\to v}(m), \qquad m = 1, ..., M \tag{2.13}$$

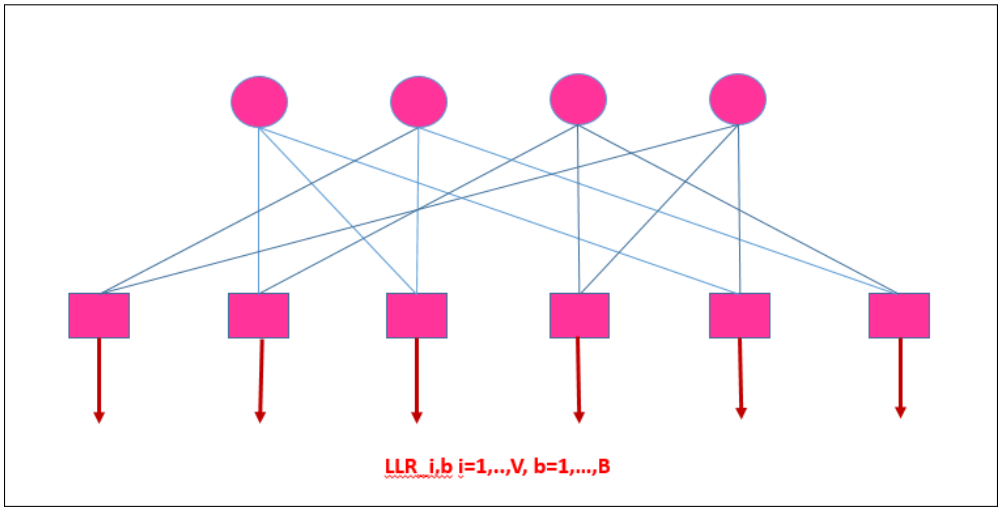

Figure 2.10 Message Passing Part 3

After guessing the codeword we compute the LLRs (i.e., Figure 2.10) to determine the bit at each position i:

$$LLR_i = log\left(\frac{P(b_i = 0)}{P(b_i = 1)}\right) \tag{2.14}$$

$$LLR_i = log\left(\frac{\sum_{m:b_{m,i}=0}^{m} G_V(m)}{\sum_{m:b_{m,i}=1}^{m} G_V(m)}\right) = log\left(\sum_{m:b_{m,i}=0}^{m} G_V(m)\right) - log\left(\sum_{m:b_{m,i}=1}^{m} G_V(m)\right) \tag{2.15}$$

2.3.4 Advanced SCMA applications and architectures

In Nikopour & Baligh (2013), a SCMA scheme based on LDS is proposed where:

- The modulator and spreading are replaced by a single block, which is the SCMA encoder that directly encodes binary data to multidimensional complex domain codewords.
- Multiple access is achievable by multiple layers for each user.
- Sparse codewords are used and the MPA is implemented with moderate complexity.

In Nikopour & Baligh (2013), the authors proposed a systematic sub-optimal algorithm, based on a multi-stage optimization approach, for SCMA codebook design. The simulation results show that SCMA has lower block error rate (BLER) than LDS. In Taherzadeh *et al.* (2014), a new approach to design SCMA codebooks is derived from the design basics of lattice constellations. In this work, a sub-optimal solution for the codebook design challenge following a multi-stage optimization approach, is employed. Here, the codebook design consists of three main steps. The first step is to select the mapping matrix and aims to determine the number of layers interfering at each OFDM tone (frequency), which also leads to an estimation of the complexity of the MPA decoder. It is noted that the complexity of SCMA codebook design increases with the number of layers that are multiplexed with diverse codebooks (as they belong to different users). The second step consists in defining the constellations of the users, that are expressed as functions of a mother constellation and layer-specific operators. Here the mother constellation and the operators are determined separately. Finally, the last step is an optimization over the layer-specific operators, which may include phase rotation and low power offset. The authors in Taherzadeh *et al.* (2014) showed a performance gain achieved by SCMA compared to LDS and orthogonal frequency division multiple access (OFDMA). SCMA takes all the advantages of LDS while avoiding the poor link performance of LDS systems.

In Li & Yang (2009), a coalitional game for blind group decoding in a multi-cell CDMA system was devised. First, a study of the effect of the coalition size on the system level was conducted by using models of transferable payoffs. Second, the study sought to find the best coalition from the individual nodes' side using a non-transferable payoff model. Results showed that for transferable-payoffs scenarios, the grand coalition was the most stable. However, from the

individual nodes' side, the grand coalition is not guaranteed to be the best choice. Another interesting application for cooperative game theory in SCMA was in Yang & Sun (2019), which aimed to maximize the system rate considering the user fairness in massive machine-type communications. This was achieved in two steps where, in the first step, the optimal coalitions to be formed are determined, while codebook assignment is performed in the second step. The results showed a small difference in rates between users, which is a clear indication of fairness achievement.

The first SCMA model to make use of Deep Neural Networks (DNNs) was proposed in Kim, Kim, Lee & Cho (2018). Precisely, a DNN was used for codebook generation and in the decoding of the received signal. The results showed less computational complexity and a lower BER than the conventional MPA-based SCMA decoder. In Lu, Xu, Shen, Zhang & You (2018), a new idea of converting the sparse design of the MPA to a neural network with sparseness applied as the weights of that network was proposed. Here, instead of MPA iterations, we have network layers. The neural network design showed better performance than the MPA, especially for the high signal-to-noise-ratio (SNR) regime.

In Wu, Zhang & Chen (2015a), an iterative multiuser receiver, that explores the coding and shaping gains of SCMA, is studied. In that work, the computation of the soft decision, i.e. the a posteriori LLRs, was expressed as the sum of the priori LLRs obtained from the previous iteration and the extrinsic LLRs. The iterative decoder showed a better result than the non-iterative one, with a BLER that does not degrade much when we go from a load of 100% to 300%. In Qin, Qin, Wang & Wang (2018), the effect of multipath is considered in recovering the SCMA signal. Here, the equalization is done at the transmitter instead of the receiver for less design complexity. This semi-blind receiver leads to a lower BER.

2.3.5 SCMA in Grant-Free Multiple Access

A usual request for transmission consists of sending a request and waiting for an accept to send data. This leads to delays in wireless communications. A new model of communication that overcomes this delay is the grant-free model where a user can transmit without asking for

permission. Grant-free is very important especially in mMTC where we have a high number of low rate transmissions Evangelista, Sattar & Kaddoum (2019a), Evangelista, Sattar, Kaddoum, Selim & Sarraf (2021b). Also, grant-free is important for scenarios with stringent latency requirements Evangelista, Kaddoum & Sattar (2021a). In this context, SCMA is a promising technology since it can accommodate a higher number of users and enables massive connections due to its overloading capabilities, mostly with codebook reusability possibility. In Figure 2.11, we show two types of grant-free scenario.

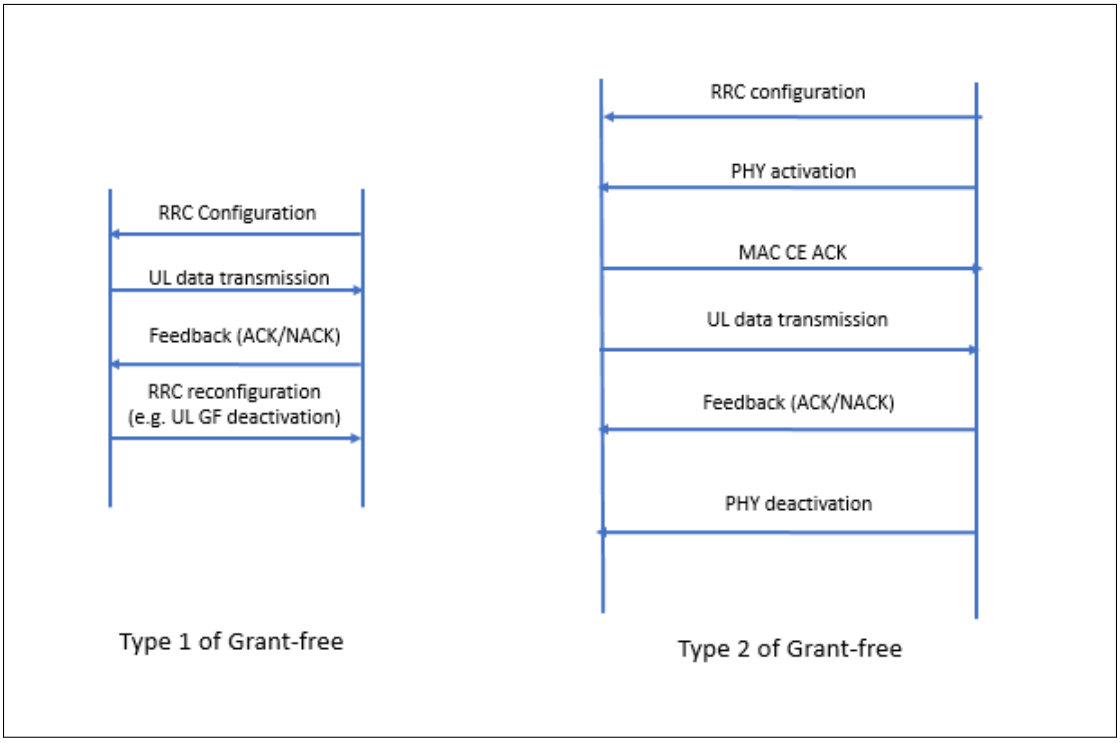

Figure 2.11 Types of grant-free multiple access Li *et al.* (2018b)

In OFDM, a Resource Block (RB) is the smallest amount of resources that can be allocated to a user. A RB is defined in frequency as a set of 12 subcarriers with a separation of 15 kHz between consecutive frequencies, i.e. a total of 180 kHz in frequency. Meanwhile, in time, it is the equivalent of 7 timeslots Au, Zhang, Nikopour, Yi, Bayesteh, Vilaipornsawai, Ma & Zhu (2014). In SCMA, the basic resource for UL grant-free is the contention transmission unit (CTU). A

CTU is a combination of time, frequency, codebook, and pilot sequence where multiple users are contending for the same resource Au *et al.* (2014). Each user has a different pilot sequence. An example of a CTU is shown in Figure 2.12.

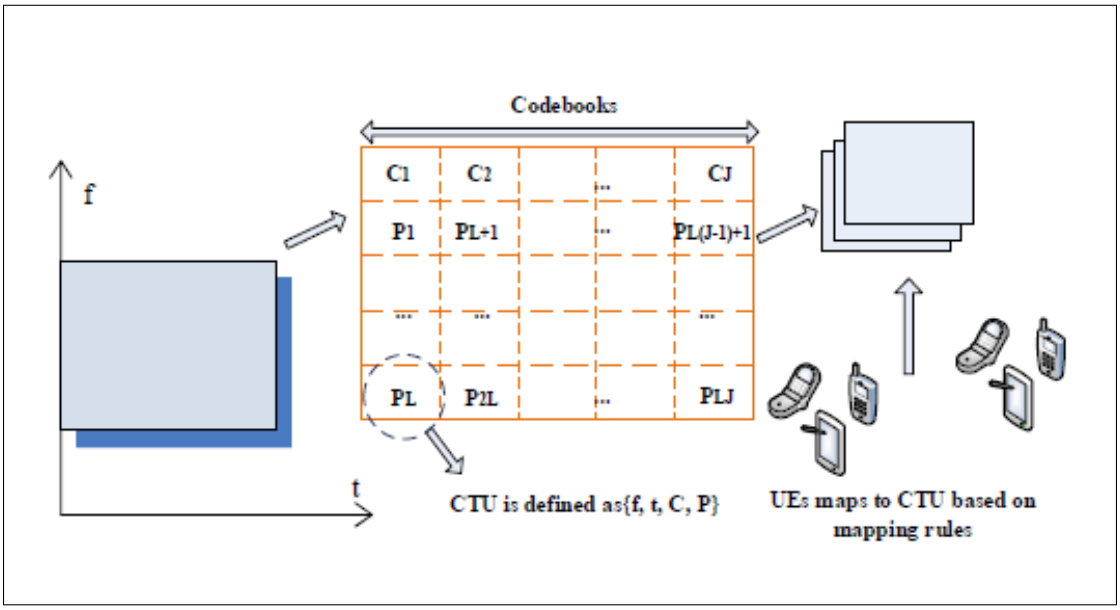

Figure 2.12 The relationship among time-frequency resources, codebooks, CTUs and UEs Sun *et al.* (2018)

Many works have studied the use of SCMA for grant-free scenarios, especially when we need to recover the actual active UEs at the receiver Sun *et al.* (2018),Bayesteh, Yi, Nikopour & Baligh (2014),Liu, Wu, Li & Tirkkonen (2017a).

2.3.6 MIMO-SCMA

As multiple-input multiple-output (MIMO) multiplexes in space and SCMA multiplexes in code, a joint study of the benefits of combining the two technologies was conducted in Liu, Li & Qiu (2015b). The study, showed that the capacity of the combined system is increased compared to MU-SCMA, and the sum rate is higher than that of MIMO MU-OFDMA. Moreover, in Yuan, Wu, Guo, Li, Xing & Kuang (2018), another combination of MIMO with SCMA was proposed for downlink transmission over frequency-selective channels. In that work, a hybrid

belief propagation (BP) and expectation propagation (EP) receiver was proposed to guarantee convergence.

2.3.7 Optimizations for SCMA scheme

As the case for every other resource allocation technique, optimizations can be employed in order to maximize the overall sum rate of the network, maximize the fairness which is achieved by maximizing the minimum rate, or reduce the energy consumption in SCMA. Optimizing all these aspects in the same scheme is impossible; however we can depict some trade-offs for many scenarios. In Evangelista, Sattar, Kaddoum & Chaaban (2019b), two algorithms are proposed, one for the overall sum-rate maximization, while the other is for the minimum rate maximization, which leads to higher fairness. Another study on energy saving in downlink and uplink was conducted in Zhai (2017). In Klimentyev & Sergienko (2017), the authors proposed a method based on genetic algorithm to maximize the minimum euclidean distance of the SCMA signal set. The obtained codebook presented a gain of 0.8 dB with respect to other codebooks. Another optimization study for the codebook design is proposed in Dong, Gao, Niu & Lin (2018). This codebook optimization is based on the maximization of the mutual information between the discrete input and continuous output. The optimization uses Karush-Kuhn-Tucker (KKT) conditions. The authors showed that in AWGN conditions the obtained codebook can approach the gaussian capacity upper bound.

2.3.8 Impairments in SCMA

As with every new technology, numerous inevitable obstacles and hurdles emerge during its implementation within practical wireless communications ecosystems. Additionally, the proliferation of the number of connected devices and the increased need for higher data rates will lead to growing interference levels, which need mitigation solutions to prevent performance degradation. Impairments, such as frequency offset Chen, Yin & Wei (2018), in-phase/quadrature-phase imbalance (IQI) Selim, Muhaidat, Sofotasios, Sharif, Stouraitis, Karagiannidis & Al-Dhahir (2018), impulsive noise Selim, Alam, Kaddoum & Agba (2020b),

hardware nonlinearity Mitra & Bhatia (2017b) imperfect channel estimation and mobility Jain, Mitra & Bhatia (2020) have been studied in several wireless communication technologies. As for SCMA, the studies on impairments available in the literature are still limited. In Liu, Zhang & Xin (2015a), the authors considered frequency offset impairment, where they studied filter bank-based multicarrier (FBMC) with SCMA and showed that it is more robust against the residual frequency offset (RFO). In Li, Li, Mathiopoulos, Zhang, Li & Jin (2018a), the authors studied the impact of hardware impairments and imperfect channel state information (ICSI) on the performance of energy harvesting (EH) cooperative NOMA multi-relay systems. On the other hand, SCMA is being studied for implementation within new use cases, such as visible light communication (VLC) Mitra & Bhatia (2017b) and reconfigurable intelligent surface (RIS) Al-Nahhal, Dobre & Basar (2021). Therefore, there is an imminent and undeniable need for studying and considering the effects of possible inevitable impairments and proposing solutions to mitigate their effect.

CHAPTER 3

RFF BASED DETECTION FOR SCMA IN PRESENCE OF PA NONLINEARITY

Elie Sfeir[1] , Rangeet Mitra[1] , Georges Kaddoum[1] , and Vimal Bhatia[2]

[1] Department of Electrical Engineering, École de Technologie Supérieure,
1100 Notre-Dame Ouest, Montréal, Québec, Canada H3C 1K3
[2] Department of Electrical Engineering, École de Technologie Supérieure,
Discipline of Electrical Engineering, IIT Indore,Indore 453552, India

Paper published in IEEE Communication Letters, 2020.

3.1 Abstract

The next-generation of communication systems must be capable of serving a significantly higher traffic generated by a large number of devices. To support massive connectivity over limited time-frequency resources, several non-orthogonal multiple access (NOMA) paradigms have emerged. In this context, sparse code multiple access (SCMA) based NOMA is particularly attractive due to its robustness to error-propagation, and its potentially high coding-gain with appropriate codebook design. However, the performance of SCMA based systems is severely degraded by distortions introduced by non-ideal hardware, e.g. power-amplifier (PA) nonlinearity. To mitigate such artefacts, in this letter, a random Fourier feature (RFF) based hybrid message passing algorithm (MPA) is proposed, and validated through computer simulations. Lastly, an analytical proof is presented that indicates that the use of RFFs significantly improves the convergence of the MPA in the presence of impairments, and renders error-rate performance equivalent to that of a linear Gaussian channel under approximate MPA.

Index Terms— Hardware impairments, SCMA, random Fourier features.

3.2 Introduction

THE next-generation of communication systems will experience a spectrum crunch due to significantly higher traffic caused by massive connectivity triggered by upcoming internet of

things (IoT) ecosystems, tactical environments, and healthcare applications Giordani, Polese, Mezzavilla, Rangan & Zorzi (2020). To enhance the capacity of next-generation communication systems and serve a multitude of devices, non-orthogonal multiple access (NOMA) has emerged as a disruptive multiple-access paradigm which supports several users over limited time-frequency resources Liu, Qin, Elkashlan, Ding, Nallanathan & Hanzo (2017b), Evangelista *et al.* (2019b). NOMA can be broadly classified as: a) power-domain NOMA(PD-NOMA), and b) code-domain NOMA Vaezi, Ding & Poor (2019). Though computationally simple, PD-NOMA is well known to be impaired by error-propagation due to imperfect successive interference cancellation (SIC) Liu *et al.* (2017b), as well as for its dependence on suitable power-allocation techniques and knowledge of channel-state information. On the other hand, the paradigm of sparse code multiple access (SCMA) (a kind of code-domain NOMA) Nikopour, Yi, Bayesteh, Au, Hawryluck, Baligh & Ma (2014) has been found to be particularly useful for supporting numerous users with high throughput by exploiting coding/shaping gains of the SCMA-codebook Moltafet, Yamchi, Javan & Azmi (2017). Here, by exploiting sparsity in the SCMA-codewords, the symbols are detected at the receiver using message passing algorithm (MPA) Sharma, Deka, Bhatia & Gupta (2019b). Though promising, the performance of SCMA is severely impaired by the non-ideal device characteristics such as the power-amplifier (PA) nonlinearity, which affects convergence of the MPA and are also known to be a serious impairment in upcoming communication systems Gharaibeh (2011), Rajasekaran, Vameghestahbanati, Farsi, Yanikomeroglu & Saeedi (2019). While some recent works explore iterative detection for the mitigation of PA nonlinearities Yang, Lin, Ma & Li (2018), these approaches rely on explicit knowledge of the PA characteristics at the receiver. Among several available signal processing solutions for mitigation of device nonlinearity, reproducing kernel Hilbert spaces (RKHS)based signal-processing has emerged as viable in the context of several nonlinear and non-Gaussian signal-processing applications Mitra & Bhatia (2017a), Mitra & Bhatia (2018a) and Mitra *et al.* (2018). RKHS based approaches are well-known for their computational simplicity, guarantee of exact representation of a wide-class of nonlinear functions, and generalization to changes in the nonlinear characteristics Schölkopf *et al.* (2001). These advantages of RKHS based solutions have enabled their application in the context of PD-NOMA systems Awan, Cavalcante,

Yukawa & Stanczak (2018). However, such existing detection methods for PD-NOMA primarily rely on dictionary based methods. In-general, the dictionary based RKHS algorithms are prone to noisy observations (particularly in the initial adaptive iterations), and incur non-negligible computational overhead in evaluation of appropriate criterion for selectively adding observations. This drawback is mitigated by using explicit approximations (also called random Fourier Features (RFF)) of the feature-map obtained by Monte-Carlo sampling of an RKHS Bouboulis, Chouvardas & Theodoridis (2017), Bouboulis *et al.* (2017).[1]

Contributions: In this letter, we propose an RFF based SCMA-detection technique which unwarps/recovers the received observations prior to the MPA based detection to mitigate the impairments caused by PA nonlinearity. Simulation results are presented which indicate that using the unwarped observations using RFF, the MPA delivers a bit error-rate (BER) performance comparable to that of an ideal linear Gaussian channel. Further, the proposed approach achieves several orders of BER gain as compared to performing MPA directly on the impaired codewords. Lastly,an optimality-proof of the proposed RFF based detection technique is outlined.

3.3 System Model

Considering a downlink scenario, where the information bits of the users are mapped to K-dimensional codeword, $\mathbf{x}_j \in \mathbb{C}^K$ for the j^{th} user, which is drawn from the corresponding codebook C_j. The channel gain vector $\mathbf{h} \in \mathbb{C}^K$ is modelled as a quasi-static Rayleigh fading channel, and the noise vector $\mathbf{n} \sim \mathcal{CN}(0, \sigma_n^2 \mathbf{I}_{K\times K})$ (where $\mathbf{I}_{K\times K}$ denotes an identity matrix of size $K \times K$) is modelled as an additive white Gaussian noise (AWGN). Using this terminology, the received observation $\mathbf{y} \in \mathbb{C}^K$ can be rewritten as

$$\mathbf{y} = \text{diag}(\mathbf{h}) f\left(\sum_{j=1}^{J} \mathbf{x}_j\right) + \mathbf{n}, \tag{3.1}$$

where diag $(\cdot)$ is a diagonal matrix with $(\cdot)$ as its diagonal elements, J denotes the number of overlapped users. Denoting x_{sat} as the saturation voltage, and p as the severity/slope of the PA

[1] Note that in Mitra *et al.* (2020a), it is proved than an RFF delivers significantly lower approximation error than any polynomial based solution under a fixed implementation budget.

nonlinearity. The PA nonlinearity $f(\cdot)$ is either modelled as an AM-AM type Rapp nonlinearity Gharaibeh (2011), which is expressed as

$$f(x) = \frac{x}{\left(1 + \left|\frac{x}{x_{\text{sat}}}\right|^{2p}\right)^{\frac{1}{2p}}} \tag{3.2}$$

or as a Modified (AM-PM) Rapp nonlinearity Dudak & Kahyaoglu (2012) which is expressed as

$$\begin{aligned} |f(x)| &= \frac{|x|}{\left(1 + \left|\frac{x}{x_{\text{sat}}}\right|^{2p}\right)^{\frac{1}{2p}}}, \\ \angle f(x) &= \angle x + \frac{\epsilon\,|x|^{q_1}}{1 + \left(\frac{|x|}{\gamma}\right)^{q_2}}, \end{aligned} \tag{3.3}$$

where $\epsilon = 0.0747$, $\gamma = 0.1281$, $q_1 = -0.03462$, $q_2 = -1.758$, $|\cdot|$ denotes the absolute value, and $\angle(\cdot)$ denotes the angle of $(\cdot)$.

3.4 Proposed Detection Algorithm

In this section, we outline a supervised technique for recovering/unwarping the distorted received signal, and proceed to performing MPA to recover the users' bits.

3.4.1 RFF Based Unwarping

In this section, we outline the technique of unwarping y using the pilots $\mathbf{p}_j$ in each user's transmission frame for each coherence-time. It is further assumed that the pilot-sequences are commonly agreed upon between the transmitter and the receiver Tse & Viswanath (2005), and that there is no interference between the users' pilots (or pilot contamination). Using these pilots, the reference signal, $\mathbf{y}_{\text{ref}}$, is formed as follows

$$\mathbf{y}_{\text{ref}} = \text{diag}(\mathbf{h}) \sum_{j=1}^{J} \mathbf{p}_j. \tag{3.4}$$

Next, to mitigate nonlinearity, the received signal during the training-phase, denoted by $\mathbf{y}_{\text{tr}}$, is mapped to an approximate RKHS using an RFF map $\boldsymbol{\Psi} : \mathbb{R}^{2K} \rightarrow \mathbb{R}^{n_G}$ as follows

$$\boldsymbol{\Psi}(\boldsymbol{\xi}) = \sqrt{\frac{2}{n_G}} \begin{bmatrix} \cos(\boldsymbol{\omega}_1^T \mathbf{z} + b_1) \\ \vdots \\ \cos(\boldsymbol{\omega}_{n_G}^T \mathbf{z} + b_{n_G}) \end{bmatrix} \tag{3.5}$$

where $\boldsymbol{\xi} \in \mathbb{C}^K$ denotes an independent variable, the variable $\mathbf{z} \in \mathbb{R}^{2K}$ is defined as follows:

$$\mathbf{z} = (\text{real}[\boldsymbol{\xi}], \ \ \text{imag}[\boldsymbol{\xi}])^T,$$

and each $\{\boldsymbol{\omega}_i\}_{i=1}^{n_G}$ is a Gaussian vector, with zero mean and covariance $\frac{1}{\sigma^2}\mathbb{I}_{n_G}$, with $\mathbb{I}_{n_G}$, σ , and n_G denoting the identity matrix of size n_G , the kernel-width, and the number of RFF-dimensions respectively. Finally, $(\cdot)^T$ denotes the transpose operation.

Next, the unwarping weights $\mathbf{W}$ are estimated using zero-forcing in RKHS as

$$\mathbf{W} = \boldsymbol{\Psi}(\mathbf{y}_{\text{tr}})^{T^{\dagger}}_{(1:\mathcal{P})} \mathbf{y}_{\text{ref}_{(1:\mathcal{P})}} \tag{3.6}$$

where $(\cdot)^{\dagger}$ denotes the pseudo-inverse operation, $\mathcal{P}$ denotes the number of pilots, and $(\cdot)_{1:\mathcal{P}}$ denotes a matrix consisting of the vectors $(\cdot)$ sampled/indexed by the pilots $1 : \mathcal{P}$. Finally, after estimating $\mathbf{W}$ during the training interval, the refined unwarped observations are obtained as

$$\mathbf{y}' = \boldsymbol{\Psi}(\mathbf{y})^T \mathbf{W}. \tag{3.7}$$

3.4.2 Message Passing Algorithm

Using the recovered unwarped observation $\mathbf{y}'$, the MPA is performed assuming an AWGN channel to recover the users' bits. We denote the set of variable nodes (VN) corresponding to user-symbols as $\mathcal{J} = \{1, 2, \cdots, J\}$, and function nodes (FN) corresponding to y as $\mathcal{F} = \{1, 2, \cdots, K\}$. Further, in the context of message-passing, we denote the graph-neighborhood of a vertex i as $\mathcal{B}_i$. Let I_{jk} be the message between the j^{th} vertex to the k^{th} vertex, the users' bits are detected using MPA as outlined in Algorithm 3.1, where $\sum_{j=1}^{J} \mathbf{x}_j$ and $(\cdot)\,[k]$ denotes the k^{th} component of $(\cdot)$.

Algorithm 3.1 Message-Passing using RFF

1 Recover $\mathbf{y}'$ from $\mathbf{y}$ as per (3.7)

2 Initialize $I_{kj} = p(x_j)$ as a uniform distribution.

3 Initialize:

4 $$I_{jk} = p\left(\mathbf{y}'\,[k]\,|\mathbf{X}\right)$$

5 $$= \frac{1}{2\pi\sigma_n^2} \exp\left(- \frac{\left| y'[k] - h[k] \sum\limits_{j \in B_k} x_j[k] \right|^2}{\sigma_n^2} \right)$$

6 Initialize *MAXITER*.

7 **while** $c <$ *MAXITER* **do**

8 $I_{jk} := \log(p(\mathbf{x}_j)) + \sum\limits_{j \in \mathcal{B}_k} I_{kj}.$

9 $I_{kj} := \max\limits_{\forall \mathbf{x}_j \in C_j, k \in \mathcal{B}_j} \log(p(y'[k]|\mathbf{X})) + \sum\limits_{k \in \mathcal{B}_j} I_{jk}$

10 $c := c + 1$

11 **end while**

12 Using the converged messages I_{jk} and codebook C_j detect the user-symbols as in [Vaezi *et al.* (2019), eq. (12.12)]

In Algorithm 3.1, the received observations $\mathbf{y}$ are unwarped using an RFF for mitigating the PA nonlinearity in Step 1. Next, the a-priori messages are initialized in Step 2 and Step 3, and the

number of MPA iterations is fixed in Step 4. Consequently generic MPA is performed on the unwarped observations $\mathbf{y}'$ as detailed in Step 5, and the symbols are detected using the converged LLRs in Step 6.

3.5 Optimality of the Proposed Detection Algorithm

In this section, we attempt to explore optimality of the above mentioned algorithm. Revisiting the system model in (3.1), and invoking the Representer Theorem Schölkopf *et al.* (2001), we can alternatively write (3.1) as follows in RKHS $\mathcal{H}$ [2]

$$\mathbf{y} = \text{diag}(\mathbf{h}) < k_x, \mathbf{X} >_{\mathcal{H}} + \mathbf{n}, \tag{3.8}$$

where k_x is the evaluation functional for $f(\cdot)$, and $< \cdot, \cdot >_{\mathcal{H}}$ denotes an inner-product over RKHS $\mathcal{H}$. Further, using the closure property of RKHS, one can state that there exists an operator k_y on $\mathbf{y}$ such that

$$< k_y, \mathbf{y} >_{\mathcal{H}} = \text{diag}(\mathbf{h})\mathbf{X} + < k_y, \mathbf{n} >_{\mathcal{H}}, \tag{3.9}$$

Hence, it can be inferred from the above equation that the application of MPA on $< k_y, \mathbf{y} >_{\mathcal{H}}$, achieves a BER performance equivalent to an AWGN channel.

Although, $< k_y, \mathbf{y} >_{\mathcal{H}}$ is difficult to evaluate in general, it can be conveniently expressed using Gaussian kernels (or other Mercer kernels). Additionally, this inner product may also be approximated using RFFs Rahimi *et al.* (2007), i.e., we can write

$$\mathbf{y}' \approx < k_y, \mathbf{y} >_{\mathcal{H}} = \text{diag}(\mathbf{h})\mathbf{X} + < k_y, \mathbf{n} >_{\mathcal{H}} . \tag{3.10}$$

[2] Notably, we never utlize any explicit knowledge of the nature of $f(\cdot)$ for detection. Also, $f(\cdot)$ can change from one deployment scenario to the other;however, we would still be guaranteed a unique representation in RKHS.

Hence, it is concluded that in the presence of arbitrary PA nonlinearity, applying MPA on the unwarped observations $\mathbf{y}'$ delivers a detection-performance asymptotically equivalent to a linear AWGN channel.[3]

3.6 Effect of Unmitigated Nonlinearities

In this section, we investigate the deleterious effect on the convergence of the MPA in the hypothetical scenario where the nonlinear device characteristics remain unmitigated. By Bussgang's theorem Price (1958), another alternative expression of (3.1) can be written as

$$\mathbf{y} = \mathrm{diag}(\mathbf{h})\zeta\mathbf{X} + \mathrm{diag}(\mathbf{h})\mathbf{v} + \mathbf{n}, \tag{3.11}$$

where $0 < \zeta < 1$ denotes the statistical correlation coefficient between x and $f(x)$, and $\mathbf{v}$ denotes the distortion noise (whose exact probability density function is difficult to quantify in general and depends on the nonlinearity type). In the scenario where a hypothetical "naive" receiver makes an assumption of a linear Gaussian channel, it can be readily inferred that the incorrect choice of likelihood (i.e. hypothetically assuming a Gaussian likelihood as in Step-3 of Algorithm 1 without mapping to RFF) presents an irreducible error-floor in messages, which leads to error propagation in the MPA (in the terms I_{jk} and I_{kj}), which lead to convergences to a suboptimal solution, or even possible divergence depending on the dynamics of the error-propagation.

3.7 Simulations

In this section, computer simulations are presented to validate the presented analytical results. Without loss of generality, two complex codebooks are considered, with $K = 4$ and $J = 6$, to demonstrate the applicability of the proposed algorithm: i) a complex codebook from Klimentyev & Sergienko (2016) (denoted by CB1), and ii) a mutual information based codebook

[3] It can also be noted that the additive noise variance is conserved if a Gaussian kernel is used/approximated. This is due to the fact that $\|k_y\|^2_{\mathcal{H}} = 1$ for a Gaussian kernel.

Zhang *et al.* (2016) (denoted by CB2).[4] In addition, another codebook (denoted by CB3) that supports 9 users Sharma, Deka, Bhatia & Gupta (2018) was also considered with $K = 6$, and $J = 9$.

Without loss of generality number of RFF dimensions, n_G, was set to 50.[5] Furthermore, the kernel-width was estimated using the Silverman's rule of thumb. The nonlinearity was modeled using a Rapp nonlinearity (where we consider here both the AM-AM and AM-PM cases defined in (3.2) and (3.3) respectively) with a saturation voltage of 2.8[6] and results are presented for $p = 0.5, 1, 2$ (i.e. decreasing order of severity). The training is performed over temporal coherence-blocks, with pilots being transmitted in the beginning of each coherence-interval Zou, Kim, Ding, Wichman, Hamalainen, Lin & Chiang (2019). For the current treatment, orthogonal-pilots using pseudo-random bit sequences are utilized, which are widely deployed in LTE based systems Korowajczuk (2011). For the presented simulations, 50 pilots were utilized, which is in the same order as the number used in Klimentyev & Sergienko (2016). The slightly higher of pilots needed is understandable given the severity of the AM-AM and AM-PM nonlinearities. From the BER results depicted for the AM-AM nonlinearity in Fig. 3.1 and AM-PM nonlinearity in Fig. 3.2, it can be noted that for the unmitigated scenario, the effect of the nonlinearity on generic message-passing and the dynamics of the distortion over MPA iterations is quite unpredictable. Indeed, one can observe artefacts such as degradation in the BER upon reducing the AWGN variance and saturation of the BER at values of the order of 10^{-1}. In addition, it is also observed that the proposed RFF based MPA delivers improved BER performance compared to the MPA under the unmitigated scenario, and closely approaches the performance corresponding to MPA based detection for SCMA over an "ideal" linear channel

[4] Optimal codebook design remains out of the scope of the current study, as we primarily aim to mitigate the impairments using appropriate signal processing techniques.

[5] While n_G can be chosen arbitrarily high, since there is a monotonously decreasing dependence of the approximation error energy with increasing n_G Mitra *et al.* (2020a); however increasing n_G arbitrarily increases the computational complexity which necessitates truncation of n_G to a value that meets a sufficient level of performance/QoS.

[6] Choice of the saturation voltage is arbitrary; however it should be chosen lesser than the dynamic range of the input symbols to model sufficient degradation/impairment due to nonlinearity.

without any PA distortion. This renders the proposed approach attractive for practical SCMA based systems impaired by PA nonlinearities.

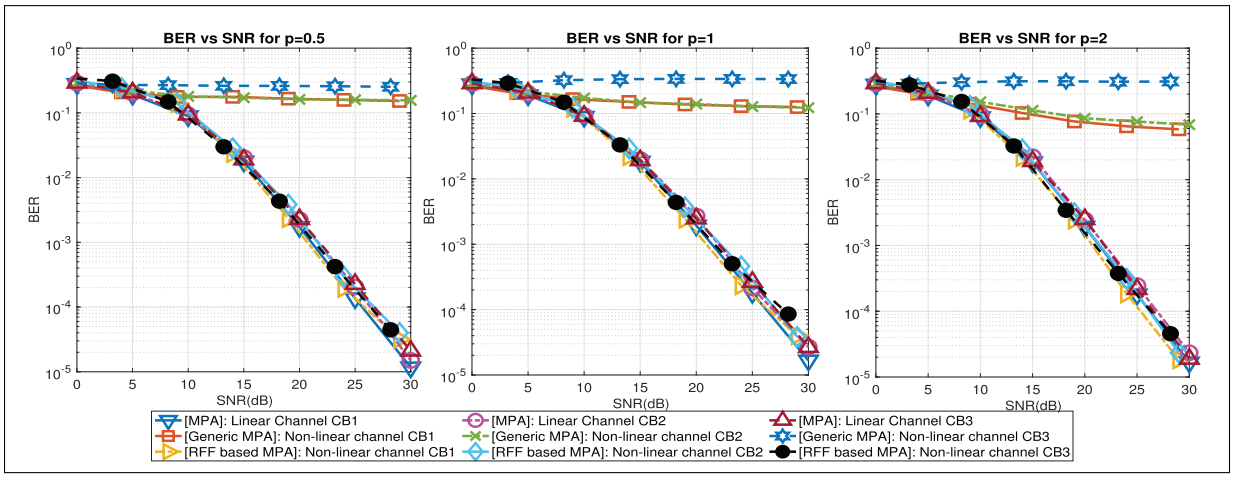

Figure 3.1 BER vs SNR comparison for SCMA in presence of AM-AM Rapp nonlinearity

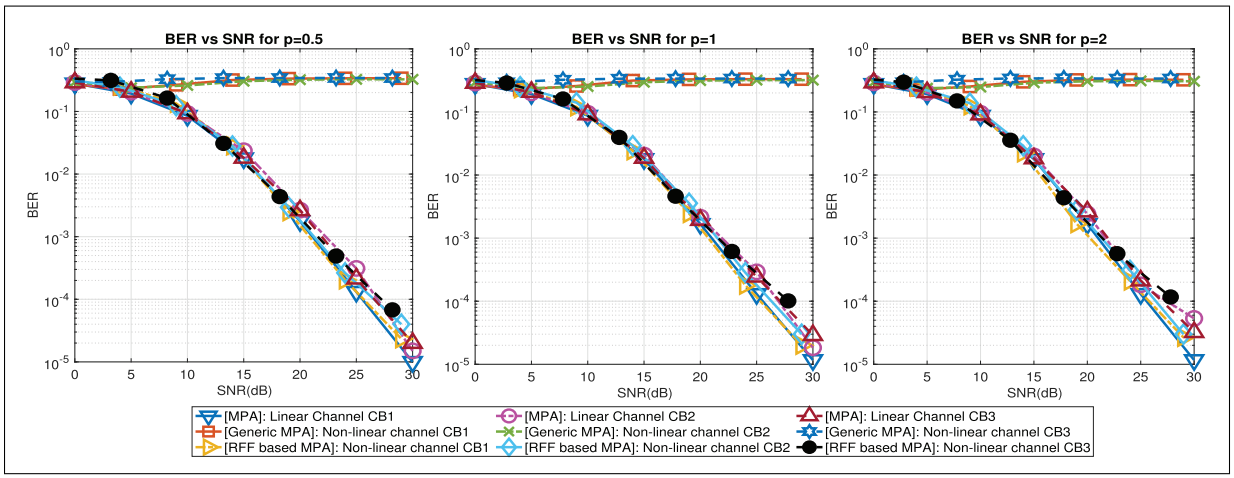

Figure 3.2 BER vs SNR comparison for SCMA in presence of AM-PM Rapp nonlinearity

3.8 Conclusion

In this letter an RFF based MPA detection technique for SCMA is proposed for mitigating PA nonlinearity. Analytical proofs are outlined that guarantee convergence of the proposed detection technique to the ideal linear AWGN channel in the presence of arbitrary PA nonlinearities and

the deleterious impact of unmitigated nonlinearities on the classical MPA based detection is highlighted. Furthermore, computer simulations are presented over Rayleigh fading channels, validating the above analytical results. Lastly, the presented simulations reveal that the proposed RFF based MPA detection technique delivers significantly improved BER performance compared to the classical MPA in the presence of PA nonlinearities, which makes the proposed algorithm viable for practical deployments.

CHAPTER 4

PERFORMANCE ANALYSIS OF MAXIMUM-CORRENTROPY BASED DETECTION FOR SCMA

Elie Sfeir[1] , Rangeet Mitra[1] , Georges Kaddoum[1] , and Vimal Bhatia[2]

[1] Department of Electrical Engineering, École de Technologie Supérieure,
1100 Notre-Dame Ouest, Montréal, Québec, Canada H3C 1K3
[2] Discipline of Electrical Engineering, IIT Indore,Indore 453552, India

Paper published in IEEE Communication Letters, 2020.

4.1 Abstract

Non-orthogonal multiple access (NOMA) has emerged as a promising multiple-access technique capable of accommodating many users over limited time-frequency resources. Among several NOMA techniques, sparse code multiple access (SCMA) has emerged as viable due to its promise of high coding-gain by appropriate codebook-design and simplistic detection using message-passing algorithm (MPA). However,the performance of classic SCMA based systems are severely impaired by impulsive noise (IN), which causes outages and therefore non-negligible degradations to the bit-error-rate (BER)performance. Exploiting the robustness of the maximum correntropy criterion (MCC) to non-Gaussian noise processes, an MPA based detector is formulated with message-functions derived from the MCC criterion. Based on the said MCC criterion, concurrent-adaptation of the MCC's spread-parameter is proposed in this letter. Lastly, analytical results for the proposed approach's BER performance are presented with corresponding validation by computer-simulations.

Index Terms— Impulsive noise, sparse code multiple access,information theoretic learning, maximum correntropy criterion.

4.2 Introduction

THE next-generation of communication systems must be able to service numerous users/devices with a reasonable quality-of-service over massively-connected ecosystems such as the industrial internet of things (IIoT) and several applications in industry 4.0 Dai, Wang, Ding, Wang, Chen & Hanzo (2018). In this regard,non-orthogonal multiple access (NOMA) has emerged as a disruptive solution for accommodating multiple users over limited time-frequency resources. NOMA can be broadly classified into Dai *et al.* (2018), Ding, Lei, Karagiannidis, Schober, Yuan & Bhargava (2017), Makki, Chitti, Behravan & Alouini (2020) and Vaezi *et al.* (2019): a) Power-domain NOMA (PD-NOMA), and b) Code-domain NOMA. PD-NOMA overlaps the users using superposition-coding, and detection is commonly done using successive interference cancellation (SIC) or message-passing algorithms (MPA) at the receivers. However, the number of users that can be supported by PD-NOMA is limited due to error-propagation across user-layers and dependence on power-diversity Bhatia, Swami, Sharma & Mitra (2020), Mitra & Bhatia (2017b) and Mitra & Bhatia (2018b). On the other hand, sparse code multiple access (SCMA) has emerged as a specific genre of code-domain NOMA Nikopour & Baligh (2013), Moltafet *et al.* (2017), Sharma *et al.* (2019b) and Sergienko & Klimentyev (2017), which enables coding/shaping-gains offered by codebook-design, the possibility of near-optimal detection using MPA, and robustness to error-propagation. However, most existing analyses of SCMA are performed assuming idealistic additive distortions, such as additive white Gaussian noise (AWGN). Notably, several of the beyond 5G ecosystems, such as IIoT, smart grid, and Industry 4.0, are significantly impaired by instantaneous outages in the signal to noise ratio caused by impulsive noise (IN) Lampe (2011), Yin, Zhu, Huang & Jiang (2018), Sharma, Bhatia & Mishra (2019a) and Selim, Alam, Evangelista, Kaddoum & Agba (2020a). Several models exist in the literature for various IN-distributions such as Middleton-Class A,Middleton-Class B, and Middleton Class C, which are further classified into either memoryless/memory-based approaches Spaulding & Middleton (1977), Bhatia, Mulgrew & Georgiadis (2006), Ndo, Labeau & Kassouf (2013) and Alam, Selim, Kaddoum & Agba (2020). From generic analytical studies on the achievable information-limits under these noise-models, and also from studies

specific to NOMA, a saturation in bit-error-rate(BER)/sum-rate is observed under these IN models due to the intermittent signal-to-noise ratio (SNR)-outages induced by the IN processes Wiklundh, Stenumgaard & Tullberg (2009).In the specific context of log-likelihood ratio (LLR) based message-passing algorithm (MPA) for SCMA-detection, to the best of our knowledge and belief, there is no existing work providing a generic solution for the mitigation of the effect of IN processes (though there is literature which rigorously addresses PD-NOMA in Selim *et al.* (2020b)). Additionally, specific works in the context of detection under IN suggest LLR-clipping to reject the IN-induced outliers Alam *et al.* (2020), Mestrah (2019). However, it is noteworthy that a poor choice of the thresholds causes these clipping methods to adversely affect the shape of the LLR for the samples that are not affected by IN, which in turn affects the performance of LLR-based detection.

Contributions: Motivated by notions of information-potentials (IP) Chen *et al.* (2013) in information-theoretic learning (ITL),a maximum-correntropy criterion (MCC) based detection method (which can be motivated as an online estimate of the Renyi-α information-potential with $\alpha = 2$) is formulated in this letter. The proposed method counters the IN-induced outliers by propagating these IP-gradients across the MPA iterations, whose robustness to IN is established through the presented analytical proofs. In addition, a concurrent online method of estimating the spread-parameter of the MCC criterion is derived. Using the notion of generalized SNR (GSNR) Polcari (2013), the converged LLR is linked to the BER performance to quantify the achieved performance gains analytically. Lastly, the presented analysis is validated by relevant computer-simulations over various fading channel distributions.

4.3 System Model

In this section, the considered system model is outlined for IN-impaired downlink SCMA. In this regard, a binary independent and identically distributed (i.i.d) bit-stream is considered, which is grouped and consequently mapped to respective codewords $\left\{\mathbf{x}^{(j)} \in C^{(j)}\right\}_{j=1}^{J}$, where $\mathbf{x}^{(j)} \in \mathbb{C}^{V}$, and the number of codewords in each codebook is denoted as $\text{Card}[C^{(u)}] = M$, with M denoting the modulation-order and Card $[\cdot]$ denotes the number of vectors in the codebook. Consequently,

the codewords are overlapped to form the overall superposition $\mathbf{X}$ and transmitted through the wireless channel.The observations at the receiver, denoted as $\mathbf{y}$, is expressed as[Vaezi *et al.* (2019), Eq. (12.3)]:

$$\mathbf{y} = \text{diag}(\mathbf{h}) \underbrace{\sum_{j=1}^{J} \mathbf{x}^{(j)}}_{\mathbf{x}} + \mathbf{n}, \tag{4.1}$$

where $\text{diag}(\cdot)$ denotes a diagonal matrix consisting of the elements of $(\cdot)$, and $\mathbf{h}$ denotes the channel-gains drawn from a distribution with probability denisty function (p.d.f) $p(h)$. In this letter, no a-priori assumptions are enforced on the distribution of $\mathbf{h}$. Furthermore, the complex noise vector, denoted as $\mathbf{n} = [n_1, n_2, \cdots, n_V]^T$, where each $n_i \sim p(n)$ is drawn from a two-component memoryless approximation of the Middleton Class A noise-model (which is widely followed due to its tractability Selim *et al.* (2020b)), which can be expressed as:

$$p_A(n) = \frac{\alpha}{2\pi\sigma_n^2} \exp\left(-\frac{|n|^2}{2\sigma_n^2}\right) + \frac{\beta}{2\pi\sigma_I^2} \exp\left(-\frac{|n|^2}{2\sigma_I^2}\right), \tag{4.2}$$

where $\alpha, \beta < 1$ are probabilistic weights (i.e, $\alpha + \beta = 1$) for the Gaussian-mixture in the above equation and σ_n^2 and σ_I^2 denotes the variances of the AWGN and the IN-components, respectively. In the sequel, quantities corresponding to AWGN are denoted using the suffix $(\cdot)_n$, and quantities corresponding to IN by the suffix $(\cdot)_I$. Notably, the ratio between these components, denoted as $\Gamma = \frac{\sigma_I^2}{\sigma_n^2}$, is a measure for severity of the additive noise.

4.4 Proposed Max-Correntropy Receiver

In this section, the proposed detection technique is outlined based on the system-model derived above. In this regard, an MCC Chen *et al.* (2013) based message-passing algorithm is formulated, which provides robustness to outliers introduced by IN. This technique may be physically interpreted as a "flow of IP", which has roots in statistical physics, and is thus guaranteed to achieve "thermal-equilibrium" at convergence. In this regard, it can also be noted that the MCC can be treated as an online estimate of the Renyi-α information potential with $\alpha = 2$.

In general, the MPA based detection is performed by propagating the log $(\cdot)$ of the conditional p.d.f between the function-nodes $j = 1, 2, \cdots, V$ and the variable nodes $k = 1, 2, \cdots, J$ [Vaezi *et al.* (2019), pp. 377]. In what follows, $\mathcal{B}_k$ denotes a graph-theoretic neighborhood of a node k of the resulting Tanner-graph between the function nodes and variable nodes [Vaezi *et al.* (2019), Sec. 12.1.1.3].

Under AWGN, The conditional p.d.f of y conditioned on $\mathbf{X}$ is denoted as:

$$p(y[k]|\mathbf{X}) = \frac{1}{2\pi\sigma_n^2} \exp\left(- \frac{\left| y[k] - h[k] \sum\limits_{\forall j \in \mathcal{B}_k} x[k] \right|^2}{\sigma_n^2} \right).$$

In the context of the log-max MPA for generic AWGN channels, the propagated messages m_{jk} are $\log[p(y[k]|\mathbf{X})]$, which for the AWGN case is denoted as:

$$m_{jk} = \frac{-\left| y[k] - h[k] \sum\limits_{\forall j \in \mathcal{B}_k} x[k] \right|^2}{\sigma_n^2}. \tag{4.3}$$

However, in the case of IN there are instantaneous outages in the detection due to the errors in the messages m_{jk} . In the considered two-component Gaussian-mixture IN, the expected value of the error in the messages for the classical MPA, Δm_{jk} , is expressed as follows using the expression for the Kullback-Leibler divergence between two zero-mean Gaussians Cover (1999):

$$\begin{aligned} \mathbb{E}[\Delta m_{jk}] &= -\mathbb{E}_p[m_{jk}] + \mathbb{E}_{p_A}[m_{jk}] \\ &= \underbrace{\beta(\Gamma - 1)}_{\Omega} \end{aligned} \tag{4.4}$$

where $\mathbb{E}[\cdot]$ denotes statistical expectation. It can be noted that these IN-induced transients occur with probability β, which is small in general; however the energy of these transients is large which makes Ω non-negligible.

To mitigate the effect of these erroneous messages in MPA, and to suppress outliers, it is proposed to propagate the energy of the gradients of MCC, which is more robust to IN-induced outliers as a learning criterion. Mathematically, this is re-expressed as:

$$\begin{aligned}\xi_{jk} = &\frac{-\left|y[k] - h[k] \sum\limits_{\forall j \in \mathcal{B}_k} x[k]\right|^2}{\sigma_n^2} \\ &\times \exp\left(-\theta\left|y[k] - h[k] \sum_{\forall j \in \mathcal{B}_k} x[k]\right|^2\right),\end{aligned} \tag{4.5}$$

with θ denoting the hyperparameter of the MCC. Using the definition of m_{jk} in (4.3), (4.5) is re-expressed as:

$$\xi_{jk} = m_{jk} \exp(\theta \sigma_n^2 m_{jk}). \tag{4.6}$$

Thus, the instantaneous error in the derived message is expressed as:

$$\Delta\xi_{jk} = \Delta m_{jk} \exp(\theta \sigma_n^2 m_{jk})(1 + \theta \sigma_n^2 m_{jk}). \tag{4.7}$$

From the above expression for the instantaneous error in the message, the corresponding expected value under the two-component Gaussian-mixture p.d.f can be written as:

$$\begin{aligned}\mathbb{E}[\Delta\xi_{jk}] = &\alpha\Omega\mathbb{E}_{e[k]\sim\mathcal{N}(0,\sigma_n^2)}[\exp(-\theta|e[k]|^2)(1 - \theta|e[k]|^2)] \\ &+ \beta\Omega\mathbb{E}_{e[k]\sim\mathcal{N}(0,\sigma_I^2)}[\exp(-\theta|e[k]|^2)(1 - \theta|e[k]|^2)].\end{aligned} \tag{4.8}$$

Denoting $e[k] = y[k] - h[k] \sum\limits_{\forall j \in \mathcal{B}_k} x\,[k]$, the expected value of $\Delta\xi_{jk}$ can therefore be expressed as:

$$\mathbb{E}[\Delta\xi_{jk}] = \frac{\alpha(1 + \theta\sigma_n^2)\Omega}{(1 + 2\sigma_n^2\theta)^{\frac{3}{2}}} + \frac{\beta(1 + \theta\sigma_I^2)\Omega}{(1 + 2\sigma_I^2\theta)^{\frac{3}{2}}}. \tag{4.9}$$

To counter IN, it is essential to derive an appropriate value of θ which ensures an improvement over the unmitigated scenario, i.e.,

$$\frac{\alpha(1+\theta\sigma_n^2)\Omega}{(1+2\sigma_n^2\theta)^{\frac{3}{2}}}+\frac{\beta(1+\theta\sigma_I^2)\Omega}{(1+2\sigma_I^2\theta)^{\frac{3}{2}}}\leq \nu\Omega, \tag{4.10}$$

for $0<\nu<1$. Denoting constants $\phi_1=\log(1+\theta\sigma_n^2)$, $\phi_2=\frac{3}{2}\log(1+2\theta\sigma_n^2)$, $\phi_3=\log(1+\theta\sigma_I^2)$, and $\phi_4=\frac{3}{2}\log(1+2\theta\sigma_I^2)$. Using these variables, and assuming $\sigma_n^2\rightarrow 0$ at high SNR, from (4.10) the following approximation is derived:

$$\nu\approx\alpha\exp\left(-\frac{2\theta\sigma_n^2}{1+2\theta\sigma_n^2}\right)+\beta\sqrt{\frac{1}{2\sigma_I^2\theta}}. \tag{4.11}$$

From inspection of the above equation, ν is guaranteed to be less than one, which guarantees the existence of a "rich" range of values of θ for which $0<\nu<1$. It should be additionally noted that achieving $\nu=0$ is infeasible for any value of θ, which implies that there is always a (though a significantly reduced) gap between the performance of the proposed MCC based MPA and the MPA under AWGN.

Though the central theme of this letter aligns with the formulation of an MCC based MPA for IN impaired SCMA, an analytical result is presented below, which holds for generic noises which may/may not be drawn from a Middleton Class-A distribution. To simplify the following exposition, an error-term, $e[k]$, is defined below as:

$$e[k]=y[k]-h[k]\sum_{\forall j\in\mathcal{B}_k}x[k]. \tag{4.12}$$

Using a batch of B error samples denoted as $\{e_i\}_{i=1}^{B}$ with arbitrary statistics, the p.d.f of e is expressed by a non-parametric Parzen window representation as follows Bhatia *et al.* (2006),

Bhatia & Mulgrew (2007):

$$p_{\mathrm{NP}}(e) = \frac{1}{B}\sum_{i=1}^{B}\kappa_{\gamma}(e - e_i), \tag{4.13}$$

where $\kappa_{\gamma}(\cdot)$ is a Gaussian function denoted as:

$$\kappa_{\gamma}(\cdot) = \frac{1}{\sqrt{2\pi\gamma^2}}\exp\left(-\frac{(\cdot)^2}{2\gamma^2}\right). \tag{4.14}$$

(4.3) is simplified as follows under the distribution $p(e)$:

$$\mathbb{E}_{p_{\mathrm{NP}}}[\Delta m_{jk}] = \frac{\sum_{i=1}^{B}(e_i^2 + \gamma^2)}{B\sigma_n^2}. \tag{4.15}$$

Notably, $\mathbb{E}[\Delta m_{jk}]$ derived above for the classical MPA is not guaranteed to converge since the error-energy is not guaranteed to be bounded in general for the α-stable noise distribution. On the other hand, (4.5) is expressed as:

$$\mathbb{E}_{p_{\mathrm{NP}}}[\Delta \xi_{jk}] = \mathbb{E}_{p_{\mathrm{NP}}}[\Delta m_{jk}\exp(\theta\sigma_n^2 m_{jk})(1 + \theta\sigma_n^2 m_{jk})]. \tag{4.16}$$

Assuming independence of Δm_{jk} and m_{jk} , the following simplification is achieved:

$$\mathbb{E}_{p_{\mathrm{NP}}}[\Delta \xi_{jk}] = \frac{\sum_{i=1}^{B}(e_i^2 + \gamma^2)}{B\sigma_n^2}\mathbb{E}_{p_{\mathrm{NP}}}[\exp(-\theta e^2)(1 - \theta e^2)], \tag{4.17}$$

which is further simplified as:

$$\mathbb{E}_{p_{\mathrm{NP}}}[\Delta\xi_{jk}] = \left[\frac{\sum_{i=1}^{B}(e_i^2+\gamma^2)}{B\sigma_n^2\sqrt{2\gamma^2\theta+1}} - \frac{\theta\sum_{i=1}^{B}\sum_{j=1}^{B}(e_j^2+\gamma^2)\left(e_i^2+\frac{\gamma^2}{2\gamma^2\theta+1}\right)}{B^2\sigma_n^2}\right]. \tag{4.18}$$

From (4.15) and (4.18) it is directly concluded that for appropriately chosen θ , $\mathbb{E}_{p_{\mathrm{NP}}}[\Delta\xi_{jk}] < \mathbb{E}_{p_{\mathrm{NP}}}[\Delta m_{jk}]$ which leads us to the following theorem:

Theorem 1: *As compared to the classical MPA which is ML-optimal for AWGN, the proposed MCC based MPA offers higher robustness to errors in the messages caused by generic non-Gaussian noise processes.*

4.5 Recursive Information-Theoretic Estimation of θ

In this section, a recursive information-theoretic estimation technique is proposed for tracking θ. Under the considered two-component Middleton Class-A model for the additive noise n, the difference in the messages is given by:

$$\Delta\xi_{jk} \propto \log m - \log p_A \exp(\theta\sigma_n^2 \log p_A), \tag{4.19}$$

where $\log p$ corresponds to the potential under AWGN, and $\log p_A$ corresponds to the potential under the considered Middleton class A model for the additive noise vector $\mathbf{n}$. Here, (4.19) is be factorized as:

$$\Delta\xi_{jk} \propto \log p_A \left[\frac{\log p}{\log p_A} - p_A^{\theta(t)\sigma_n^2}\right]. \tag{4.20}$$

The above equation is re-expressed as:

$$\Delta\xi_{jk} = -\frac{\alpha|e|^2}{\Gamma\sigma_n^2}(1 - p_A^{\theta(t)\sigma_n^2}) + \beta\left(\frac{|e|^2(\Gamma-1)}{\Gamma\sigma_n^2}\right). \tag{4.21}$$

Assuming $\sigma_n^2 \to 0$, $\alpha \approx 1$, and letting $\Delta\xi_{jk} \to 0$, θ is expressed as follows:

$$\theta = \frac{\beta\Gamma\sigma_n^2}{|e|^2[1+\beta(\Gamma-1)]}. \tag{4.22}$$

Therefore, one arrives at the following moving-average update for θ :

$$\theta := \Xi\theta + (1-\Xi)\frac{\Gamma\sigma_n^2}{|e|^2[1+\beta(\Gamma-1)]}, \tag{4.23}$$

where $0 < \Xi < 1$ denotes the forgetting factor. Based on the presented MCC based MPA in the previous section and the hyperparameter-estimation/tracking outlined in this section, the proposed algorithm is summarized in Algorithm 4.1.

Algorithm 4.1 MCC Based MPA

Initialize $I_{kj} = p(x_j)$ as a uniform distribution.
Initialize: $I_{jk} := |\Delta J_{MCC}|^2$
where, $|\Delta J_{MCC}|^2$ is calculated as per (4.5).
Initialize *MAXITER*.
while $c <$ *MAXITER* **do**
$I_{jk} := \log(p(\mathbf{x}_j)) + \sum_{j \in \mathcal{B}_k} I_{kj}$.
$I_{kj} := \max_{\forall \mathbf{x}_j \in C_j, k \in \mathcal{B}_j} \log(p(y'[k]|\mathbf{X})) + \sum_{k \in \mathcal{B}_j} I_{jk}$
Adapt θ as per (4.23). $c := c + 1$
end while
Using the converged messages I_{jk} and codebook C_j detect the user-symbols as in [Vaezi *et al.* (2019), eq. (12.12)]

4.6 BER Analysis

In this section, analytical results are presented to link the error-rate performance of the proposed approaches, with the expression for the errors in messages. For this purpose, the concept of GSNR, which links the converged LLR to the BER is invoked. Under AWGN, the generalized SNR is proportional to the converged LLR upto a scaling factor.

Hence, the error in the message floor can be directly converted to a corresponding SNR floor as mentioned next. First, a given channel $\mathbf{h}$ with arbitrary statistics is assumed and the converged

GSNR is denoted as SNR^* , under which the BER achieved under AWGN, BER_{AWGN} , is denoted as a function that depends on the statistics of the channel-gain, say $\psi_{p(h)}(\text{SNR}^*)$[1]

$$\text{BER}_{\text{AWGN}} = \psi_{p(h)}(\text{SNR}^*). \tag{4.24}$$

Using the definition of generalized SNR, and from (4.4), one can re-write the above BER-expression for the unmitigated IN-impaired scenario as follows:

$$\text{BER}_{\text{IN}} \approx \psi_{p(h)}(\text{SNR}^*) + |\psi'(\text{SNR}^*)|\mathbb{E}[\Delta m_{jk}]. \tag{4.25}$$

Further, the BER expression for the MCC based MPA is quantified as:

$$\text{BER}_{\text{IN}} \approx \psi_{p(h)}(\text{SNR}^*) + |\psi'_{p(h)}(\text{SNR}^*)|\mathbb{E}[\Delta \xi_{jk}]. \tag{4.26}$$

In the next section, the validity of these BER expressions is verified and the robustness of our approach to varying IN-levels is demonstrated using computer simulations.

4.7 Results and Discussion

In this section, computer-simulations are presented to validate the proposed MCC based MPA. The simulated and analytical results are depicted in Fig. 4.1 for one-sided Gaussian fading and Fig. 4.2 for Rayleigh fading, where, [S] and [A] denote simulated and analytical curves, respectively. From Figs. 4.1 and 4.2, it is observed that the proposed MCC based MPA successfully mitigates the IN. Moreover, it is noticed from Fig. 4.1, that MCC based MPA does not fully nullify the effect of IN, which is in line with the analysis presented in Section V.

[1] $\psi_{p(h)}$ arises as expectation of Q-function under the distribution for the channel-gain of $\mathbf{h}$.Some specific works in the context of the Rayleigh channel are found in [Vaezi *et al.* (2019), Sec. 12.2.1], Bao, Ma, Xiao, Ding & Zhu (2017), and for VLC systems with random waypoint mobility model Mitra, Sharma, Kaddoum & Bhatia (2020c).

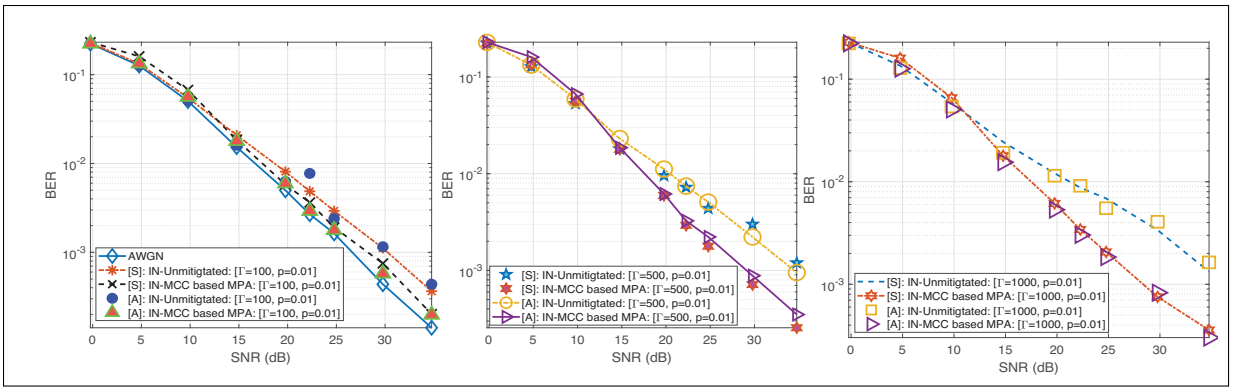

Figure 4.1 BER vs SNR comparison for SCMA in presence of AM-AM Rapp nonlinearity under One-sided Gaussian fading

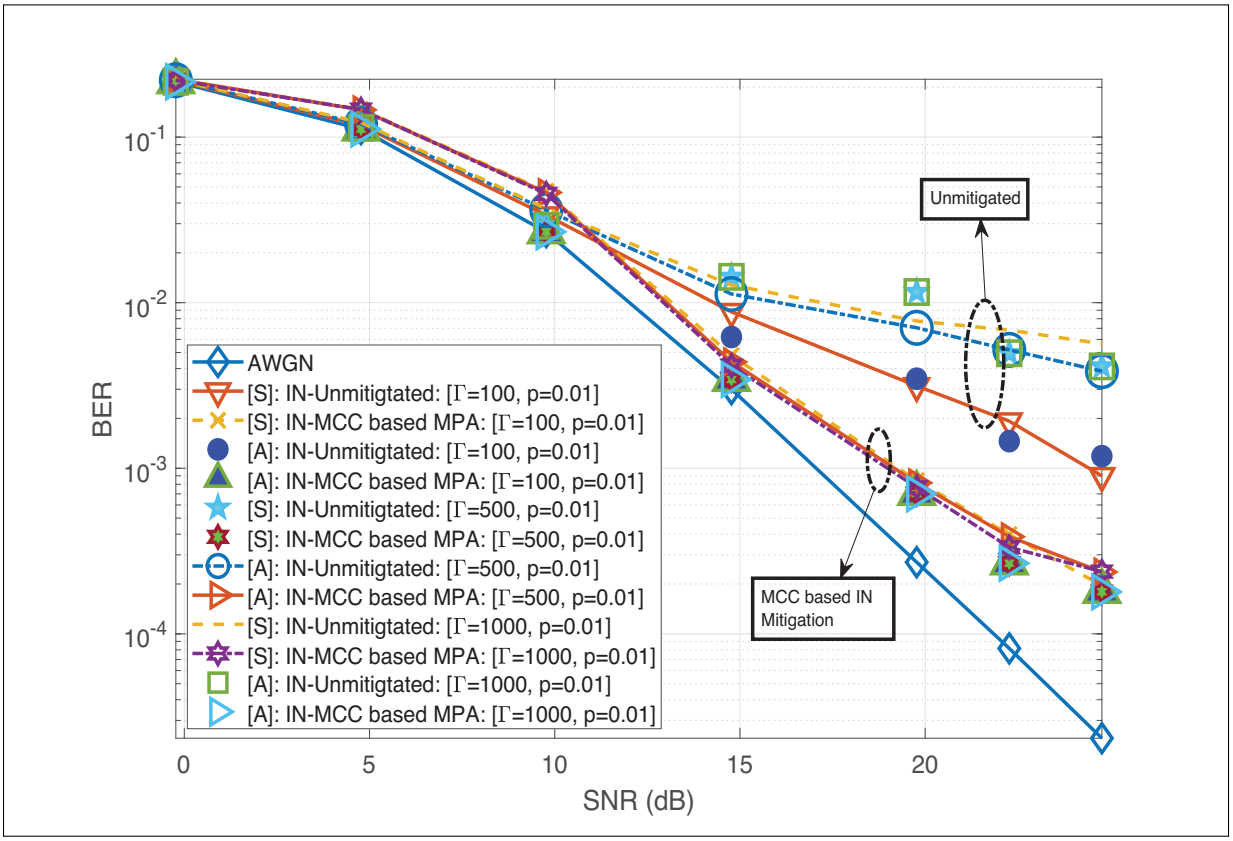

Figure 4.2 BER vs SNR comparison for SCMA in presence of AM-AM Rapp nonlinearity under Rayleigh fading

However, one can observe that the extent of degradation caused by increasing magnitudes of IN is significantly lower for the proposed MCC-based MPA as compared to the unmitigated scenario. In this regard, one can observe from Figs. 4.1 and 4.2 that the performance of the MCC based MPA is almost invariant across varying IN levels and gives performance gains ranging from half a decade to a full decade of BER as Γ increases from 100 to 1000 at SNR above an SNR of 20 dB. Furthermore, in Figs. 4.1 and 4.2, the corresponding simulated BER plots are validated using analytical results obtained using (4.25) and (4.26). To implement (4.25) and (4.26) by obtaining the analytical coordinates corresponding to the unmitigated scenario and for the MCC based MPA, the BER-coordinates corresponding to the AWGN performance, $\psi(\cdot)$, are used. Additionally, for substitution in (4.25) and (4.26), $\psi'(\cdot)$ is estimated by performing numerical-differences on the BER curve corresponding to the AWGN scenario. Furthermore, one can observe a close agreement between the simulated and the analytical plots, which, together with the BER performance gains and achieved robustness to IN, ratifies the presented analysis and makes the proposed algorithm viable for IN-impaired scenarios.

Computational Complexity: The classical MPA has a computational complexity $\mathcal{O}(MJV^{d_f})$ Vaezi *et al.* (2019), Vameghestahbanati, Bedeer, Marsland, Gohary & Yanikomeroglu (2017), Al-Nahhal, Dobre, Basar & Ikki (2019), Al-Nahhal, Dobre & Ikki (2020), where d_f denotes the number of layers occupying each resource. It is noted that the proposed MPA based approach has similar complexity since the only difference lies in calculation of the messages as in (4.5). For the proposed approach, one more multiplication and an extra exponentiation is required for each message-calculation, and in that it has slightly higher implementation complexity than the classical MPA. However, the order of complexity for the proposed approach is not affected by the extra computations, and is still $\mathcal{O}(MJV^{d_f})$. Furthermore,[2] the proposed MCC based MPA offers significantly higher robustness to IN and independence across various deployment-scenarios/IN-parameter-values, which offsets the slight increase in the computational complexity.

[2] Notably, this makes our analytical framework independent of channel statistics; one can directly "measure" the IN-induced degradation in BER by benchmarking with the AWGN performance.

4.8 Conclusion

In this letter, an MCC based MPA was proposed for SCMA detection that relies on the propagation of IP-gradients rather than classical LLR-based approaches. The proposed MCC based method was analytically found to deliver improved BER performance and offer improved robustness to different IN levels. Furthermore, BER-expressions were derived for the proposed MCC based MPA and the unmitigated scenario. For both scenarios, a close agreement is observed between the corresponding analytical and simulated BER values. The achieved performance-gains, and the robustness to IN offered by the MCC based MPA make the proposed approach viable for practical SCMA systems over IN-impaired scenarios.

ACKNOWLEDGMENT

The authors acknowledge the Richard J. Marceau (RJM) Chair.

CHAPTER 5

COMPARATIVE ANALYTICAL STUDY OF SCMA DETECTION METHODS FOR PA NONLINEARITY MITIGATION

Elie Sfeir[1] , Rangeet Mitra[1] , Georges Kaddoum[1] , and Vimal Bhatia[2]

[1] Department of Electrical Engineering, École de Technologie Supérieure,
1100 Notre-Dame Ouest, Montréal, Québec, Canada H3C 1K3
[2] Discipline of Electrical Engineering, IIT Indore,Indore 453552, India

Paper published in MDPI sensors Journal, December 2021.

5.1 Abstract

Non-orthogonal multiple access (NOMA) has emerged as a promising technology that allows for multiplexing several users over limited time-frequency resources. Among existing NOMA methods, sparse code multiple access (SCMA) is especially attractive; not only for its coding gain using suitable codebook design methodologies, but also for the guarantee of optimal detection using message passing algorithm (MPA). Despite SCMA's benefits, the bit error rate (BER) performance of SCMA systems is known to degrade due to nonlinear power amplifiers at the transmitter. To mitigate this degradation, two types of detectors have recently emerged, namely, the Bussgang-based approaches and the reproducing kernel Hilbert space (RKHS)-based approaches. This paper presents analytical results on the error-floor of the Bussgang-based MPA, and compares it with a universally optimal RKHS-based MPA using random Fourier features (RFF). Although the Bussgang-based MPA is computationally simpler, it attains a higher BER floor compared to its RKHS-based counterpart. This error floor and the BER's performance gap are quantified analytically and validated via computer simulations.

Keywords: PA nonlinearity; Bussgang-based approach; SCMA; RKHS

5.2 Introduction

Next-generation communication systems must be capable of providing several users/ devices with appropriate service levels for the industrial internet of things (IIoT) and Industry 4.0 Dai *et al.* (2018). In the context of multiple-access techniques for these ecosystems, non-orthogonal multiple access (NOMA) has emerged as a promising solution that has the potential to support several users over a finite number of temporal/spectral resources. NOMA-based approaches are broadly categorized into the following types Dai *et al.* (2018); Vaezi *et al.* (2019): (a) power domain NOMA (PD-NOMA), and (b) code domain NOMA. PD-NOMA uses superposition coding to overlap multiple users and detects corresponding user symbols on the receiver side by successive interference cancellation (SIC) or message passing algorithms (MPAs). However, PD-NOMA is known to support a limited number of users due to inter-layer error propagation, and its reliance on power diversity Bhatia *et al.* (2020); Mitra & Bhatia (2017b, 2018b). Apart from PD-NOMA, specific code-domain NOMA-based approaches, like sparse code multiple access (SCMA) have recently been found to be particularly promising Nikopour & Baligh (2013); Moltafet *et al.* (2017); Sharma *et al.* (2019b); Sergienko & Klimentyev (2017), as they not only allow for potential coding/shaping gains through codebook design, but also enable near-optimal detection using MPAs. Besides, SCMA is also known for its robustness to error propagation.

However, transmit-side power amplifier (PA) nonlinearities have been found to degrade the performance of generic SCMA systems. From Bussgang's theorem Price (1958), transmit-side PA nonlinearity is known to add an independent equivalent distortion noise term that lowers the overall signal-to-noise ratio. Two types of competing MPA-based detection methods exist to mitigate this degradation: (a) Bussgang decomposition-based MPA detectors Yang *et al.* (2018) and (b) random Fourier feature (RFF)-based detectors Sfeir, Mitra, Kaddoum & Bhatia (2020b). While decomposition-based approaches achieve commendable performance under a limited implementation budget, the RFF based approaches offer benefits like universal approximation and generalization across various types of nonlinear PA characteristics. However, RFF-based approaches have slightly more computational overhead, and in certain hardware limited IIoT ecosystems, the implementation complexity of algorithms outweighs the error-floor reached

subject to the achievement of a minimum level of quality of service (QoS) Samie, Tsoutsouras, Xydis, Bauer, Soudris & Henkel (2016); Baek & Kaddoum (2020); Evangelista *et al.* (2019b). Therefore, it is compelling to compare and derive analytical insights/comparisons on the error floors of the Bussgang-based MPA methods and to decide on the suitability of a detector for a given bit error rate (BER)-based on the QoS. Several works in the literature have studied the nonlinearity effect not only in SCMA but also in other environments, such as Guerreiro, Dinis, Montezuma & Campos (2020), where a Bussgang-based receiver design was proposed for nonlinear PD-NOMA. Moreover, in Sfeir *et al.* (2020b), a nonlinear SCMA system model was studied, and a RFF-based solution was proposed to improve BER performance as equivalent to that obtained in the presence of a linear AWGN channel, whereas an iterative method based on clipping noise was proposed in Yang *et al.* (2018). Additionally, in Anand *et al.* (2021), RFF-KLMS based algorithm was proposed to mitigate nonlinearity in MIMO-VLC channels.

Contributions: In this paper, we present rigorous analytical studies and insights on the optimality of the Bussgang-based MPA for downlink SCMA with PA impairments. From our analysis, the Bussgang-based MPA detector is found to reach a non-negligible BER floor compared to the universally optimal RFF-based MPA, and the analytical results are presented to quantify the BER floor. Next, these results are validated using computer simulations under different fading distributions. The quantification of this error floor could potentially allow for switching between detection methods in hardware-constrained IIoT environments, where meeting a specific QoS constraint with minimal computations is of paramount importance.

5.3 System Model

In this section, we describe the system model considered. We consider a downlink SCMA scenario, in which the users' bitstreams (considered binary, independent and identically distributed) are grouped and mapped to respective codewords from a codebook $\left\{\mathbf{x}^{(j)} \in C^{(j)}\right\}_{j=1}^{J}$, where each codeword, $\mathbf{x}^{(j)} \in \mathbb{C}^{V}$. Furthermore,the number of codewords in each codebook is denoted by $\text{Card}[C^{u}] = M$, with M denoting the modulation order, and $\text{Card}[\cdot]$ denoting the number of vectors in a codebook. In this paper, we consider a downlink SCMA system as

in (Vaezi *et al.* (2019) Equation (12.3)), where the users' codewords are overlapped and the superposition, $\mathbf{x}$, is broadcast through the channel $\mathbf{h}$. At the receiver, the received vector, $\mathbf{y}$, is used for MPA-based detection. This is in contrast with the possible uplink scenario presented in (Vaezi *et al.* (2019) Equation (12.1)) where the users' codewords could arrive asynchronously. For this hypothetical case, there is indeed a possibility of interference between the codewords that could impair their sparsity/algebraic-structure; however, this issue does not arise for downlink SCMA.

For V non-interfering resources, the observation at the receiver, $\mathbf{y} \in \mathbb{C}^V$, is given as Vaezi *et al.* (2019), (Sfeir *et al.* (2020b) Equation (12.3)):

$$\mathbf{y} = \text{diag}(\mathbf{h}) f(\underbrace{\sum_{j=1}^{J} \mathbf{x}^{(j)}}_{\mathbf{x}}) + \mathbf{n}, \tag{5.1}$$

where $f(\cdot)$ denotes the PA nonlinearity, $\mathbf{x}$ denotes the instantaneous superposition of the users' codewords, $\text{diag}(\cdot)$ is a diagonal matrix that contains elements of $(\cdot)$ in its diagonal, and $\mathbf{h} \in \mathbb{C}^V$ is a vector of channel gains sampled according to a probability density function (PDF) $p(h)$. The contribution in this work is not constrained by prior statistical assumptions on $\mathbf{h}$. Furthermore, the complex additive white Gaussian noise (AWGN) vector is given by $\mathbf{n} = [n_1, n_2, \cdots, n_V]^T$, with each $n_i \sim p(n)$. Without sacrificing generality, we consider AM-AM Rapp nonlinearity for the PA model, $f(x)$, which is expressed as follows Gharaibeh (2011):

$$f(x) = \frac{x}{\left(1 + \left|\frac{x}{x_{\text{sat}}}\right|^{2p}\right)^{\frac{1}{2p}}}, \tag{5.2}$$

where p denotes the parameter that controls the severity of the nonlinearity, and x_{sat} is the PA saturation voltage. It is noted that the RFF-based detectors' performance is not dependent on the nonlinear PA characteristics or their knowledge at the receiver, and existing works show their generalization across different PA characteristics Sfeir *et al.* (2020b).

The components of the system model are pictorially depicted in Figures 5.1–5.3. The transmitter model described mathematically in (5.1) is shown pictorially in Figure 5.1. Figure 5.2 pictorially depicts the overlap of the codewords from each users' dictionary. Finally, the dependence on the user-resources and the variable-nodes is shown by a Tanner graph in Figure 5.3.

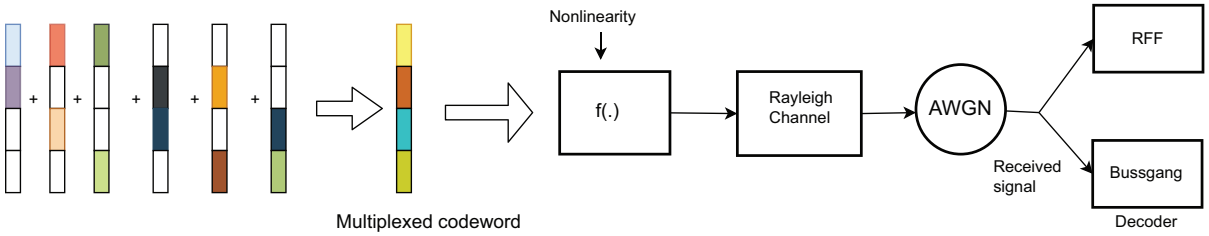

Figure 5.1 Depiction of the System Model for SCMA

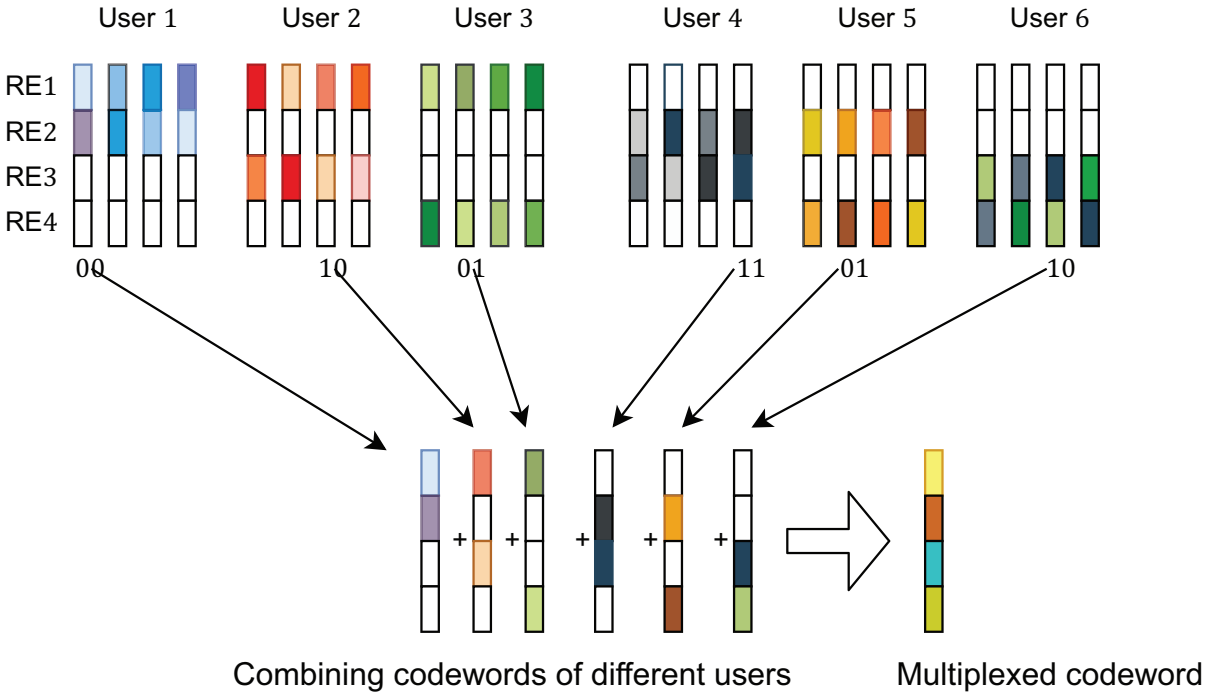

Figure 5.2 Depiction of the overlapping of codewords for different users

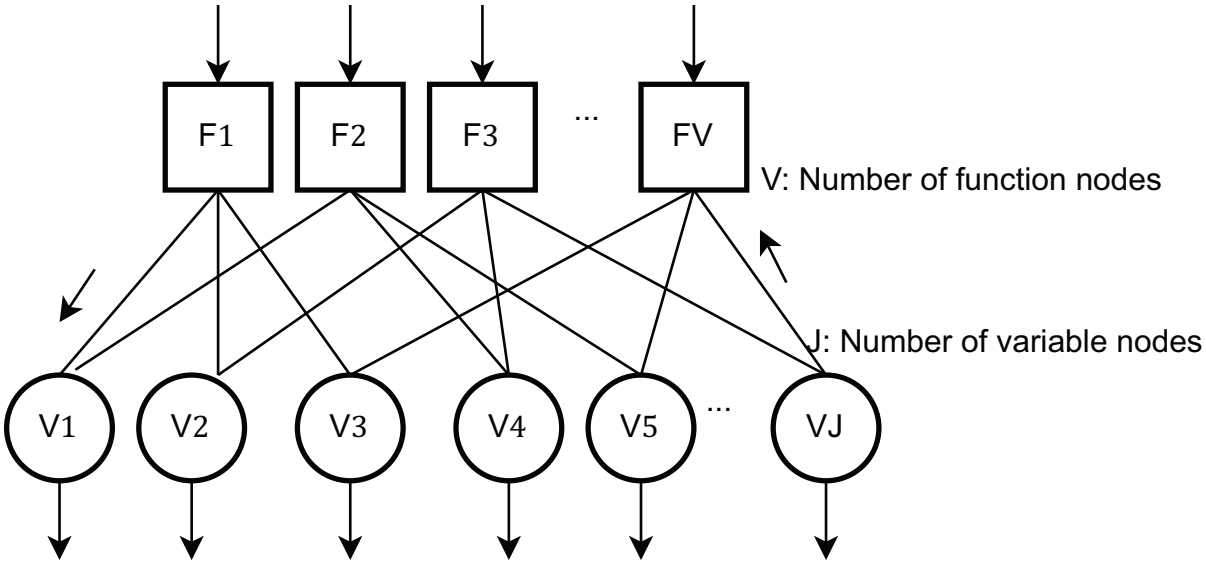

Figure 5.3 Depiction of the Tanner Graph

5.4 Bussgang Decomposition-Based MPA

In this section, we elaborate on the Bussgang decomposition-based MPA detector. The MPA detector iteratively exchanges the $\log(\cdot)$ of the conditional likelihood as messages across the function nodes, indexed as $j = 1, 2, \cdots, V$, and the variable nodes, indexed as $k = 1, 2, \cdots, J$. Also, for the resulting Tanner graph of the function nodes and variable nodes (Vaezi *et al.* (2019) Section 12.1.1.3), the graph neighborhood of node k is denoted as $\mathcal{B}_k$. In this regard, we invoke the Bussgang theorem Price (1958), and re-express (5.1) as:

$$\mathbf{y} = \alpha \text{diag}(\mathbf{h})\mathbf{x} + \mathbf{v} + \mathbf{n}, \tag{5.3}$$

where α denotes a correlation-coefficient and $\mathbf{v}$ denotes an independent distortion term with variance σ_v^2. Using this equivalent form, we obtain the following expression for the conditional

PDF, $p(y[k]|\mathbf{x})$:

$$p(y[k]|\mathbf{x}) = \frac{1}{2\pi\sigma_n^2} \exp\left[-\frac{\left| y[k] - \alpha h[k] \sum\limits_{\forall j \in B_k} x[k] \right|^2}{\sigma_n^2 + \sigma_v^2} \right]. \tag{5.4}$$

Generally, classical MPA-based detection propagates the $\log(\cdot)$ of the conditional PDF across the function nodes, j, and variable nodes, k (Vaezi *et al.* (2019) p. 377). For AWGN channels, the conditional PDF of $y[k]$ given $\mathbf{x}$ is provided below:

$$\log p(y[k]|\mathbf{x}) = -\log\left(2\pi\sigma_n^2\right) - \frac{\left| y[k] - \alpha h[k] \sum\limits_{\forall j \in B_k} x[k] \right|^2}{\sigma_v^2 + \sigma_n^2}. \tag{5.5}$$

The parameters α and σ_v^2 are estimated using the available pilots and the channel estimates $\mathbf{h}$ from (5.1) as follows:

$$\begin{aligned} \alpha &= \frac{\mathbb{E}\left[\mathbf{y}^T \mathrm{diag}(\mathbf{h})\mathbf{x}\right]}{\mathbb{E}\left[\|\mathrm{diag}(\mathbf{h})\mathbf{x}\|^2\right]}, \\ \sigma_v^2 &= (1-\alpha)^2 \mathbb{E}\left[\|\mathrm{diag}(\mathbf{h})\mathbf{x}\|^2\right]. \end{aligned} \tag{5.6}$$

For the log-max MPA approaches over AWGN channels, the messages, m_{jk}, are essentially given by the log likelihood $\log\left[p(y[k]|\mathbf{x})\right]$. Considering the Bussgang representation of (5.1) in (5.3), m_{jk} is explicitly written as:

$$m_{jk} = \frac{-\left| y[k] - \alpha h[k] \sum\limits_{\forall j \in \mathcal{B}_k} x[k] \right|^2}{\sigma_n^2 + \sigma_v^2}. \tag{5.7}$$

The difference between the value of this message and its corresponding ideal value is expressed as follows:

$$\Delta m_{jk} = \frac{\underbrace{\left| y[k] - h[k] \sum_{\forall j \in \mathcal{B}_k} x[k] \right|^2 \left(\sigma_n^2 + \sigma_v^2\right)}_{\mathcal{P}} - \underbrace{\left| y[k] - \alpha h[k] \sum_{\forall j \in \mathcal{B}_k} x[k] \right|^2 \sigma_n^2}_{\mathcal{Q}}}{\sigma_n^2 \left(\sigma_n^2 + \sigma_v^2\right)}. \tag{5.8}$$

If the appropriate expression for the Kullback–Leibler divergence between Gaussian PDFs having zero mean and variances σ_n^2 and $\sigma_n^2 + \sigma_d^2$ is invoked, the difference between m_{jk} and its corresponding ideal value, $\mathbb{E}\left[\Delta m_{jk}\right]$ (with $\alpha = 1$ and $\sigma_v^2 = 0$), is given by Cover (1999):

$$\mathbb{E}\left[\Delta m_{jk}\right] = \frac{1}{2}\log\left[\frac{\sigma_n^2 + (1-\alpha)^2 \sigma_h^2 \sigma_x^2 + \sigma_n^2}{\sigma_n^2}\right] + \frac{\sigma_n^2}{2\left(\sigma_n^2 + (1-\alpha)^2 \sigma_h^2 \sigma_x^2\right)} - \frac{1}{2}, \tag{5.9}$$

where

$$\begin{aligned} \sigma_h^2 &= \mathbb{E}\left[h^2\left[k\right]\right], \\ \sigma_x^2 &= \mathbb{E}\left[\left(\sum_{\forall j \in \mathcal{B}_k} x\left[k\right]\right)^2\right]. \end{aligned} \tag{5.10}$$

Next, we directly link the converged log likelihood ratio for the ideal linear channel to the generalized signal-to-noise ratio (GSNR) Sfeir, Mitra, Kaddoum & Bhatia (2020a), ref. Polcari (2013) achieved at convergence, SNR*, which is in turn a function of $\psi_{p(h)}$ (the PDF of the channel gain) Sfeir *et al.* (2020a):

$$\mathrm{BER}_{\mathrm{Linear}} = \psi_{p(h)}\left(\mathrm{SNR}^*\right). \tag{5.11}$$

From the expression for the message error derived in (5.9), the BER of the proposed Bussgang detector, $\mathrm{BER}_{\mathrm{Bussgang}}$, is approximately expressed as:

$$\mathrm{BER}_{\mathrm{Bussgang}} = \psi_{p(h)}\left(\mathrm{SNR}^{*}\right) + \psi'_{p(h)}\left(\mathrm{SNR}^{*}\right) \times \mathbb{E}\left[\Delta m_{jk}\right], \tag{5.12}$$

where the $\mathbb{E}\left[\Delta m_{jk}\right]$ is derived in (5.9). The following insights are drawn from the above analytical result:

- Notably, (5.12) quantifies the gap between the BER of the proposed approach and that of a universally optimal MPA (the RFF-based MPA in Sfeir *et al.* (2020b)). As mentioned before, this quantification helps when trading off computational complexity with BER performance subject to achieving a given BER-based level of QoS.
- It is further noted that the above deviation is independent of the fading distribution. In this context, it is indeed worth mentioning that the ideal BER, $\psi_{p(h)}(\mathrm{SNR}^{*})$, is mostly an integral of a Q-function over the concerned PDF $p(h)$ Vaezi *et al.* (2019). However, when $\psi_{p(h)}(\mathrm{SNR}^{*})$ (and hence its derivative $\psi'_{p(h)}$) are known, the optimality gap is found to be independent of the underlying distribution.
- It is possible to further improve the error approximation in (5.12) as follows:

$$\mathrm{BER}_{\mathrm{Bussgang}} = \sum_{l=0}^{\infty} \frac{\psi^{(l)}_{p(h)}(\mathrm{SNR}^{*})}{l!} \mathbb{E}\left[\Delta m^{l}_{jk}\right], \tag{5.13}$$

  where $\psi^{(l)}_{p(h)}(\cdot)$ represents the l^{th} derivative of $\psi_{p(h)}(\cdot)$. To simplify, we note from (5.7) that $\mathcal{P}, \mathcal{Q} \sim \mathrm{Exp}\left[\sigma_n^2\left(\sigma_n^2 + \sigma_v^2\right)\right]$ are even powers of normal random variables with average energy $\sigma_n^2\left(\sigma_n^2 + \sigma_v^2\right)$. Therefore, we obtain the following for $\mathbb{E}\left[\Delta m^{l}_{jk}\right]$:

$$\mathbb{E}\left[\Delta m^{l}_{jk}\right] = \sum_{s=0}^{l} \binom{l}{s} \mathbb{E}\left[\mathcal{P}^{s}\mathcal{Q}^{l-s}\right]. \tag{5.14}$$

From (Kan (2008) p. 546), this is simplified as:

$$\mathbb{E}\left[\Delta m_{jk}^{l}\right] = \sum_{s=0}^{l} \sum_{u=0}^{\min[s,(l-s)]} \binom{l}{s} \frac{2s!\left[2\left(l-s\right)!\right]\left(\alpha\sigma_h^2\sigma_x^2\right)^{2u}}{2^l\left[\left(s-u\right)!\right]\left[\left(l-s-u\right)!\right]2u!}, \tag{5.15}$$

which yields the final expression:

$$\mathrm{BER}_{\mathrm{Bussgang}} = \sum_{l=0}^{\infty} \frac{\psi_{p(h)}^{(l)}(\mathrm{SNR}^*)}{l!} \mathbb{E}\left[\Delta m_{jk}^{l}\right]. \tag{5.16}$$

A summary of the proposed Bussgang-based MPA is provided in Algorithm 5.1.

Algorithm 5.1 Bussgang based MPA

1: Initialization:

$I_{kj} = p\left(\mathbf{x}_j\right)$ according to a uniform distribution.

2: Initialization:

$$I_{jk} := \frac{1}{2\pi\sigma_n^2} \exp\left[-\frac{\left|y[k]-\alpha h[k] \sum\limits_{\forall j \in \boldsymbol{B}_k} x[k]\right|^2}{\sigma_v^2+\sigma_n^2}\right]$$

$$\alpha = \frac{\mathbb{E}\left[\mathbf{y}^T \mathrm{diag}(\mathbf{h})\mathbf{x}\right]}{\mathbb{E}\left[\|\mathrm{diag}(\mathbf{h})\mathbf{x}\|^2\right]},$$

$$\sigma_v^2 = (1-\alpha)^2\mathbb{E}\left[\|\mathrm{diag}(\mathbf{h})\mathbf{x}\|^2\right].$$

3: Initialize the maximum number of iterations, *ITER*.

4: **while** $c <$ ITER **do**

$$I_{jk} := \log\left(p\left(\mathbf{x}_j\right)\right) + \sum_{j \in \mathcal{B}_k} I_{kj}.$$

$$I_{kj} := \max_{\forall \mathbf{x}_j \in C_j, k \in \mathcal{B}_j} \log(p(y[k]|\mathbf{x})) + \sum_{k \in \mathcal{B}_j} I_{jk}$$

$c := c + 1$

end while

5: Detect user-symbols as per (Vaezi *et al.* (2019) eq. (12.12)) using the steady-state message-values I_{jk} and codebook C_j

5.5 Simulations

In this section, we present the simulation results to validate the Bussgang decomposition-based MPA. Without sacrificing generality, a simplistic codebook from Klimentyev & Sergienko (2016) is considered in our simulations. We set $p = 1$ and x_{sat} to be equal to the maximum dynamic range of $\mathbf{x}$. Furthermore, the BER simulations are performed over 10^7 bits, and 15 MPA iterations are used. The simulation results for a Rayleigh channel are depicted in Figure 5.4. The simulation parameters are summarized in Table 5.1.

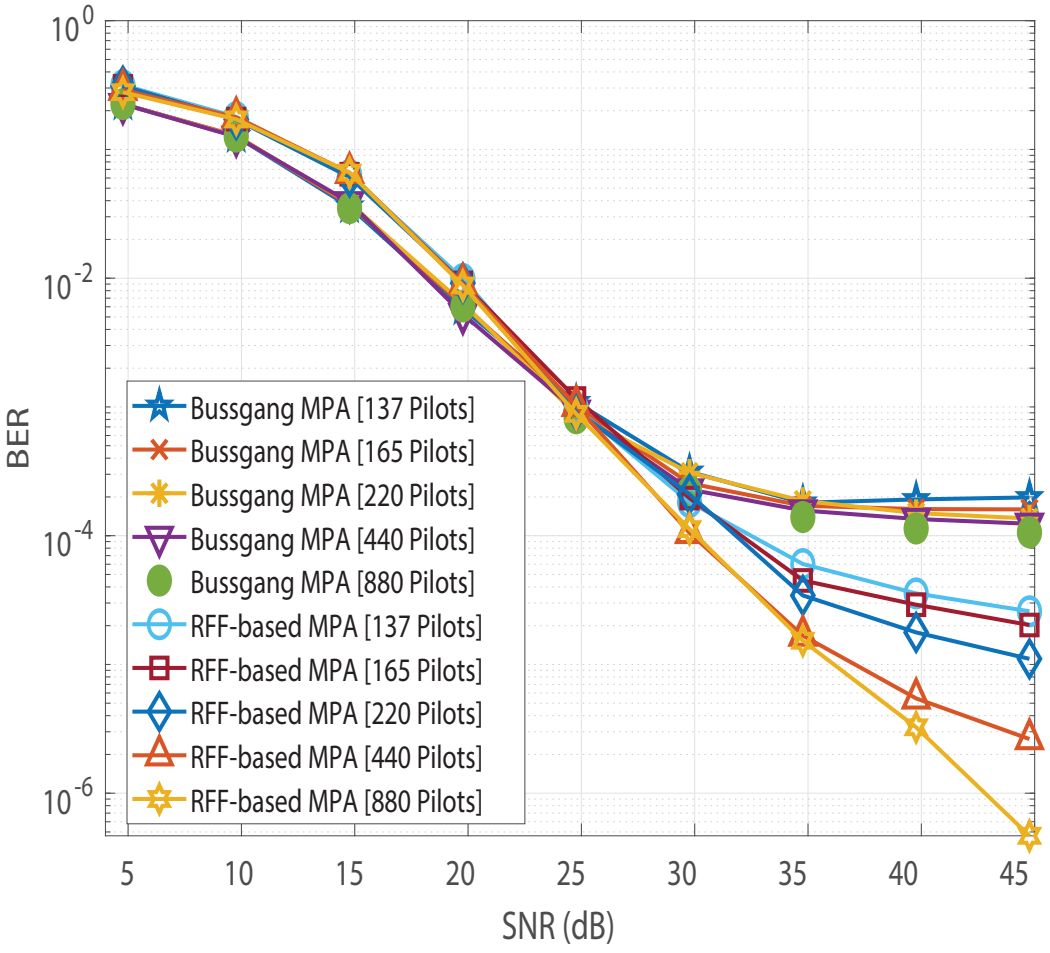

Figure 5.4 BER vs. SNR comparison of the Bussgang-based detector with RFF-based detector for a Rayleigh Channel by varying the number of pilots

Table 5.1 Simulation Parameters

Codebook	Section II.A Klimentyev & Sergienko (2016)
Modulation	OOK
Value of p	1
Kernel-width assignment	Silverman's rule Silverman (2018)
Number of MPA iterations	15
Number of transmitted bits	10^7
Parameter values for Rayleigh distribution	$\sigma_h^2 = 1$
Parameter values for the Nakagami-m distribution	Shape: $m = 0.5$, Spread parameter: 1
n_G	110

In Figure 5.4, saturation is observed in Bussgang-based MPA's BER performance. In addition, we observe no significant change in Bussgang-based MPA's BER floor when the number of pilots is increased from 137 to 880. However, for the RFF-based MPA detection in Sfeir *et al.* (2020b), its BER performance is found to improve as the number of pilots increases, and the saturation due to the BER floor is completely invisible at 880 pilots. Furthermore, the analytical expression for the BER of the Bussgang-based detector derived in (5.12) is validated in Figure 5.5, which illustrates close agreement between the analytical BER (denoted by [A]) and the simulated BER (denoted by [S]). Figure 5.6 shows a similar validation of the analytical result derived in (5.12) assuming a Nakagami-m distributed $\mathbf{h}$, with $m = 0.5$. Since the mode of the Nakagami-m distribution (with $m = 0.5$) is zero, we observe degraded BER performance for Nakagami-m fading as compared to the BER performance for the Rayleigh channel presented in Figure 5.5. However, due to the distribution-independent quantification of the performance gap presented in (5.12), a close match is observed between the simulated BER and the analytical BER for the Bussgang-based detector in Figure 5.6. This quantification of the BER floor helps when predetermining the viability of using a lightweight Bussgang-based MPA (which has a complexity of $O(TKM^{d_f})$, where d_f denotes the free distance) over a complex RFF-based detector (which has a complexity of $O(TKM^{d_f} + n_G^2)$, where n_G denotes the number of RFFs) subject to achieving a BER-based level of QoS.

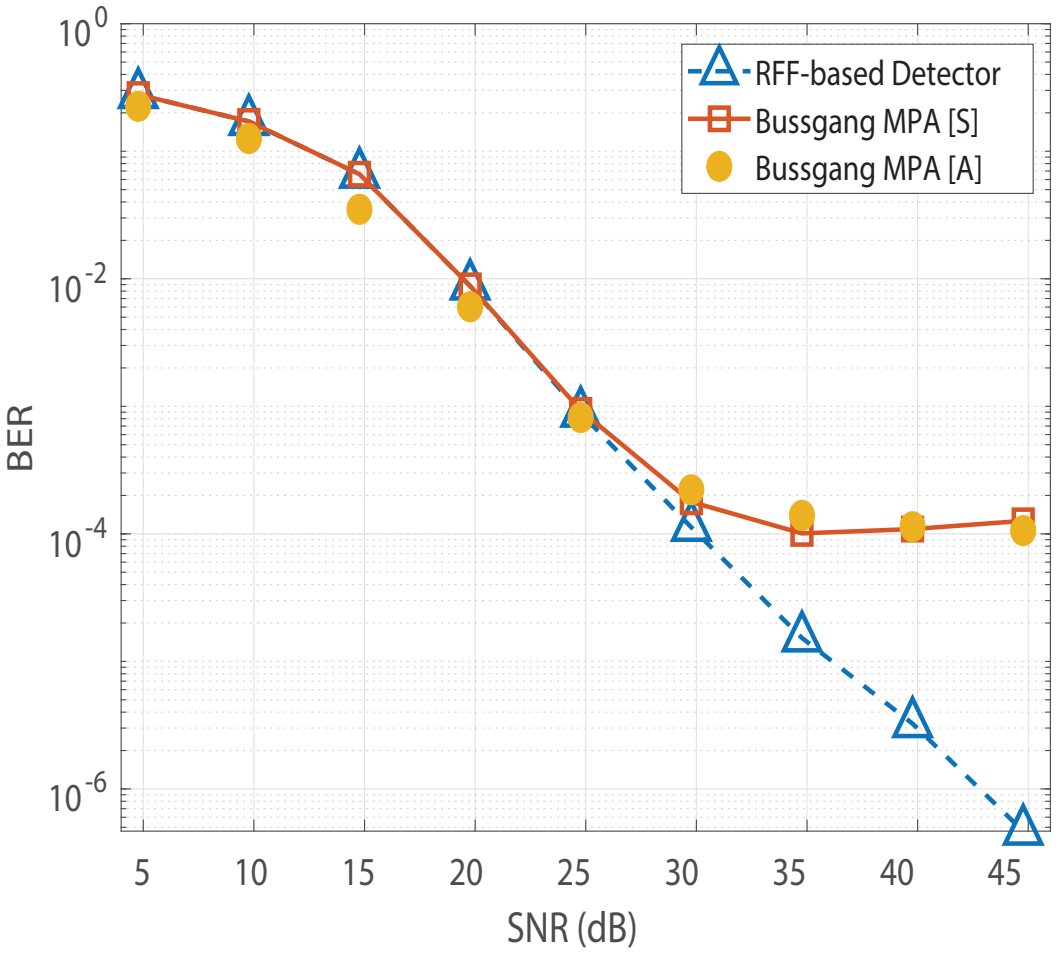

Figure 5.5 BER vs. SNR validation for the Bussgang-based detector for a Rayleigh channel

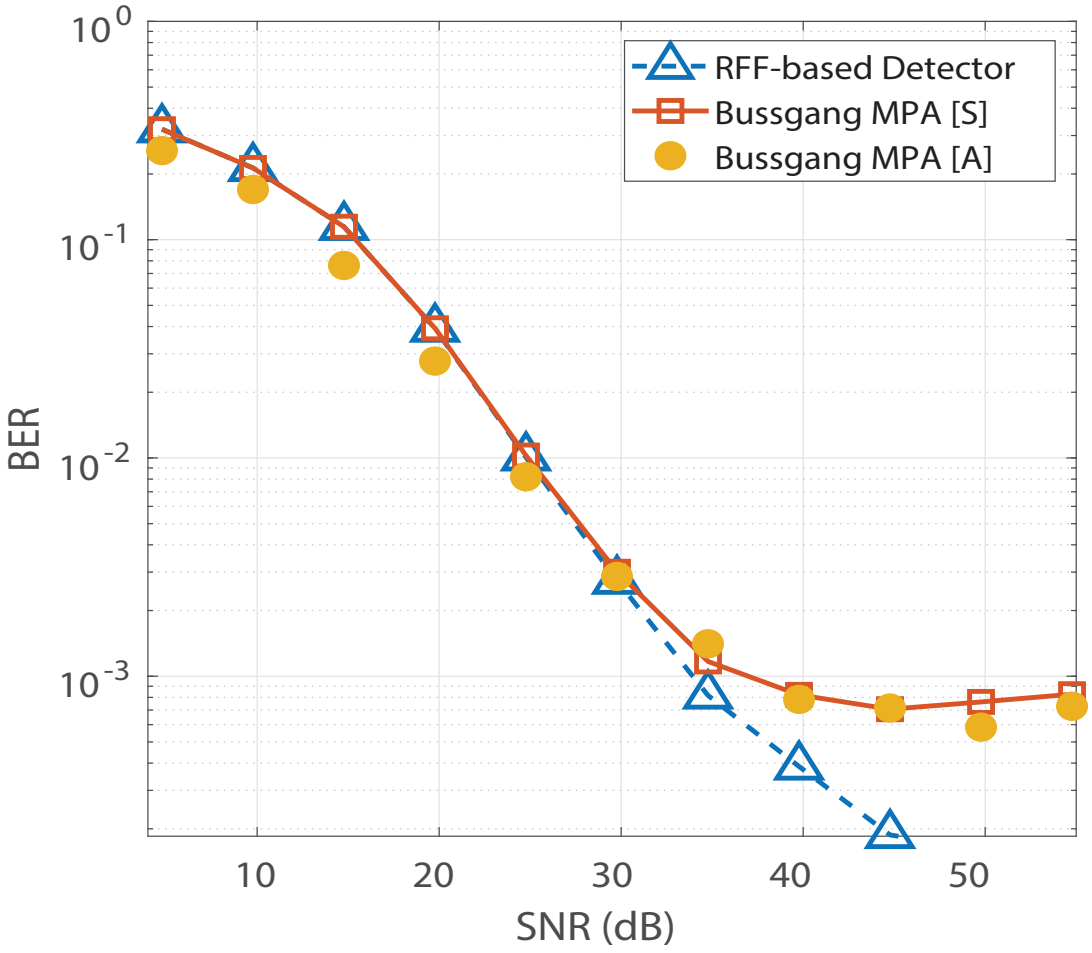

Figure 5.6 BER vs. SNR validation for the Bussgang-based detector for a Nakagami-m channel with $m = 0.5$

5.6 Conclusions

In this paper, a low-complexity detector, the Bussgang-based MPA, was derived, and its BER performance was quantified. The proposed detector was found to present a BER floor comparable to that of existing RFF-based approaches. The BER floor was quantified analytically relative to the optimal RFF-based MPA without specific assumptions about the nature of the PA nonlinearity or the fading distribution. Additionally, the analytical results were validated by computer simulations considering different channel distributions. The detector is attractive

despite its error floor due to its simplicity and suitability for hardware-limited IIoT systems, wherein achieving a certain level of QoS with low computational cost outweighs the requirement of obtaining a universally optimal BER performance.

Author Contributions: The contributions to this paper are classified as follows: E.S.: writing-original draft preparation, conceptualization, software and visualization. R.M.: writing—Review and editing, supervision, formal analysis and validation. G.K.: writing—Review and editing, validation, methodology and project administration. V.B.: Review and editing. All authors have read and agreed to the published version of the manuscript.

Funding: This work was supported by the Richard J. Marceau (RJM) research chair, and by the grantfrom the National Natural Sciences and Engineering Research Council of Canada (NSERC).

Conflicts of Interest: The authors declare no conflict of interest.

CHAPTER 6

A RANDOM FOURIER FEATURE BASED RECEIVER DETECTION FOR ENHANCED BER PERFORMANCE IN NONLINEAR PD-NOMA

Elie Sfeir[1] , Rangeet Mitra[1] , Georges Kaddoum[1]

[1] Department of Electrical Engineering, École de Technologie Supérieure,
1100 Notre-Dame Ouest, Montréal, Québec, Canada H3C 1K3

Paper published in IEEE Transactions on Vehicular Technology Journal, October 2022.

6.1 Abstract

Non-orthogonal multiple access (NOMA) has been proposed as a potential enabler for massive connectivity. Among the different NOMA schemes, power-domain (PD-NOMA) is particularly appealing as it improves user fairness while enhancing spectral efficiency. However, the practical implementation of NOMA faces several challenges, including radio frequency impairments, such as power-amplifier (PA) nonlinearity, which can limit its performance. In this paper, we study the impact of PA nonlinearity on the detection performance of PD-NOMA, and propose a random Fourier feature (RFF) based solution to mitigate the effects of such imperfections. Computer simulations carried out assuming different PA nonlinearity types demonstrate that the proposed RFF based algorithm considerably improves the BER performance and achieves results that are close to the ideal case. Lastly, the analytical proof of our proposed algorithm's performance is provided to support our simulation results.

Index Terms—Hardware impairments, PD-NOMA, nonlinearity, RFF.

6.2 Introduction

Multiple access techniques have been the cornerstone of every new wireless generation. Nowadays, the continuous increase in the number of connected devices and the explosive growth

in the data rate requirements is pushing researchers to conceive new multiple access techniques that enable massive connectivity, and achieve higher spectral efficiency and throughput Giordani, Polese, Mezzavilla, Rangan & Zorzi (2020). In this context, traditional orthogonal multiple access (OMA) techniques, used in previous generations of mobile communications, have been found ill-equipped toward accommodating the overwhelming traffic that will be required by the upcoming beyond fifth generation (B5G) and sixth generation (6G) communication systems. In this regard, non-orthogonal multiple access (NOMA) has emerged as a potential candidate for supporting massive connectivity, increasing spectral efficiency and achieving fairness, in upcoming generations of wireless networks Liu *et al.* (2017b). In contrast to OMA techniques, NOMA offers higher spectral efficiency by enabling the allocation of multiple users on the same resource block (RB). In general, NOMA is classified into two broad categories: Power domain NOMA (PD-NOMA), where multiplexing is performed in the power domain, and code domain NOMA (CD-NOMA), where multiplexing is achieved in the code domain. CD-NOMA, seen as an extension of code division multiple access (CDMA), has multiple variants such as low density spreading sequence-based CDMA (LDS-CDMA) and sparse code multiple access (SCMA) Vaezi *et al.* (2019),Wang, Zhang, Yang & Hanzo (2018). In CD-NOMA, codes are assigned to users. For instance, for each user, SCMA, defines a multidimensional codebook consisting of a set of codewords enabling a shaping gain in addition to the coding gain Wu *et al.* (2017); Evangelista *et al.* (2019b); Sfeir *et al.* (2020a); Sfeir, Mitra, Kaddoum & Bhatia (2021). Unlike CD-NOMA, PD-NOMA separates the users in the power domain, leveraging their channel gain differences. Here, the users are assigned different power levels according to their channel gain, i.e. users suffering from bad channel conditions (typically users who are far from the transmitter) are assigned higher power levels. In contrast, those enjoying better SNRs (typically users that are close to the transmitter) will be allocated lower amounts of powerDai *et al.* (2018), Mitra & Bhatia (2017b), Farah *et al.* (2017). This difference in power allocation, in addition to achieving fairness between users, facilitates decoding at the user end. Specifically, the user with bad channel conditions is allocated more power and therefore perceives the other user's signal as noise while performing his decoding as normal. Meanwhile, the user with good channel conditions is assigned less power and thus should decode the other user's information and subtract

that information from the received signal to recover his message. This decoding then subtracting is known as successive interference cancellation (SIC). SIC suffers from error-propagation, which saturates/degrades the performance of PD-NOMA systems with a large number of users Sun, Xie, Hu & Wu (2016). Furthermore, when the number of multiplexed users on the same resource increases, the complexity of SIC increases Islam, Avazov, Dobre & Kwak (2016),Islam, Zeng & Dobre (2017) which is why, in most related works, only two users are multiplexed.

That being said, PD-NOMA enables fairness between unequal users while achieving massive connectivity and integrates well with ecosystems like the internet of things (IoT) Lv, Ma, Zeng & Mathiopoulos (2018).

However, impairments, such as nonlinearities in the power amplifier (PA), severely degrade the performance of PD-NOMA based systems. Pitfalls of nonlinear distortion in wireless communication were studied in Gharaibeh (2011), where system models and simulations were provided for single and multichannel wireless communication systems. In Belkacem, Ammari & Dinis (2020), the performance of PD-NOMA is studied in 5G with high-power amplifiers (HPAs) nonlinearities. In Guerreiro *et al.* (2020), an iterative receiver design is performed to mitigate nonlinearity.

Among several signal processing algorithms, reproducing kernel Hilbert spaces (RKHS) tools have been found to offer practically effective solutions for recovering information in the presence of impairments, such as intersymbol interference (ISI) and hardware nonlinearity. In Jain, Mitra & Bhatia (2019b), a RKHS based algorithm was proposed for mitigating nonlinearity and ISI in visible light communication (VLC). In Sfeir *et al.* (2020b), a technique based on random Fourier feature (RFF) was proposed to mitigate the effect of PA nonlinearities on CD-NOMA, and specifically SCMA. Additionally, a RFF-based detection showed attractive results for mitigating impairments over nonlinear multi user massive multiple input multiple output (MU-m-MIMO) Chhangani *et al.* (2020). Therefore, in this work, we propose a RFF-based solution for nonlinear downlink PD-NOMA.

Contributions: In this paper, we consider the impact of the PA nonlinearities on BER performance of PD-NOMA systems and propose a new RFF based solution that recovers the distorted NOMA

signal before performing SIC. Our simulations show that, under different types of PA nonlinearity and severity levels, the proposed method greatly reduces the effects of PA nonlinearities and delivers a performance that is comparable to ideal scenarios. Further, analytical proofs and theorems are given that support the generated results.

6.3 Preliminaries

In PD-NOMA, the same RB is shared between different users. The users are paired and assigned different power levels based on their distinct channel gains. Because several users share the same resources, precise pairing and power allocation strategies are essential for optimum resource utilization, resulting in reduced interference and increased system capacity. Hence, the downlink transmitted signal to the k^{th} user is expressed as:

$$y_k = h_k \sum_{j=1}^{J} \sqrt{P_j} x_j + n_k, \quad j = 1, .., J \quad , \tag{6.1}$$

where J denotes the number of multiplexed users per subcarrier, $h_k \in \mathbb{C}$ is the channel gain of the k^{th} user on subcarrier n, P_j represents the amount of power allocated to user j, x_j the information sequence corresponding to user j and $n_j \sim \mathcal{CN}(0, \sigma_n^2)$ is the additive white Gaussian noise (AWGN) with zero mean and variance σ_n^2. At the receiver end, SIC is performed to identify messages for the different users from the superposed signal. Moreover, decoding at the receiver end should follow an optimal decoding order based on the assigned power levels. Thus, if user k has the highest power level, he perceives the other user's information as noise, and decodes his information. However, if the user k does not have the highest power level, the user decodes messages of all the users whose power levels are higher than his before decoding his own information. Hence, the recovered signal is obtained as:

$$\hat{y}_k = y_k - \sum_{l \in \mathcal{L}} h_l \sqrt{P_l} \hat{x}_l, \tag{6.2}$$

where $\mathcal{L}$ is the set of users whose power level P_l is greater than the power level of user k, P_k. While there are no explicit limitations on the number of multiplexed users per subcarrier, SIC complexity and error propagation both rise as the number of users sharing a RB increases. Thus, in this work, we will consider a multiplexing of two users per subcarrier multiplexing scenario.

6.4 System Model

We consider a downlink PD-NOMA system consisting of a single base station, N subcarriers, and U users, where $U > N$ and perfect channel state information (CSI) is available at the receiver. The users are separated based on their locations within the cell into two sets: users far from the base station which are considered as weak users and users close to the base station who are considered as strong users. In the following, we assume a two-users superposition, where the first user is the one suffering from a low channel gain, and the second having the best channel conditions. The transmitted signals for user 1 are generated from a binary PSK (BPSK) modulation where $\mathbb{S}_1 = \{b_0 = 0, b_1 = 1\}$ and those of user 2 are generated from a quadrature PSK (QPSK) where $\mathbb{S}_2 = \{a_0 = 00, a_1 = 01, a_2 = 10, a_3 = 11\}$. The received signal at the k^{th} user's receiver is given by:

$$y_k = h_k f\left(\underbrace{\sum_{j=1}^{J} \sqrt{P_j} x_j}_{\mathrm{X}}\right) + n_k, \quad j = 1, .., J \quad , \tag{6.3}$$

where f represents the nonlinear distortion function of the HPA. The nonlinearities of the PA can be modelled by the amplitude modulation–amplitude modulation (AM-AM) Rapp nonlinearity function $f(\cdot)$ given as Gharaibeh (2011)

$$f(x) = \frac{x}{\left(1 + \left|\frac{x}{x_{\text{sat}}}\right|^{2p}\right)^{\frac{1}{2p}}}, \tag{6.4}$$

or by the amplitude modulation–phase modulation (AM-PM) nonlinearity function given by Dudak & Kahyaoglu (2012)

$$\begin{aligned} |f(x)| &= \frac{|x|}{\left(1 + \left|\frac{x}{x_{\text{sat}}}\right|^{2p}\right)^{\frac{1}{2p}}}, \\ \angle f(x) &= \angle x + \frac{\epsilon\,|x|^{q_1}}{1 + \left(\frac{|x|}{\gamma}\right)^{q_2}}, \end{aligned} \tag{6.5}$$

where x_{sat} represents the saturation value, p represents the severity of the nonlinearity, $|\cdot|$ denotes the absolute value operation, $q_1 = -0.03462$, $q_2 = -1.758$, $\epsilon = 0.0747$, $\gamma = 0.1281$, and $\angle(\cdot)$ represents the angle of $(\cdot)$.

6.5 Proposed RFF based Post-distortion Algorithm for NOMA

In this section, we present our RFF based algorithm for decoding PD-NOMA messages in the presence of hardware nonlinearities. RFF enables us to approximate the feature map space in RKHS using randomized feature mapping $\Psi : \mathbb{R}^d \rightarrow \mathbb{R}^D$, defined as Anand *et al.* (2021), Bouboulis *et al.* (2016), Mitra *et al.* (2020a)

$$\Psi(\boldsymbol{\gamma}) = \sqrt{\frac{2}{D}} \begin{bmatrix} \cos\left(\boldsymbol{\omega}_1^T \mathbf{v} + \eta_1\right) \\ \cos\left(\boldsymbol{\omega}_2^T \mathbf{v} + \eta_2\right) \\ \vdots \\ \cos\left(\boldsymbol{\omega}_D^T \mathbf{v} + \eta_D\right) \end{bmatrix}, \tag{6.6}$$

where each $\{\boldsymbol{\omega}_i\}_{i=1}^{D}$ is generated from the Gaussian filter kernel Fourier transform, expressed as Anand *et al.* (2021), Bouboulis *et al.* (2016)

$$K_{\mathbf{G}}(\omega) = \left(\frac{\sigma}{2\pi}\right)^{D} e^{(-0.5\sigma^2\|\omega\|^2)}, \tag{6.7}$$

which is equivalent to the normal distribution $\mathcal{N}\left(\mathbf{0}_D, \frac{1}{\sigma^2}\mathbf{I}_D\right)$, with $\mathbf{I}_D$, σ and D representing the identity matrix of dimension D, the kernel-width hyperparameter, and the number of RFFs, respectively. Moreover, $(\cdot)^T$ denotes the transpose operator, each $\{\eta_i\}_{i=1}^{D}$ is drawn from a uniform distribution on the interval $[0, 2\pi]$ Bouboulis *et al.* (2016), Anand *et al.* (2021), $\boldsymbol{\gamma} \in \mathbb{C}$ represents an independent random variable, and $\mathbf{v} \in \mathbb{R}^2$ expressed as:

$$\mathbf{v} = (\text{real}[\boldsymbol{\gamma}], \ \ \text{imag}[\boldsymbol{\gamma}])^T, \tag{6.8}$$

With the CSI available at the receiver, we use a supervised learning technique based on pilots to recover the distorted signal. Pilots are assumed to be known at the transmitter, and the receiver Tse & Viswanath (2005), with no pilot contamination. Hence, the corresponding pilot channel response is obtained as:

$$y_{\text{p}} = h \sum_{j=1}^{J} \sqrt{P_j} x_{pj}. \tag{6.9}$$

This received pilot signal will be used to estimate the weights matrix by performing zero-forcing in the feature space as follows:

$$\mathbf{W} = \boldsymbol{\Psi}(y_{\text{tr}})_{(1:\mathcal{P})}^{T^{\dagger}} y_{\text{p}_{(1:\mathcal{P})}}, \tag{6.10}$$

where $(\cdot)^{T^{\dagger}}$ indicates the pseudo-inverse operator and $\mathcal{P}$ represents the number of pilots. Lastly, upon getting $\mathbf{W}$ from the training phase, the unwraped received signal is derived as:

$$y' = \boldsymbol{\Psi}(y)^T \mathbf{W}. \tag{6.11}$$

The RFF based decoding is performed at each user before the SIC operation.

Algorithm 6.1 RFF-SIC based PD-NOMA decoding

Input: y_k, h, N_0, p

Initialization:
1. Generate $\{\boldsymbol{\omega}_i\}_{i=1}^{D}$ from Gaussian distribution $\mathcal{N}\left(\mathbf{0}_D, \frac{1}{\sigma^2}\mathbf{I}_D\right)$ expressed in (6.7).
2. Generate $\{\eta_i\}_{i=1}^{D}$ from the uniform distribution $U\,[0, 2\pi]$.

Computation:
1. Compute reference signal y_{p} using pilots (6.9).
2. Derive RFF's unwarping weights $\mathbf{W}$ using (6.10).
3. Compute the RFF vector at each user end (6.11)
   $\mathbf{y'}_k = \mathbf{\Psi}(y)^T\mathbf{W}$.
4. Perform SIC at users with better channel conditions, as in (6.2).

Output: Data bits for each user $\hat{x}_1, \hat{x}_2$

6.6 Effect of Nonlinearities in PD-NOMA

When assessing the performance of systems with nonlinear components, the Bussgang decomposition is a common approach. In sum, it reveals an accurate probabilistic link between the input and the output of the nonlinearity, where the output is equivalent to a scaled version of the input plus an uncorrelated distortion term. Hence, the nonlinear signal of (6.3) is represented as:

$$\begin{aligned} z_k =& h_k\left(\alpha X + \eta\right) + n_k \\ =& \alpha h_k X + h_k \eta + n_k, \end{aligned} \tag{6.12}$$

where α, known as Bussgang gain, is given by

$$\alpha = \frac{\mathbb{E}\left[z_k^T h_k X\right]}{\mathbb{E}\left[\|h_k X\|^2\right]}, \tag{6.13}$$

and η represents the uncorrelated distortion. For user k, who has to first perform SIC and decode the other user's information, the decoded signal is expressed as:

$$\hat{z}_k = z_k - \alpha h_k \sqrt{P_l} \hat{x}_l \tag{6.14}$$

It is clear from the above equation that errors in estimating the correct information of user k results from:

- Wrong estimation of $\hat{x}_l$.
- Incorrectly assuming that the channel gain is h_k whereas it is modified to αh_k due to the nonlinearity.

The combination of SIC error propagation and error in the effective channel gain due to the nonlinearity induces degradation in performance and hence convergence to less optimal solutions or even divergence, based on the severity of the nonlinearity.

6.7 On the analytical proofs of RFF performance

Revisiting our system model and following functional analysis theory, specifically Riesz representer theorem Schölkopf *et al.* (2001), we can find an evaluation functional k_x for $f(\cdot)$ such that the nonlinearity is expressed in the RKHS $\mathcal{H}$ as:

$$f(X) = \langle k_x, X \rangle_{\mathcal{H}}, \tag{6.15}$$

where $\langle \cdot, \cdot \rangle_{\mathcal{H}}$ represents the inner-product rule over RKHS $\mathcal{H}$.
Following the RKHS properties, a kernel k_y can be found such that

$$< k_y, y >_{\mathcal{H}} = hX + < k_y, n >_{\mathcal{H}}, \tag{6.16}$$

However, since kernel computation is computationally expensive, randomization is recommended to reduce the computation complexity and approximate the kernel computation. Hence, we

select the RFF Rahimi *et al.* (2007) to approximate the kernel calculation

$$y' \approx < k_y, y >_{\mathcal{H}} = hX + < k_y, n >_{\mathcal{H}}, \tag{6.17}$$

where y' represents the obtained RFF transform.

As a result, using RFF unwarped data, an approximately linear characteristic is generated. Hence, the BER performance of the RFF based algorithm in the presence of nonlinear hardware, approaches the achieved performance in the linear AWGN scenario, alleviating the degradation revealed in section 6.6.

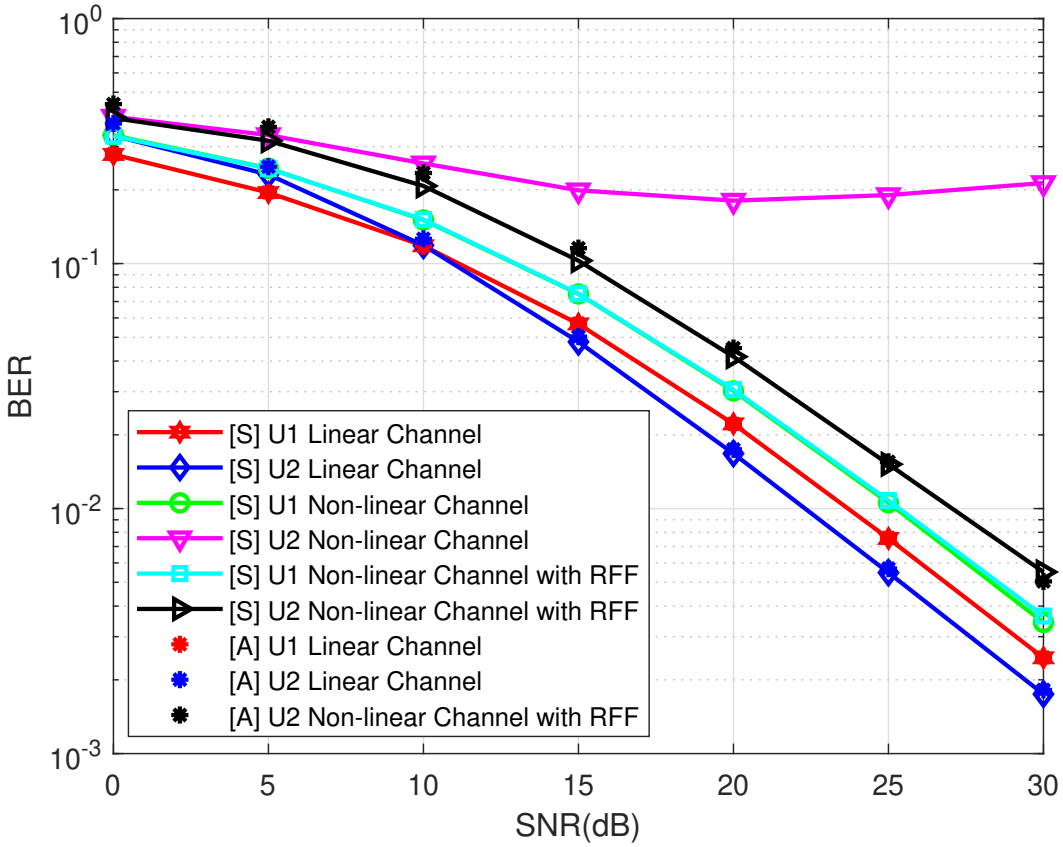

Figure 6.1 BER as a function of SNR for downlink PD-NOMA in the presence Rayleigh fading and AM-AM nonlinearity with p=1

6.8 Bit Error rate analysis for PD-NOMA RFF based decoding algorithm

6.8.1 PD-NOMA decoding algorithm

Below we reveal the analytical expressions for the PD-NOMA scenarios of superposed users.

6.8.1.1 BER of user 1

User 1, being the far user, does not have to perform SIC at his end; therefore, following an analytical approach similar to the study in Kara & Kaya (2018a),Assaf, Al-Dweik, El Moursi & Zeineldin (2019), the BER of user 1 is expressed as follows Kara & Kaya (2018a)

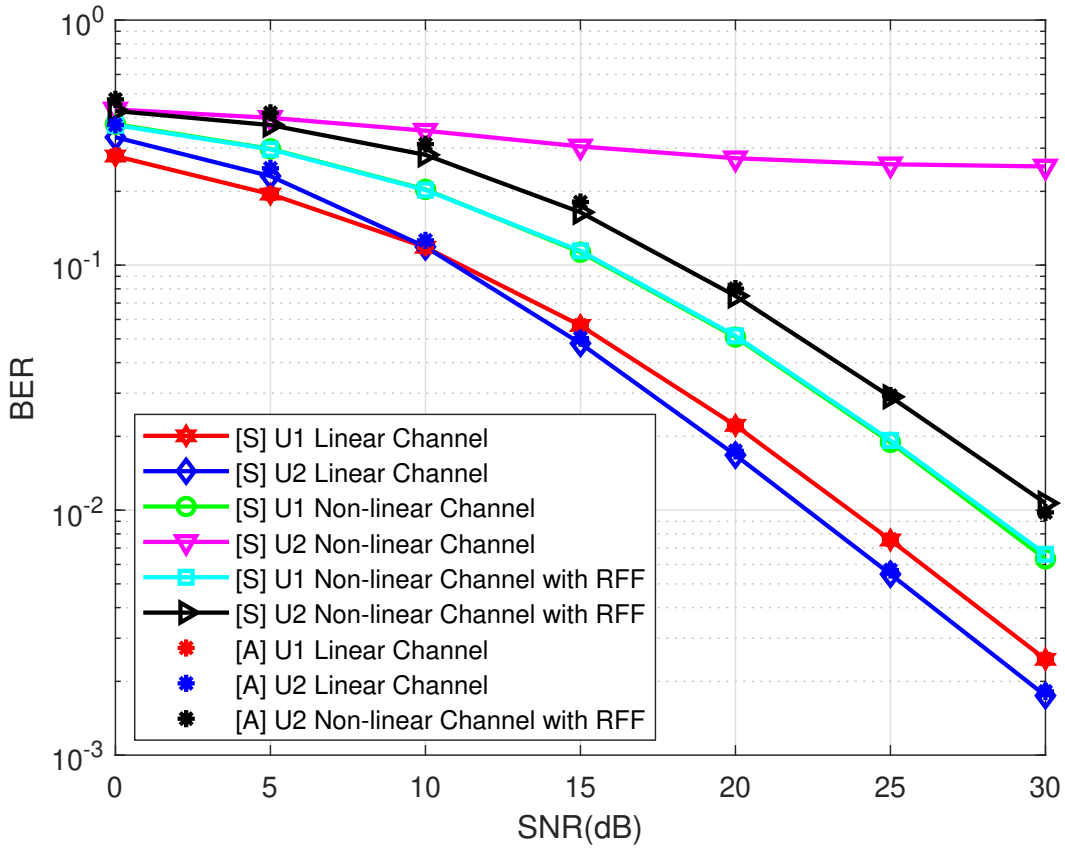

Figure 6.2 BER as a function of SNR for downlink PD-NOMA in the presence Rayleigh fading and AM-AM nonlinearity with p=0.5

$$\mathrm{BER}_1 = \frac{1}{4}\left[\left(1-\sqrt{\frac{\overline{\gamma_A}}{2+\overline{\gamma_A}}}\right)+\left(1-\sqrt{\frac{\overline{\gamma_B}}{2+\overline{\gamma_B}}}\right)\right], \tag{6.18}$$

where

$$\begin{aligned}\overline{\gamma_A} &= \frac{\left(\sqrt{2P_1}+\sqrt{P_2}\right)^2}{N_0}E\left[|h_1|^2\right],\\ \overline{\gamma_B} &= \frac{\left(\sqrt{2P_1}-\sqrt{P_2}\right)^2}{N_0}E\left[|h_1|^2\right].\end{aligned} \tag{6.19}$$

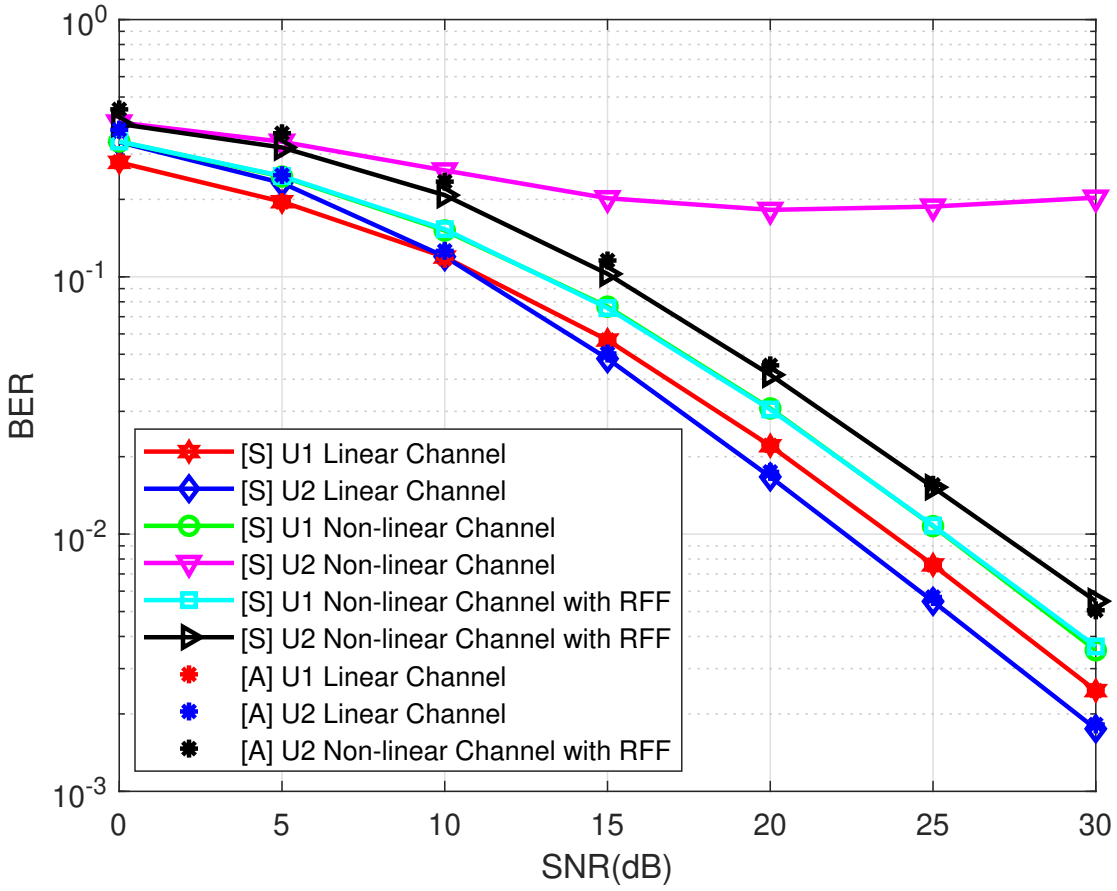

Figure 6.3 BER as a function of SNR for downlink PD-NOMA in the presence of AM-PM nonlinearity and Rayleigh fading

6.8.1.2 BER of user 2

To detect its own symbol s_2, the near user should first detect s_1 as in (6.2), by following a similar approach to Kara & Kaya (2018a), the BER of the second user

$$\begin{aligned}\mathrm{BER}_2 =&\frac{1}{2}\left(1-\sqrt{\frac{\overline{\gamma_C}}{2+\overline{\gamma_C}}}\right)+\frac{1}{8}\left[\sqrt{\frac{\overline{\gamma_D}}{2+\overline{\gamma_D}}}\right.\\&\left.-\sqrt{\frac{\overline{\gamma_E}}{2+\overline{\gamma_E}}}+\sqrt{\frac{\overline{\gamma_F}}{2+\overline{\gamma_F}}}-\sqrt{\frac{\overline{\gamma_G}}{2+\overline{\gamma_G}}}\right],\end{aligned} \tag{6.20}$$

where

$$\begin{aligned}\overline{\gamma_C}=\frac{P_2}{N_0}E\left[|h_2|^2\right],\overline{\gamma_D}=\frac{\left(\sqrt{2P_1}+\sqrt{P_2}\right)^2}{N_0}E\left[|h_2|^2\right],\\ \overline{\gamma_E}=\frac{\left(\sqrt{2P_1}-\sqrt{P_2}\right)^2}{N_0}E\left[|h_2|^2\right].\end{aligned} \tag{6.21}$$

6.8.2 RFF based PD-NOMA decoding algorithm

Revisiting (6.17), the RFF transform y' is AWGN with variance Mitra & Kaddoum (2022)

$$\sigma_{\tilde{n}}^2=\mathrm{var}\left[<k_y,\mathbf{y}>_{\mathcal{H}}\right]=<k_y,k_y>_{\mathcal{H}}\sigma_n^2, \tag{6.22}$$

Hence from Theodoridis (2015)

$$\sigma_{\tilde{n}}^2=\left\|k_y\right\|_{\mathcal{H}}^2*\sigma_n^2 \tag{6.23}$$

Hence adapting the obtained equations in (6.18),(6.20) with the new noise variance, we can derive the new BERs.

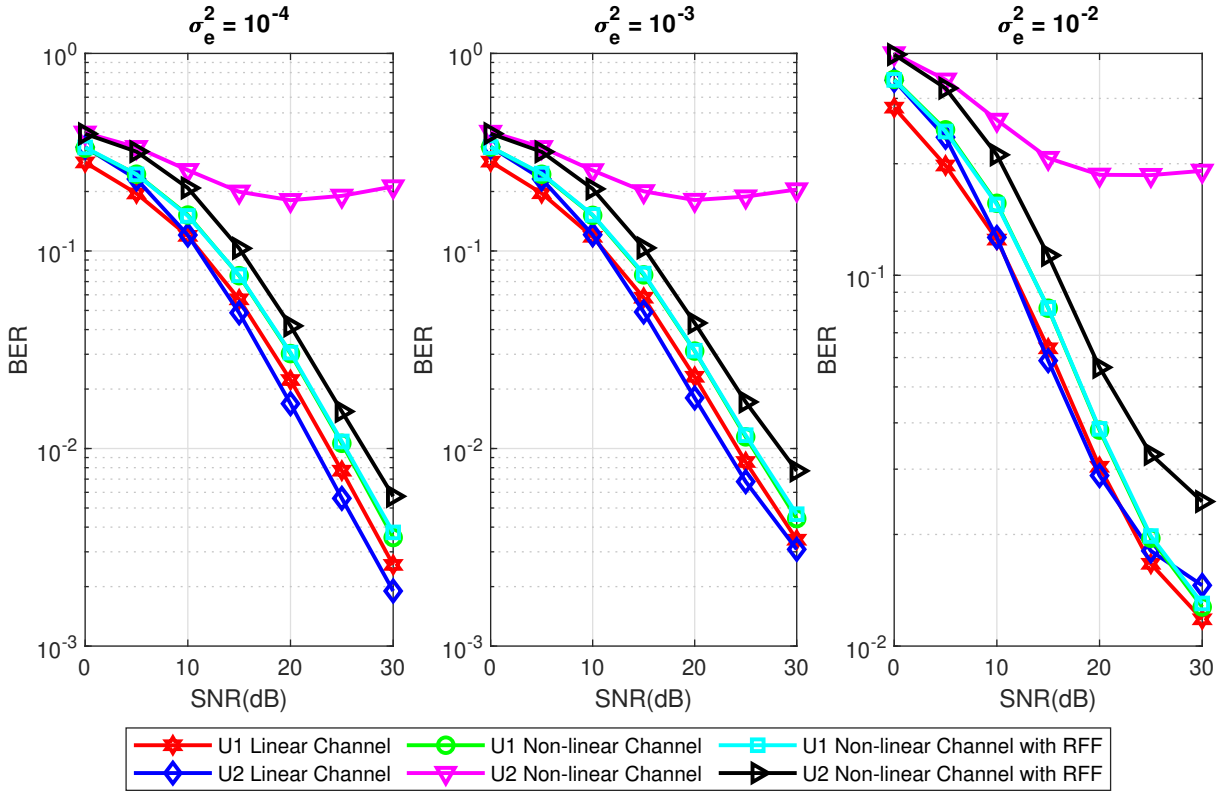

Figure 6.4 BER as a function of SNR for downlink PD-NOMA in the presence of AM-AM nonlinearity and Rayleigh fading for three different levels of channel estimation errors

6.9 Computational complexity

The computational complexity study motivates the use of RFF over other kernel trick based methods for nonlinearity approximation and mitigation.

$$f(\mathbf{x}) = \frac{1}{nh} \sum_{i=1}^{N} K\left(\frac{\mathbf{x} - \mathbf{x_i}}{h}\right) \tag{6.24}$$

Using kernel density estimation (KDE), expressed in (6.24), each evaluation point requires $O(N * d)$ kernel evaluations and $O(N * d)$ multiplications and additions Raykar *et al.* (2010b). However, RFF requires deriving the hyperplane $\mathbf{W}$ before mapping to the RKHS space of dimension D as per equation (6.11). Thus, the added complexity with respect to the conventional

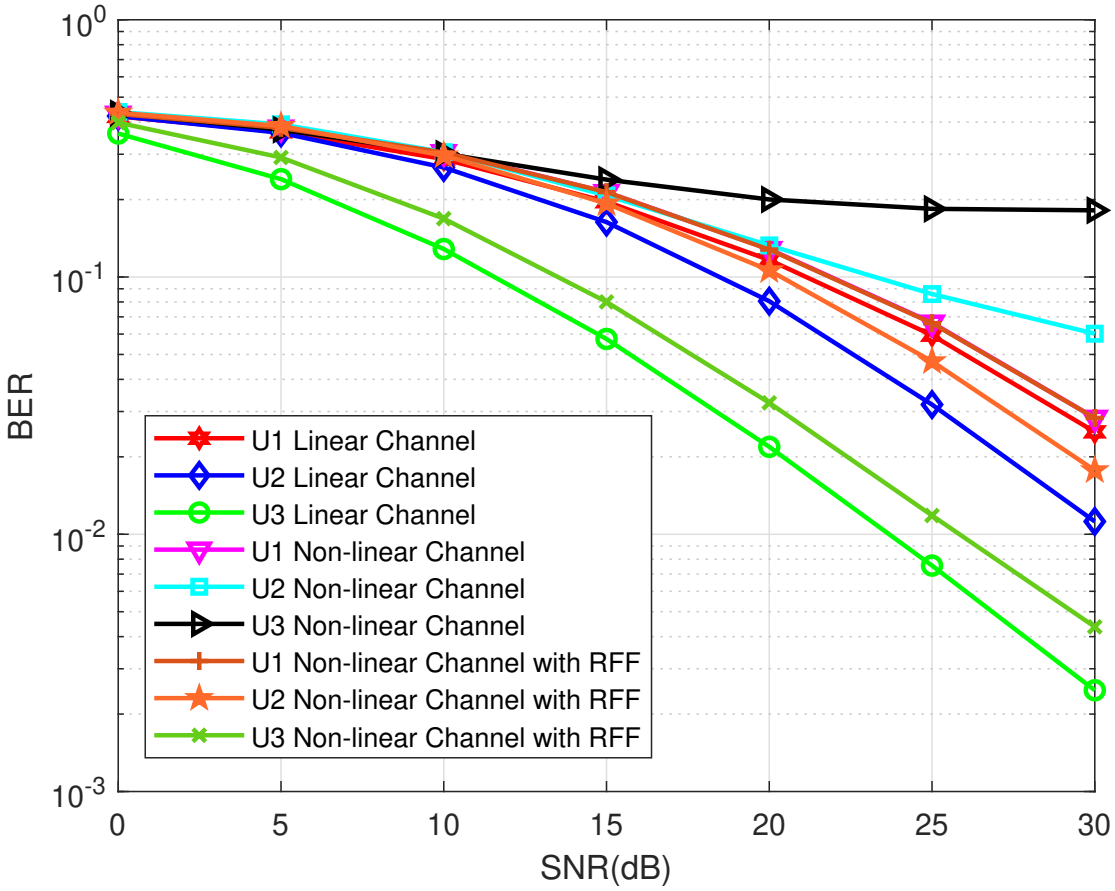

Figure 6.5 BER as a function of SNR for downlink PD-NOMA in the presence of AM-AM nonlinearity and Rayleigh fading for three superposed QPSK users

PD-NOMA decoding algorithm is limited to $O(D + d)$ for each evaluation point Rahimi *et al.* (2007). This last result shows the alleviation in computational complexity through using RFF instead of the generic kernel density estimation. It is also worth mentioning the induced lessening in storage.

6.10 Simulation Results

In this section, we assess the performance of our proposed method in different practical scenarios. Perfect knowledge of the channel is assumed to be available at the receiver. Also, we consider

two superposed users per subcarrier, where user 1, denoted by U1, is far from the base station (i.e. user with poor channel conditions) and user 2, denoted by U2, is close to the base station (i.e. user with good channel conditions). Without loss of generality, the number of RFF dimensions, D, is fixed to 100 and 100 pilots were utilized. We consider both AM-AM and AM-PM Rapp nonlinearities given in (6.4) and (6.5), respectively, with a saturation voltage x_{sat} of 1 and order of severity p of 1 and 0.5. Fig. 6.1, 6.2 show the BER as a function of the SNR in the presence of Rayleigh fading and AM-AM nonlinearity for p=1 and p=0.5 respectively. Another scenario considering AM-PM nonlinearity in Rayleigh fading is presented in Fig. 6.3. In Fig.6.4, we assume imperfect CSI, and we study different levels of channel estimation error variances, using the imperfect CSI model of Wei, Ng, Yuan & Wang (2017), for channel estimation variance, σ_e^2, ranging from 10^{-4} to 10^{-2}. In Fig. 6.5, we consider three superposed users with QPSK modulation, Rayleigh fading, and AM-AM nonlinearity with p=1. The three users are such that U1 is the far user, U2 is the mid user, and U3 is the near user. From Fig. 6.5, it is clear that BER performance has declined, particularly for SIC users, as a result of SIC error propagation that is amplified by the presence of more superposed users. In all the presented scenarios, we see the performance degradation caused to users who have to decode the other users' information before decoding their own and whose BER saturates at values in the order of 10^{-1}. On the other hand, it is shown that our proposed RFF based method mitigates the nonlinearity effects, especially for the SIC users, and achieves a performance that is close to that obtained over a linear channel without distortions. This makes the developed model appealing for PD-NOMA based systems with PA nonlinearities.

6.11 Conclusion

In this paper, we considered the problem of detecting PD-NOMA symbols in the presence of PA nonlinearities. We showed the deleterious impact of the nonlinearity on PD-NOMA systems, specifically on the near user who has to perform SIC. We proposed a RFF based solution to mitigate the degradations caused by this impairment. Simulations of our solution were carried out under different types of nonlinearities and severity levels. Our proposed method was shown

to be comparable to the performance of linear systems. Furthermore, we provided the theorems and analytical proofs that support the achieved performance of RFF based method. Hence, this work provides a more practical framework for PD-NOMA to mitigate PA nonlinearities in practical imperfect environments.

CONCLUSION AND RECOMMENDATIONS

7.1 Conclusion and Learned Lessons

The field of wireless communications will continue to evolve to satisfy the increasing needs for data coming from conventional and emerging applications, such as vehicular technologies, IoT, and healthcare. In the presence of a scarce and limited spectrum, NOMA, through its two categories, code domain and power domain, prevails as a powerful candidate for matching connectivity needs and increased spectral efficiency in future networks. However, several inevitable teething impairments, such as PA nonlinearity and impulsive noise, arise during the practical implementation of new technology. The main goal of this thesis was to study the effect of these impairments on the performance of SCMA and PD-NOMA and to propose decoding algorithms for mitigating the damage caused by these impairments. As we saw in this thesis, using machine learning, information-theoretic learning, and signal processing, NOMA techniques can be improved and adapted to face multiple impairment scenarios, and thus were found viable within the various ecosystems of wireless communications. To be more specific, our contributions are further detailed as follows:

In the third chapter, we studied the impact of PA nonlinearity on the performance of SCMA. We showed that the BER performance of SCMA in the presence of nonlinearity is severely deteriorated. Hence, we proposed an RFF-based SCMA solution for mitigating nonlinearity. Our algorithm was simulated, and our results showed convergence of the proposed solution to the MPA performance of the linear scenario. Additionally, using RKHS properties and the representer theorem, analytical proofs were provided to support our simulated results.

In the fourth chapter, we studied the impact of impulsive noise on the performance of SCMA. A maximum-correntropy based MPA algorithm was developed, which consists in propagating the IP instead of the LLRs. The Maximum-Correntropy based SCMA successfully mitigated the impulsive noise and converged to the MPA without impulsive noise. Mathematical proofs were

also provided for this approach.

In the fifth chapter, as a continuation of methods of mitigating nonlinearity in SCMA that was studied in the first chapter, another method based on Bussgang decomposition was proposed. The BER performance was studied under various nonlinearity severity levels as well as several channel models. Our results were benchmarked against the results of our first work, which was based on RFF. Due to its low computational complexity, this proposed method was found suitable for IIoT systems with limited computational capabilities.

In the sixth chapter, we studied the impact of nonlinearity in PD-NOMA and revealed the degradation in BER performance, especially for the user performing SIC. Hence, we proposed an RFF based algorithm to mitigate PA nonlinearity. Our simulation results showed improvement in the BER performance that approaches linear performance, especially for the SIC user. Additionally, our results were validated using analytical proofs.

7.2 Future Work

Following the outcomes of this thesis and our results, new interesting research paths should be considered.

7.2.1 Further impairments to study and propose mitigation solutions

In addition to PA nonlinearity and memoryless impulsive noise, which were studied in our thesis, wireless communications environments are prone to other kinds of impairments, such as memory-based impulsive noise, in-phase (I)/quadrature-phase(Q) imbalances (IQI), DC offsets, etc. Selim, Muhaidat, Sofotasios, Al-Dweik, Sharif & Stouraitis (2019). These impairments, which could deteriorate the BER performance as well as reduce coverage performance, should be studied within the different NOMA categories. While memory-based impulsive noise has been studied in Alam, Selim, Ahmed, Kaddoum & Yanikomeroglu (2021), where a two-state Markov-Gaussian process was used, the literature on SCMA is still lacking studies considering

scenarios with memory-based impulsive noise. Hence, an exciting work would be to model memory-based impulsive noise within SCMA, study the impact on the BER and coverage performance (outage probability) and propose a suitable mitigation solution. Additionally, the presence of IQI is inevitable in some scenarios. While IQI was studied in PD-NOMA Selim *et al.* (2019), the literature on SCMA is still behind in this area.

7.2.2 User and base station mobility

The sixth generation (6G) is expected to provide ubiquitous connectivity for multiple types of mobile devices, including airplanes, UAVs, and ultra-high-speed trains You, Wang, Huang, Gao, Zhang, Wang, Huang, Zhang, Jiang, Wang et al. (2021). Hence, 6G is expected to deal with excessive mobility of up to 1000km/h Tataria, Shafi, Molisch, Dohler, Sjöland & Tufvesson (2021), which is almost three times the mobility speed target level of 5G Chen, Liang, Sun, Kang, Cheng & Peng (2020). Therefore, studying user or base station mobility scenarios within NOMA is necessary and challenging. General mobility models were developed in many works, where two main models were adopted: Random direction (RD) and random waypoint model (RWP). Hyytia, Lassila & Virtamo (2006) considered the random waypoint mobility model (RWMM). While some works studied user mobility within PD-NOMA, such as in the recent work Miridakis, Michailidis, Michalas, Skondras, Vergados & Vergados (2022), where closed-form expressions of the packet error rate (PER) of two-user uplink PD-NOMA system in the short packet transmission regime with user mobility were derived, it is interesting to study the base station mobility and derive the BER bounds as well as outage probability. Moreover, studying the user/base station mobility BER performance, outage probability, and codebook selection within mobility scenarios is also essential. This would also enable deriving mitigation techniques for mobility drawbacks.

7.2.3 New technology trends in wireless communications

New trends and technologies are emerging and drawing interest in the current and upcoming wireless networks, such as NOMA cooperative networks (C-NOMA) and rate splitting multiple access (RSMA), which are generating exciting research challenges and problems.

C-NOMA is interesting because integrating cooperative approaches into NOMA networks enables greater coverage. The key idea is to provide a set of nodes between the source and NOMA users. Hence, by combining multiple replicas from diverse pathways, a spatial diversity gain is achieved, which improves the reliability Li & Mishra (2020). That being said, we can have two main categories of cooperative networks. The first consists of relays distributed to help the NOMA users communicate with the source Men & Ge (2015). The other category consists of user cooperation, where users near the source assist far users Ding, Peng & Poor (2015). Cooperative networks within NOMA reduce the system outage probability Li & Mishra (2020). While BER performance with imperfect CSI has been studied in Kara & Kaya (2018b), it is important also to study the impact of other impairments that were considered in our thesis that could be expanded for cooperative-NOMA and develop suitable mitigation techniques.

Another emerging multiple access technique to study is RSMA which was first proposed in Mao, Clerckx & Li (2018b) as a more general multiple access technique than NOMA and space-division multiple access (SDMA). Precisely, RSMA treats interference as noise like in SDMA and decodes interference entirely like in NOMA Mao *et al.* (2018b). Interestingly, RSMA was shown to be more energy efficient and spectrally efficient than SDMA and NOMA Mao, Clerckx & Li (2018a). Hence, RSMA could be a potential multiple access technique for upcoming generations. However, RSMA is still in its beginning, and its literature lacks studies on impairments, such as PA nonlinearity, impulsive noise, and IQI. This area could be interesting to tackle because of the potential challenges that arise when considering practical imperfect scenarios.

BIBLIOGRAPHY

(2015). Imt traffic estimates for the years 2020 to 2030. *Report ITU*, 2370–0.

Abidi, I., Hizem, M., Ahriz, I., Cherif, M. & Bouallegue, R. (2019). Convolutional neural networks for blind decoding in sparse code multiple access. *2019 15th International Wireless Communications & Mobile Computing Conference (IWCMC)*, pp. 2007–2012.

Adnan, N. H. M., Rafiqul, I. M. & Alam, A. Z. (2016). Massive MIMO for fifth generation (5G): Opportunities and challenges. *2016 International Conference on Computer and Communication Engineering (ICCCE)*, pp. 47–52.

Akbar, A., Jangsher, S. & Bhatti, F. A. (2021). NOMA and 5G emerging technologies: A survey on issues and solution techniques. *Computer Networks*, 190, 107950.

Al-Nahhal, I., Dobre, O. A., Basar, E. & Ikki, S. (2019). Low-cost uplink sparse code multiple access for spatial modulation. *IEEE Transactions on Vehicular Technology*, 68(9), 9313–9317.

Al-Nahhal, I., Dobre, O. A. & Ikki, S. (2020). On the complexity reduction of uplink sparse code multiple access for spatial modulation. *IEEE Transactions on Communications*, 68(11), 6962–6974.

Al-Nahhal, I., Dobre, O. A. & Basar, E. (2021). Reconfigurable Intelligent Surface-Assisted Uplink Sparse Code Multiple Access. *IEEE Communications Letters*.

Alam, M. S., Selim, B., Kaddoum, G. & Agba, B. L. (2020). Mitigation techniques for impulsive noise with memory modeled by a two state Markov-Gaussian process. *IEEE Systems Journal*, 14(3), 4079–4088.

Alam, M. S., Selim, B., Ahmed, I., Kaddoum, G. & Yanikomeroglu, H. (2021). Bursty impulsive noise mitigation in NOMA: A MAP receiver-based approach. *IEEE Communications Letters*, 25(9), 2790–2794.

Alizadeh, R., Bélanger, N., Savaria, Y. & Boyer, F. (2016, June). Performance characterization of an SCMA decoder. *2016 14th IEEE International New Circuits and Systems Conference (NEWCAS)*, pp. 1-4. doi: 10.1109/NEWCAS.2016.7604820.

Anand, P. K., Jain, S., Mitra, R. & Bhatia, V. (2021). Random Fourier Features based Post-Distortion for Massive-MIMO Visible Light Communication. *2020 International Conference on Communications, Signal Processing, and their Applications (ICCSPA)*, pp. 1–6.

Aronszajn, N. (1950). Theory of reproducing kernels. *Transactions of the American mathematical society*, 68(3), 337–404.

Assaf, T., Al-Dweik, A., El Moursi, M. & Zeineldin, H. (2019). Exact BER performance analysis for downlink NOMA systems over Nakagami-*m* fading channels. *IEEE Access*, 7, 134539–134555.

Au, K., Zhang, L., Nikopour, H., Yi, E., Bayesteh, A., Vilaipornsawai, U., Ma, J. & Zhu, P. (2014). Uplink contention based SCMA for 5G radio access. *2014 IEEE Globecom workshops (GC wkshps)*, pp. 900–905.

Awan, D. A., Cavalcante, R. L., Yukawa, M. & Stanczak, S. (2018). Detection for 5G-NOMA: An online adaptive machine learning approach. *2018 IEEE International Conference on Communications (ICC)*, pp. 1–6.

Baek, J. & Kaddoum, G. (2020). Heterogeneous task offloading and resource allocations via deep recurrent reinforcement learning in partial observable multifog networks. *IEEE Internet Things J.*, 8(2), 1041–1056. doi: 10.1109/JIOT.2020.3009540.

Banelli, P. (2013). Bayesian estimation of a Gaussian source in middleton's class-a impulsive noise. *IEEE Signal Processing Letters*, 20(10), 956–959. doi: 10.1109/LSP.2013.2274774.

Banelli, P., Baruffa, G. & Cacopardi, S. (2001). Effects of HPA nonlinearity on frequency multiplexed OFDM signals. *IEEE Trans. Broadcast.*, 47(2), 123–136.

Bao, J., Ma, Z., Xiao, M., Ding, Z. & Zhu, Z. (2017). Performance analysis of uplink SCMA with receiver diversity and randomly deployed users. *IEEE Transactions on Vehicular Technology*, 67(3), 2792–2797.

Bariah, L., Al-Dweik, A. & Muhaidat, S. (2018). On the performance of non-orthogonal multiple access systems with imperfect successive interference cancellation. *2018 IEEE International Conference on Communications Workshops (ICC Workshops)*, pp. 1–6.

Bariah, L., Muhaidat, S., Sofotasios, P. C., El Bouanani, F., Dobre, O. A. & Hamouda, W. (2021). Large intelligent surface-assisted nonorthogonal multiple access for 6g networks: Performance analysis. *IEEE Internet of Things Journal*, 8(7), 5129–5140.

Basar, E., Di Renzo, M., De Rosny, J., Debbah, M., Alouini, M.-S. & Zhang, R. (2019). Wireless communications through reconfigurable intelligent surfaces. *IEEE access*, 7, 116753–116773.

Bayesteh, A., Yi, E., Nikopour, H. & Baligh, H. (2014). Blind detection of SCMA for uplink grant-free multiple-access. *2014 11th international symposium on wireless communications systems (ISWCS)*, pp. 853–857.

Belkacem, O. B. H., Ammari, M. L. & Dinis, R. (2020). Performance analysis of NOMA in 5G systems with HPA nonlinearities. *IEEE Access*, 8, 158327–158334.

Bennis, M., Debbah, M. & Poor, H. V. (2018). Ultrareliable and low-latency wireless communication: Tail, risk, and scale. *Proceedings of the IEEE*, 106(10), 1834–1853.

Bhatia, V. & Mulgrew, B. (2007). Non-parametric likelihood based channel estimator for Gaussian mixture noise. *Signal Processing*, 87(11), 2569–2586.

Bhatia, V., Mulgrew, B. & Georgiadis, A. T. (2006). Stochastic gradient algorithms for equalisation in α-stable noise. *Signal processing*, 86(4), 835–845.

Bhatia, V., Swami, P., Sharma, S. & Mitra, R. (2020). Non-orthogonal multiple access: an enabler for massive connectivity. *Journal of the Indian Institute of Science*, 100(2), 337–348.

Bhatia, V., Jain, S., Garg, K. & Mitra, R. (2021). Performance analysis of RKHS based detectors for nonlinear NLOS ultraviolet communications. *IEEE Transactions on Vehicular Technology*, 70(4), 3625–3639.

Björnson, E., Özdogan, Ö. & Larsson, E. G. (2020). Reconfigurable intelligent surfaces: Three myths and two critical questions. *IEEE Communications Magazine*, 58(12), 90–96.

Bockelmann, C., Pratas, N., Nikopour, H., Au, K., Svensson, T., Stefanovic, C., Popovski, P. & Dekorsy, A. (2016). Massive machine-type communications in 5G: Physical and MAC-layer solutions. *IEEE Communications Magazine*, 54(9), 59–65.

Bouboulis, P., Pougkakiotis, S. & Theodoridis, S. (2016). Efficient KLMS and KRLS algorithms: A random Fourier feature perspective. *Proc. IEEE Stat. Signal Process. Workshop*, pp. 1–5.

Bouboulis, P., Chouvardas, S. & Theodoridis, S. (2017). Online distributed learning over networks in RKH spaces using random Fourier features. *IEEE Transactions on Signal Processing*, 66(7), 1920–1932.

Bussgang, J. (1952). Crosscorrelation functions of amplitude-distorted Gaussian signals. Research Lab. Electron. *MIT, Cambridge, MA, USA, Tech. Rep*.

Chen, B., Zhu, Y., Hu, J. & Principe, J. C. (2013). *System parameter identification: information criteria and algorithms*. Newnes.

Chen, H. & Wang, Y. (2018). Kernel-based sparse regression with the correntropy-induced loss. *Applied and Computational Harmonic Analysis*, 44(1), 144–164.

Chen, S., Ren, B., Gao, Q., Kang, S., Sun, S. & Niu, K. (2016). Pattern division multiple access—A novel nonorthogonal multiple access for fifth-generation radio networks. *IEEE Transactions on Vehicular Technology*, 66(4), 3185–3196.

Chen, S., Liang, Y.-C., Sun, S., Kang, S., Cheng, W. & Peng, M. (2020). Vision, requirements, and technology trend of 6G: How to tackle the challenges of system coverage, capacity, user data-rate and movement speed. *IEEE Wireless Communications*, 27(2), 218–228.

Chen, X., Yin, H. & Wei, G. (2018). Impact of frequency offset on the performance of uplink OFDM-NOMA systems. *2018 IEEE 4th International Conference on Computer and Communications (ICCC)*, pp. 168–173.

Chen, Y.-M., González, C. D. S., Wang, P.-H. & Chen, K.-P. (2021). Reinforcement learning-based SCMA codebook design for uplink Rayleigh fading channels. *IEEE Wireless Communications Letters*, 10(8), 1717–1721.

Chen, Z., Zhang, R., Cai, L. X., Cheng, Y. & Liu, Y. (2022). A Deep Reinforcement Learning based Approach for NOMA-based Random Access Network with Truncated Channel Inversion Power Control. *arXiv preprint arXiv:2202.10955*.

Chhangani, V., Mitra, R. & Bhatia, V. (2020). RFF based parallel detection for massive MIMO. *2020 European Conference on Networks and Communications (EuCNC)*, pp. 291–295.

Chowdhury, M. Z., Shahjalal, M., Ahmed, S. & Jang, Y. M. (2020). 6G wireless communication systems: Applications, requirements, technologies, challenges, and research directions. *IEEE Open Journal of the Communications Society*, 1, 957–975.

Cover, T. M. (1999). *Elements of information theory*. John Wiley & Sons.

Crisan, D., Miguez, J. et al. (2014). Particle-kernel estimation of the filter density in state-space models. *Bernoulli*, 20(4), 1879–1929.

Dai, L., Wang, B., Yuan, Y., Han, S., I, C. & Wang, Z. (2015). Non-orthogonal multiple access for 5G: solutions, challenges, opportunities, and future research trends. *IEEE Communications Magazine*, 53(9), 74-81. doi: 10.1109/MCOM.2015.7263349.

Dai, L., Wang, B., Ding, Z., Wang, Z., Chen, S. & Hanzo, L. (2018). A survey of non-orthogonal multiple access for 5G. *IEEE communications surveys & tutorials*, 20(3), 2294–2323.

Dai, X., Chen, S., Sun, S., Kang, S., Wang, Y., Shen, Z. & Xu, J. (2014). Successive interference cancelation amenable multiple access (SAMA) for future wireless communications. *2014 IEEE International Conference on Communication Systems*, pp. 222–226.

Dangi, R., Lalwani, P., Choudhary, G., You, I. & Pau, G. (2021). Study and investigation on 5G technology: A systematic review. *Sensors*, 22(1), 26.

Daumé III, H. (2004). From zero to reproducing kernel hilbert spaces in twelve pages or less. *Online: http://pub. hal3. name/daume04rkhs. ps*.

Demir, Ö. T. & Björnson, E. (2019). Channel estimation in massive MIMO under hardware non-linearities: Bayesian methods versus deep learning. *IEEE Open J. Commun. Soc.*, 1, 109–124.

Demir, Ö. T. & Björnson, E. (2020). The Bussgang decomposition of non-linear systems: Basic theory and MIMO extensions. *arXiv preprint arXiv:2005.01597*.

Dhakal, P., Garello, R., Sharma, S. K., Chatzinotas, S. & Ottersten, B. (2016). On the error performance bound of ordered statistics decoding of linear block codes. *2016 IEEE International Conference on Communications (ICC)*, pp. 1–6.

Ding, Z., Peng, M. & Poor, H. V. (2015). Cooperative non-orthogonal multiple access in 5G systems. *IEEE Communications Letters*, 19(8), 1462–1465.

Ding, Z., Lei, X., Karagiannidis, G. K., Schober, R., Yuan, J. & Bhargava, V. K. (2017). A survey on non-orthogonal multiple access for 5G networks: Research challenges and future trends. *IEEE Journal on Selected Areas in Communications*, 35(10), 2181–2195.

Dong, C., Gao, G., Niu, K. & Lin, J. (2018). An Efficient SCMA Codebook Optimization Algorithm Based on Mutual Information Maximization. *Wireless Communications and Mobile Computing*, 2018.

Duarte, M. S. (2021). On Correntropy-Based Machine Learning Models for Nonlinear Signal Processing: Addressing Sparsity, Recursive Estimation and Outlier-Robustness.

Dudak, C. & Kahyaoglu, N. D. (2012). A descriptive study on AM-AM and AM-PM conversion phenomena through EVM-SNR relation. *2012 IEEE Topical Conference on Power Amplifiers for Wireless and Radio Applications*, pp. 69–72.

Evangelista, J. V., Sattar, Z. & Kaddoum, G. (2019a). Analysis of contention-based SCMA in mMTC networks. *2019 IEEE Latin-American Conference on Communications (LATINCOM)*, pp. 1–6.

Evangelista, J. V., Sattar, Z., Kaddoum, G. & Chaaban, A. (2019b). Fairness and sum-rate maximization via joint subcarrier and power allocation in uplink SCMA transmission. *IEEE Transactions on Wireless Communications*, 18(12), 5855–5867.

Evangelista, J. V., Kaddoum, G. & Sattar, Z. (2021a). Reliability and User-Plane Latency Analysis of mmWave Massive MIMO for Grant-Free URLLC Applications. *arXiv preprint arXiv:2107.08151*.

Evangelista, J. V., Sattar, Z., Kaddoum, G., Selim, B. & Sarraf, A. (2021b). Intelligent link adaptation for grant-free access cellular networks: A distributed deep reinforcement learning approach. *arXiv preprint arXiv:2107.04145*.

Farah, J., Sfeir, E., Nour, C. A. & Douillard, C. (2017). New resource allocation techniques for base station power reduction in orthogonal and non-orthogonal multiplexing systems. *Proc. IEEE Int. Conf. Commun. Workshops*, pp. 618–624.

Forney, G. D. & Wei, L.-F. (1989). Multidimensional constellations. I. Introduction, figures of merit, and generalized cross constellations. *IEEE journal on selected areas in communications*, 7(6), 877–892.

Fossorier, M. P. & Lin, S. (1996). First-order approximation of the ordered binary-symmetric channel. *IEEE Transactions on Information Theory*, 42(5), 1381–1387.

Gharaibeh, K. M. (2011). *Nonlinear distortion in wireless systems: Modeling and simulation with MATLAB*. John Wiley & Sons.

Giordani, M., Polese, M., Mezzavilla, M., Rangan, S. & Zorzi, M. (2020). Toward 6G Networks: Use Cases and Technologies. *IEEE Commun. Mag.*, 58(3), 55-61.

Giordani, M., Polese, M., Mezzavilla, M., Rangan, S. & Zorzi, M. (2020). Toward 6G networks: Use cases and technologies. *IEEE Communications Magazine*, 58(3), 55–61.

Guerreiro, J., Dinis, R., Montezuma, P. & Campos, M. (2020). On the Receiver Design for Nonlinear NOMA-OFDM Systems. *2020 IEEE 91st Vehicular Technology Conference (VTC2020-Spring)*, pp. 1–6.

Gui, G., Huang, H., Song, Y. & Sari, H. (2018). Deep learning for an effective nonorthogonal multiple access scheme. *IEEE Transactions on Vehicular Technology*, 67(9), 8440–8450.

Haykin, S. S. (2008). *Adaptive filter theory*. Pearson Education India.

Higuchi, T., Shimizu, N., Shingu, H., Morihiro, Y., Okumura, Y., Miyagoshi, T., Endo, M. & Asano, H. (2018). Video Sending Rate Prediction Based on Communication Logging Database for 5G HetNet. *2018 IEEE 87th Vehicular Technology Conference (VTC Spring)*, pp. 1–6.

Hojeij, M., Farah, J., Nour, C. A. & Douillard, C. (2015, May). Resource Allocation in Downlink Non-Orthogonal Multiple Access (NOMA) for Future Radio Access. *2015 IEEE 81st Vehicular Technology Conference (VTC Spring)*, pp. 1-6. doi: 10.1109/VTCSpring.2015.7146056.

Hoshyar, R., Wathan, F. P. & Tafazolli, R. (2008). Novel low-density signature for synchronous CDMA systems over AWGN channel. *IEEE Transactions on Signal Processing*, 56(4), 1616–1626.

Huang, Y., Han, S., Guo, S., Li, M. & Li, Z. (2019). Secrecy Sum Rate for Two-Way Untrusted Relay in SCMA Networks. *International Conference on Machine Learning and Intelligent Communications*, pp. 72–83.

Huawei. (2013). 5G: A Technology Vision [Format]. Huawei Technologies Co., Ltd., Shenzhen, China, Whitepaper, Consulted at http://www.huawei.com/ilink/en/download/HW314849.

Hyytia, E., Lassila, P. & Virtamo, J. (2006). Spatial node distribution of the random waypoint mobility model with applications. *IEEE Transactions on mobile computing*, 5(6), 680–694.

Islam, S., Zeng, M. & Dobre, O. A. (2017). NOMA in 5G systems: Exciting possibilities for enhancing spectral efficiency. *arXiv preprint arXiv:1706.08215*.

Islam, S. R., Avazov, N., Dobre, O. A. & Kwak, K.-S. (2016). Power-domain non-orthogonal multiple access (NOMA) in 5G systems: Potentials and challenges. *IEEE Commun. Surveys Tuts.*, 19(2), 721–742.

Jain, S. (2022). RKHS based adaptive signal processing algorithms for visible light communication.

Jain, S., Agrawal, A., Bhatia, V. & Prakash, S. (2019a). Crosstalk mitigation in long-reach multicore fiber communication systems using RKHS based nonlinear equalization. *International IFIP Conference on Optical Network Design and Modeling*, pp. 398–411.

Jain, S., Mitra, R. & Bhatia, V. (2019b). KLMS-DFE based adaptive post-distorter for visible light communication. *Optics Communications*, 451, 353–360.

Jain, S., Mitra, R. & Bhatia, V. (2020). On BER analysis of nonlinear VLC systems under ambient light and imperfect/outdated CSI. *OSA Continuum*, 3(11), 3125–3140.

Jain, S., Mitra, R. & Bhatia, V. (2021). Kernel Recursive Maximum Versoria Criterion Algorithm Using Random Fourier Features. *IEEE Transactions on Circuits and Systems II: Express Briefs*, 68(7), 2725–2729.

Kan, R. (2008). From moments of sum to moments of product. *Journal of Multivariate Analysis*, 99(3), 542–554. doi: 10.1016/j.jmva.2007.01.013.

Kantas, N., Doucet, A., Singh, S. S. & Maciejowski, J. M. (2009). An overview of sequential Monte Carlo methods for parameter estimation in general state-space models. *Proc. IFAC*

Symp. System Identification, 42(10), 774–785.

Kara, F. & Kaya, H. (2018a). BER performances of downlink and uplink NOMA in the presence of SIC errors over fading channels. *IET Commun.*, 12(15), 1834–1844.

Kara, F. & Kaya, H. (2018b). On the error performance of cooperative-NOMA with statistical CSIT. *IEEE Communications Letters*, 23(1), 128–131.

Kim, M., Kim, N.-I., Lee, W. & Cho, D.-H. (2018). Deep learning-aided SCMA. *IEEE Communications Letters*, 22(4), 720–723.

Klimentyev, V. P. & Sergienko, A. B. (2016). Detection of SCMA signal with channel estimation error. *2016 18th Conference of Open Innovations Association and Seminar on Information Security and Protection of Information Technology (FRUCT-ISPIT)*, pp. 106–112.

Klimentyev, V. P. & Sergienko, A. B. (2017). SCMA codebooks optimization based on genetic algorithm. *European Wireless 2017; 23th European Wireless Conference*, pp. 1–6.

Korowajczuk, L. (2011). *LTE, WiMAX and WLAN network design, optimization and performance analysis*. John Wiley & Sons.

Lampe, L. (2011). Bursty impulse noise detection by compressed sensing. *2011 IEEE International Symposium on Power Line Communications and Its Applications*, pp. 29–34.

Li, C. & Yang, Z. (2009). Analysis of group multiuser detection based on coalition game theory. *Journal of Electronics (China)*, 26(6), 804–811.

Li, G. & Mishra, D. (2020). Cooperative NOMA networks: User cooperation or relay cooperation? *ICC 2020-2020 IEEE international conference on communications (ICC)*, pp. 1–6.

Li, M., El Bouanani, F., Tian, L., Chen, W., Han, Z. & Muhaidat, S. (2021). Error Rate Analysis of Non-Orthogonal Multiple Access With Residual Hardware Impairments. *IEEE Commun. Lett.*, 25(8), 2522–2526.

Li, X., Li, J., Mathiopoulos, P. T., Zhang, D., Li, L. & Jin, J. (2018a). Joint impact of hardware impairments and imperfect CSI on cooperative SWIPT NOMA multi-relaying systems. *2018 IEEE/CIC International Conference on Communications in China (ICCC)*, pp. 95–99.

Li, Z., Uusitalo, M. A., Shariatmadari, H. & Singh, B. (2018b). 5g urllc: Design challenges and system concepts. *2018 15th International Symposium on Wireless Communication Systems (ISWCS)*, pp. 1–6.

Lin, J., Feng, S., Zhang, Y., Yang, Z. & Zhang, Y. (2020). A novel deep neural network based approach for sparse code multiple access. *Neurocomputing*, 382, 52–63.

Liu, B., Zhang, L. & Xin, X. (2015a). Non-orthogonal optical multicarrier access based on filter bank and SCMA. *Optics express*, 23(21), 27335–27342.

Liu, J., Wu, G., Li, S. & Tirkkonen, O. (2017a). Blind detection of uplink grant-free SCMA with unknown user sparsity. *2017 IEEE International Conference on Communications (ICC)*, pp. 1–6.

Liu, S., Wang, J., Bao, J. & Liu, C. (2018). Optimized SCMA Codebook Design by QAM Constellation Segmentation With Maximized MED. *IEEE Access*, 6, 63232–63242.

Liu, T., Li, X. & Qiu, L. (2015b). Capacity for downlink massive MIMO MU-SCMA system. *2015 International Conference on Wireless Communications & Signal Processing (WCSP)*, pp. 1–5.

Liu, W., Pokharel, P. P. & Principe, J. C. (2006). Correntropy: A localized similarity measure. *The 2006 IEEE international joint conference on neural network proceedings*, pp. 4919–4924.

Liu, W., Pokharel, P. P. & Principe, J. C. (2007). Correntropy: Properties and applications in non-Gaussian signal processing. *IEEE Transactions on signal processing*, 55(11), 5286–5298.

Liu, Y. & Chen, J. (2013). Correntropy-based kernel learning for nonlinear system identification with unknown noise: an industrial case study. *IFAC Proceedings Volumes*, 46(32), 361–366.

Liu, Y., Qin, Z., Elkashlan, M., Ding, Z., Nallanathan, A. & Hanzo, L. (2017b). Non-orthogonal multiple access for 5G and beyond. *Proceedings of the IEEE*, 105(12), 2347–2381.

Lu, C., Xu, W., Shen, H., Zhang, H. & You, X. (2018). An enhanced SCMA detector enabled by deep neural network. *2018 IEEE/CIC International Conference on Communications in China (ICCC)*, pp. 835–839.

Lv, T., Ma, Y., Zeng, J. & Mathiopoulos, P. T. (2018). Millimeter-wave NOMA transmission in cellular M2M communications for Internet of Things. *IEEE Internet Things J.*, 5(3), 1989–2000.

Makki, B., Chitti, K., Behravan, A. & Alouini, M.-S. (2020). A survey of NOMA: Current status and open research challenges. *IEEE Open Journal of the Communications Society*, 1, 179–189.

Mallinson, K. (2016). The path to 5G: as much evolution as revolution. *3GPP-The Mobile Broadband Standard*.

Mao, Y., Clerckx, B. & Li, V. O. (2018a). Energy efficiency of rate-splitting multiple access, and performance benefits over SDMA and NOMA. *2018 15th International Symposium on Wireless Communication Systems (ISWCS)*, pp. 1–5.

Mao, Y., Clerckx, B. & Li, V. O. (2018b). Rate-splitting multiple access for downlink communication systems: bridging, generalizing, and outperforming SDMA and NOMA. *EURASIP journal on wireless communications and networking*, 2018(1), 1–54.

Men, J. & Ge, J. (2015). Non-orthogonal multiple access for multiple-antenna relaying networks. *IEEE Communications Letters*, 19(10), 1686–1689.

Merchan, S., Armada, A. G. & Garcia, J. (1998). OFDM performance in amplifier nonlinearity. *IEEE Trans. Broadcast.*, 44(1), 106–114.

Mestrah, Y. (2019). *Robust Communication Systems in Unknown Environments*. (Ph.D. thesis, Université de Reims Champagne-Ardenne).

Miramirkhani, F., Karbalayghareh, M., Zeydan, E. & Mitra, R. (2022). Enabling 5G indoor services for residential environment using VLC technology. *Physical Communication*, 53, 101679.

Miridakis, N. I., Michailidis, E. T., Michalas, A., Skondras, E., Vergados, D. J. & Vergados, D. D. (2022). Performance of uplink NOMA with user mobility under short packet transmission. *Wireless Personal Communications*, 122(3), 2273–2283.

Mitra, R., Kaddoum, G. & Bhatia, V. (2020). Hyperparameter-Free Transmit-Nonlinearity Mitigation Using a Kernel-Width Sampling Technique. *IEEE Trans. Commun.*, PP(99), 1-1. doi: 10.1109/TCOMM.2020.3048045.

Mitra, R. & Bhatia, V. (2017a). Low complexity post-distorter for visible light communications. *IEEE Communications Letters*, 21(9), 1977–1980.

Mitra, R. & Bhatia, V. (2017b). Precoded chebyshev-NLMS-based pre-distorter for nonlinear LED compensation in NOMA-VLC. *IEEE Transactions on Communications*, 65(11), 4845–4856.

Mitra, R. & Bhatia, V. (2018a). Kernel-based parallel multi-user detector for massive-MIMO. *Computers & Electrical Engineering*, 65, 543–553.

Mitra, R. & Bhatia, V. (2018b). Precoding technique for ill-conditioned massive MIMO-VLC system. *2018 IEEE 87th Vehicular Technology Conference (VTC Spring)*, pp. 1–5.

Mitra, R. & Kaddoum, G. (2021). Random Fourier feature based deep learning for wireless communications. *arXiv preprint arXiv:2101.05254*.

Mitra, R. & Kaddoum, G. (2022). Random Fourier feature based deep learning for wireless communications. *IEEE Trans. on Cogn. Commun. Netw.*

Mitra, R., Miramirkhani, F., Bhatia, V. & Uysal, M. (2018). Mixture-kernel based post-distortion in RKHS for time-varying VLC channels. *IEEE Transactions on Vehicular Technology*, 68(2), 1564–1577.

Mitra, R., Jain, S. & Bhatia, V. (2020a). Least minimum symbol error rate based post-distortion for VLC using random Fourier features. *IEEE Communications Letters*, 24(4), 830–834.

Mitra, R., Miramirkhani, F., Bhatia, V. & Uysal, M. (2020b). Low complexity least minimum symbol error rate based post-distortion for vehicular VLC. *IEEE Transactions on Vehicular Technology*, 69(10), 11800–11810.

Mitra, R., Sharma, S., Kaddoum, G. & Bhatia, V. (2020c). Color-Domain SCMA NOMA for Visible Light Communication. *IEEE Communications Letters*, 25(1), 200–204.

Mitra, R., Bhatia, V., Jain, S. & Choi, K. (2021). Performance Analysis of Random Fourier Features-Based Unsupervised Multistage-Clustering for VLC. *IEEE Communications Letters*, 25(8), 2659–2663.

Moltafet, M., Yamchi, N. M., Javan, M. R. & Azmi, P. (2017). Comparison study between PD-NOMA and SCMA. *IEEE Transactions on Vehicular Technology*, 67(2), 1830–1834.

Morocho-Cayamcela, M. E., Lee, H. & Lim, W. (2019). Machine learning for 5G/B5G mobile and wireless communications: Potential, limitations, and future directions. *IEEE Access*, 7, 137184–137206.

Ndo, G., Labeau, F. & Kassouf, M. (2013). A Markov-Middleton model for bursty impulsive noise: Modeling and receiver design. *IEEE Transactions on Power Delivery*, 28(4), 2317–2325.

Nikopour, H. & Baligh, H. (2013). Sparse code multiple access. *2013 IEEE 24th Annual International Symposium on Personal, Indoor, and Mobile Radio Communications (PIMRC)*, pp. 332–336.

Nikopour, H., Yi, E., Bayesteh, A., Au, K., Hawryluck, M., Baligh, H. & Ma, J. (2014). SCMA for downlink multiple access of 5G wireless networks. *2014 IEEE global communications conference*, pp. 3940–3945.

Panda, S. & Nanda, P. K. (2021). Kernel density estimation and correntropy based background modeling and camera model parameter estimation for underwater video object detection. *Soft Computing*, 25(15), 10477–10496.

Parvez, I., Rahmati, A., Guvenc, I., Sarwat, A. I. & Dai, H. (2018). A survey on low latency towards 5G: RAN, core network and caching solutions. *IEEE Communications Surveys & Tutorials*, 20(4), 3098–3130.

Polcari, J. (2013). An informative interpretation of decision theory: The information theoretic basis for signal-to-noise ratio and log likelihood ratio. *IEEE Access*, 1, 509–522.

Price, R. (1958). A useful theorem for nonlinear devices having Gaussian inputs. *IRE Transactions on Information Theory*, 4(2), 69–72.

Principe, J. C. (2010). *Information theoretic learning: Renyi's entropy and kernel perspectives*. Springer Science & Business Media.

Príncipe, J. C., Liu, W. & Haykin, S. (2011). *Kernel adaptive filtering: a comprehensive introduction*. John Wiley & Sons.

Proakis, J. G. & Salehi, M. (2001). *Digital communications*. McGraw-hill New York.

Psaltopoulos, G. K. & Wittneben, A. (2010). Nonlinear MIMO: Affordable MIMO technology for wireless sensor networks. *IEEE Trans. Wireless Commun.*, 9(2), 824–832.

Qi, J. & Aissa, S. (2012). On the power amplifier nonlinearity in MIMO transmit beamforming systems. *IEEE Trans. Commun.*, 60(3), 876–887.

Qin, X., Qin, C., Wang, C. & Wang, W. (2018). Blind Equalization of Sparse Code Multiple Access Algorithm in Multipath Propagation. *2018 24th Asia-Pacific Conference on Communications (APCC)*, 213–218.

Rahimi, A., Recht, B. et al. (2007). Random Features for Large-Scale Kernel Machines. *NIPS*, 3(4), 5.

Rajasekaran, A. S., Vameghestahbanati, M., Farsi, M., Yanikomeroglu, H. & Saeedi, H. (2019). Resource allocation-based PAPR analysis in uplink SCMA-OFDM systems. *IEEE Access*, 7, 162803–162817.

Raykar, V. C., Duraiswami, R. & Zhao, L. H. (2010a). Fast Computation of Kernel Estimators. *J. Comput. Graphical Stat.*, 19(1), 205–220.

Raykar, V. C., Duraiswami, R. & Zhao, L. H. (2010b). Fast computation of kernel estimators. *Journal of Computational and Graphical Statistics*, 19(1), 205–220.

Razavi, R., Mohammed, A.-I., Imran, M. A., Hoshyar, R. & Chen, D. (2012). On receiver design for uplink low density signature OFDM (LDS-OFDM). *IEEE Transactions on Communications*, 60(11), 3499–3508.

Salah, S. B., Philip, P. C., Paulus, R. & Jaiswal, A. K. (2017). Comparative Analysis for Strategic Minimization of the Interference in Small Cell LTE Networks.

Samie, F., Tsoutsouras, V., Xydis, S., Bauer, L., Soudris, D. & Henkel, J. (2016). Distributed QoS management for Internet of Things under resource constraints. *Proceedings of the Eleventh IEEE/ACM/IFIP International Conference on Hardware/Software Codesign and System Synthesis*, pp. 1–10. doi: 10.1145/2968456.2974005.

Sayed, A. H. (2011). *Adaptive filters*. John Wiley & Sons.

Schölkopf, B., Herbrich, R. & Smola, A. J. (2001). A generalized representer theorem. *International conference on computational learning theory*, pp. 416–426.

Selim, B., Muhaidat, S., Sofotasios, P. C., Sharif, B. S., Stouraitis, T., Karagiannidis, G. K. & Al-Dhahir, N. (2018). Outage probability of multi-carrier NOMA systems under joint I/Q imbalance. *2018 International Conference on Advanced Communication Technologies and Networking (CommNet)*, pp. 1–7.

Selim, B., Muhaidat, S., Sofotasios, P. C., Al-Dweik, A., Sharif, B. S. & Stouraitis, T. (2019). Radio-frequency front-end impairments: Performance degradation in nonorthogonal multiple access communication systems. *IEEE Vehicular Technology Magazine*, 14(1), 89–97.

Selim, B., Alam, M. S., Evangelista, J. V., Kaddoum, G. & Agba, B. L. (2020a). NOMA-based IoT networks: Impulsive noise effects and mitigation. *IEEE Communications Magazine*, 58(11), 69–75.

Selim, B., Alam, M. S., Kaddoum, G. & Agba, B. L. (2020b). Effect of impulsive noise on uplink NOMA systems. *IEEE Transactions on Vehicular Technology*, 69(3), 3454–3458.

Sergienko, A. B. & Klimentyev, V. P. (2017). Spectral efficiency of uplink SCMA system with CSI estimation. *2017 20th Conference of Open Innovations Association (FRUCT)*, pp. 391–397.

Series, M. (2015). IMT Vision–Framework and overall objectives of the future development of IMT for 2020 and beyond. *Recommendation ITU*, 2083, 21.

Sfeir, E., Mitra, R., Kaddoum, G. & Bhatia, V. (2020a). Performance analysis of maximum-correntropy based detection for SCMA. *IEEE Commun. Lett.*, 25(4), 1114–1118. doi: 10.1109/LCOMM.2020.3047782.

Sfeir, E., Mitra, R., Kaddoum, G. & Bhatia, V. (2020b). RFF Based Detection for SCMA in Presence of PA Nonlinearity. *IEEE Commun. Lett.*, 24(11), 2604-2608. doi: 10.1109/L-COMM.2020.3010698.

Sfeir, E., Mitra, R., Kaddoum, G. & Bhatia, V. (2021). Comparative analytical study of SCMA detection methods for PA nonlinearity mitigation. *Sensors*, 21(24), 8408.

Sfeir, E., Mitra, R. & Kaddoum, G. (2022). A random fourier feature based receiver detection for enhanced BER performance in nonlinear PD-NOMA. *IEEE Trans. Veh. Technol.*

Sharma, S., Deka, K., Bhatia, V. & Gupta, A. (2018). SCMA codebook based on optimization of mutual information and shaping gain. *2018 IEEE Globecom Workshops (GC Wkshps)*, pp. 1–6.

Sharma, S., Bhatia, V. & Mishra, A. K. (2019a). Wireless consumer electronic devices: The effects of impulsive radio-frequency interference. *IEEE Consumer Electronics Magazine*, 8(4), 56–61.

Sharma, S., Deka, K., Bhatia, V. & Gupta, A. (2019b). Joint power-domain and SCMA-based NOMA system for downlink in 5G and beyond. *IEEE Communications Letters*, 23(6), 971–974.

Sharma, V., Bennis, M. & Kumar, R. (2016). UAV-assisted heterogeneous networks for capacity enhancement. *IEEE Communications Letters*, 20(6), 1207–1210.

Silverman, B. W. (1986). *Density Estimation for Statistics and Data Analysis*. CRC Press.

Silverman, B. W. (2018). *Density estimation for statistics and data analysis*. Routledge. doi: 10.1201/9781315140919.

Singh, A. & Kaur, H. (2012). Non linearity analysis of high power amplifier in OFDM system. *International Journal of Computer Applications*, 37(2), 37–41.

Slavakis, K., Bouboulis, P. & Theodoridis, S. (2014). Online learning in reproducing kernel Hilbert spaces. In *Academic Press Library in Signal Processing* (vol. 1, pp. 883–987). Elsevier.

Spaulding, A. & Middleton, D. (1977). Optimum reception in an impulsive interference environment-Part I: Coherent detection. *IEEE Transactions on Communications*, 25(9),

910–923.

Sultana, A., Woungang, I., Anpalagan, A., Zhao, L. & Ferdouse, L. (2020). Efficient Resource Allocation in SCMA-Enabled Device-to-Device Communication for 5G Networks. *IEEE Transactions on Vehicular Technology*, 69(5), 5343–5354.

Sun, H., Xie, B., Hu, R. Q. & Wu, G. (2016). Non-orthogonal multiple access with SIC error propagation in downlink wireless MIMO networks. *Proc. IEEE Veh. Technol. Conf. (VTC Fall)*, pp. 1–5.

Sun, J., Wu, W. & Wu, X. (2018). A Contention Transmission Unit Allocation Scheme for Uplink Grant-Free SCMA Systems. *2018 IEEE International Conference on Communications (ICC)*, pp. 1–5.

Taherzadeh, M., Nikopour, H., Bayesteh, A. & Baligh, H. (2014). SCMA codebook design. *2014 IEEE 80th Vehicular Technology Conference (VTC2014-Fall)*, pp. 1–5.

Tataria, H., Shafi, M., Molisch, A. F., Dohler, M., Sjöland, H. & Tufvesson, F. (2021). 6G wireless systems: Vision, requirements, challenges, insights, and opportunities. *Proceedings of the IEEE*, 109(7), 1166–1199.

Theodoridis, S. (2015). *Machine learning: a Bayesian and optimization perspective*. Academic press.

Tse, D. & Viswanath, P. (2005). *Fundamentals of wireless communication*. Cambridge university press.

Vaezi, M., Ding, Z. & Poor, H. V. (2019). *Multiple access techniques for 5G wireless networks and beyond*. Springer.

Vameghestahbanati, M., Bedeer, E., Marsland, I., Gohary, R. H. & Yanikomeroglu, H. (2017). Enabling sphere decoding for SCMA. *IEEE Communications Letters*, 21(12), 2750–2753.

Vameghestahbanati, M., Marsland, I. D., Gohary, R. H. & Yanikomeroglu, H. (2019). Multidimensional constellations for uplink SCMA systems—A comparative study. *IEEE Communications Surveys & Tutorials*, 21(3), 2169–2194.

Wang, Q., Zhang, R., Yang, L.-L. & Hanzo, L. (2018). Non-orthogonal multiple access: A unified perspective. *IEEE Wireless Commun.*, 25(2), 10–16.

Wei, F. & Chen, W. (2016). A low complexity SCMA decoder based on list sphere decoding. *2016 IEEE Global Communications Conference (GLOBECOM)*, pp. 1–6.

Wei, Z., Ng, D. W. K., Yuan, J. & Wang, H.-M. (2017). Optimal resource allocation for power-efficient MC-NOMA with imperfect channel state information. *IEEE Trans. Commun.*, 65(9), 3944–3961.

Wiklundh, K., Stenumgaard, P. & Tullberg, H. (2009). Channel capacity of Middleton's class A interference channel. *Electronics letters*, 45(24), 1227–1229.

Wu, Y., Zhang, S. & Chen, Y. (2015a). Iterative Multiuser Receiver in Sparse Code Multiple Access Systems. *2015 IEEE International Conference on Communications (ICC)*, 2918–2923.

Wu, Y., Wang, C., Chen, Y. & Bayesteh, A. (2017). Sparse code multiple access for 5G radio transmission. *Proc. IEEE Veh. Technol. Conf. (VTC Fall)*, pp. 1–6.

Wu, Z., Shi, J., Zhang, X., Ma, W., Chen, B. & Senior Member, I. (2015b). Kernel recursive maximum correntropy. *Signal Processing*, 117, 11–16.

Xiao, M., Mumtaz, S., Huang, Y., Dai, L., Li, Y., Matthaiou, M., Karagiannidis, G. K., Björnson, E., Yang, K., Chih-Lin, I. et al. (2017). Millimeter wave communications for future mobile networks. *IEEE Journal on Selected Areas in Communications*, 35(9), 1909–1935.

Yang, L., Lin, X., Ma, X. & Li, S. (2018). Iterative clipping noise elimination of clipped and filtered SCMA-OFDM system. *IEEE Access*, 6, 54427–54434.

Yang, S. & Sun, J. (2019). Joint Power and Codebook Assignment Using Cooperative Game and Coalitions for SCMA mMTC System. *2019 International Conference on Communications, Information System and Computer Engineering (CISCE)*, pp. 49–53.

Yin, J., Zhu, X., Huang, Y. & Jiang, Y. (2018). Null subcarriers assisted impulsive noise mitigation for in-vehicle power line communication in the presence of narrowband interference. *IEEE Transactions on Vehicular Technology*, 68(1), 498–508.

You, X., Wang, C.-X., Huang, J., Gao, X., Zhang, Z., Wang, M., Huang, Y., Zhang, C., Jiang, Y., Wang, J. et al. (2021). Towards 6G wireless communication networks: Vision, enabling technologies, and new paradigm shifts. *Science China Information Sciences*, 64(1), 1–74.

Yuan, W., Wu, N., Guo, Q., Li, Y., Xing, C. & Kuang, J. (2018). Iterative receivers for downlink MIMO-SCMA: Message passing and distributed cooperative detection. *IEEE Transactions on Wireless Communications*, 17(5), 3444–3458.

Yuan, Y. (2016). Non-orthogonal Multi-User Superposition and Shared Access. *Signal Processing for 5G: Algorithms and Implementations*, 115–142.

Yuan, Y., Zhao, Y., Zong, B. & Parolari, S. (2020). Potential key technologies for 6G mobile communications. *Science China Information Sciences*, 63, 1–19.

Zhai, D. (2017). Adaptive codebook design and assignment for energy saving in SCMA networks. *IEEE Access*, 5, 23550–23562.

Zhang, J., Dai, L., Li, X., Liu, Y. & Hanzo, L. (2018). On low-resolution ADCs in practical 5G millimeter-wave massive MIMO systems. *IEEE Communications Magazine*, 56(7), 205–211.

Zhang, S., Xiao, K., Xiao, B., Chen, Z., Xia, B., Chen, D. & Ma, S. (2016). A capacity-based codebook design method for sparse code multiple access systems. *2016 8th International Conference on Wireless Communications & Signal Processing (WCSP)*, pp. 1–5.

Zhao, S., Chen, B. & Principe, J. C. (2011). Kernel adaptive filtering with maximum correntropy criterion. *The 2011 International Joint Conference on Neural Networks*, pp. 2012–2017.

Zhidkov, S. V. (2016). Joint Channel Estimation and Nonlinear Distortion Compensation in OFDM Receivers. *arXiv preprint arXiv:1612.09222*.

Zou, Y., Kim, K. T., Ding, Z., Wichman, R., Hamalainen, J., Lin, X. & Chiang, M. (2019). Low-overhead multi-antenna-enabled random access for machine-type communications with low mobility. *2019 IEEE Global Communications Conference (GLOBECOM)*, pp. 1–6.